AD-A041 316 YALE UNIV NEW HAVEN CONN DEPT OF ENGINEERING AND AP--ETC F/G 20/1
BISTATIC SURFACE SCATTERING STRENGTH AT SHORT WAVELENGTHS.(U)
JUN 77 J G ZORNIG, P M SCHULTHEISS, J SNYDER N00014-75-C-1014

UNCLASSIFIED CS-9 NL

1 OF 1
ADA
041316

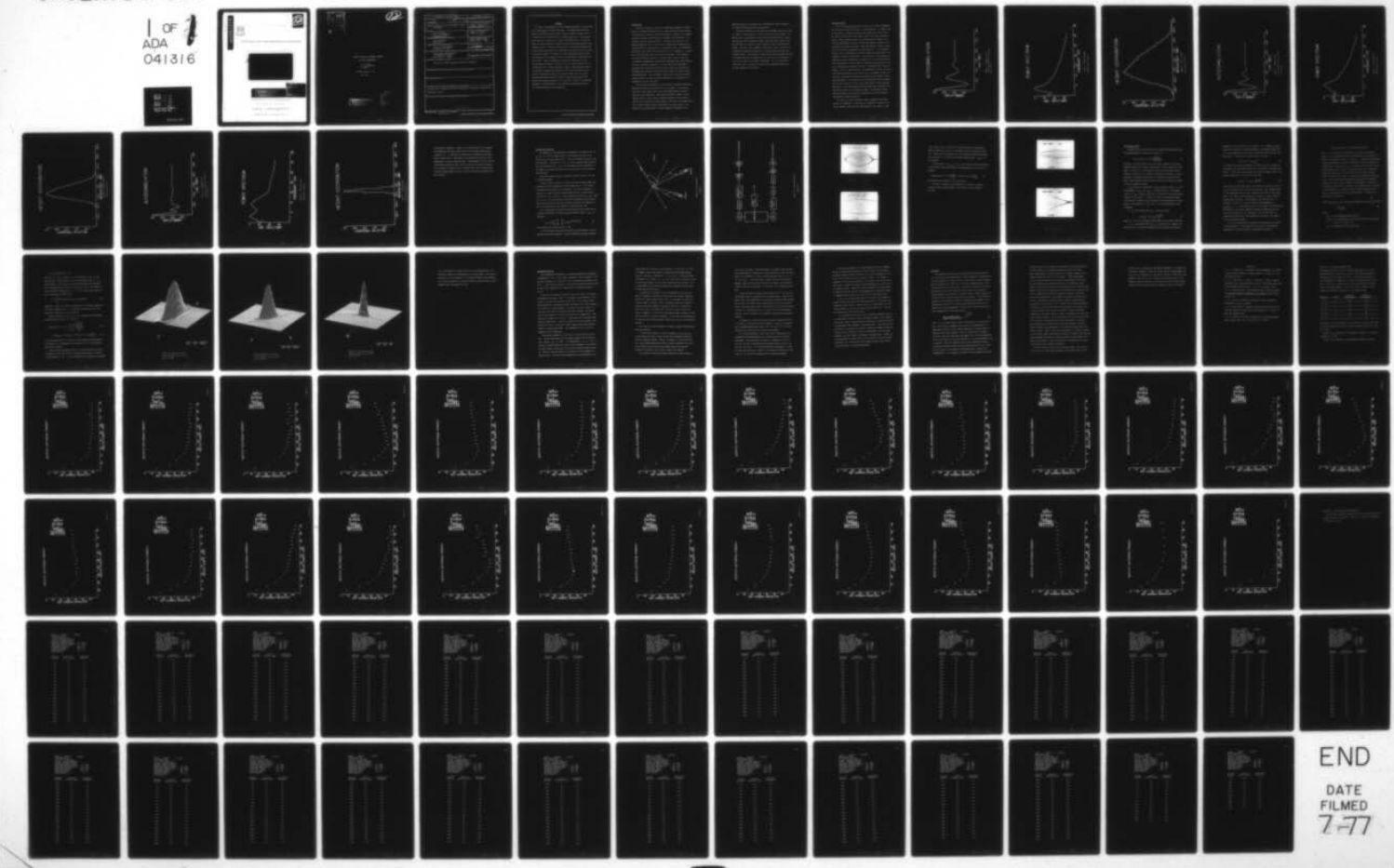

END
DATE
FILMED
7-77

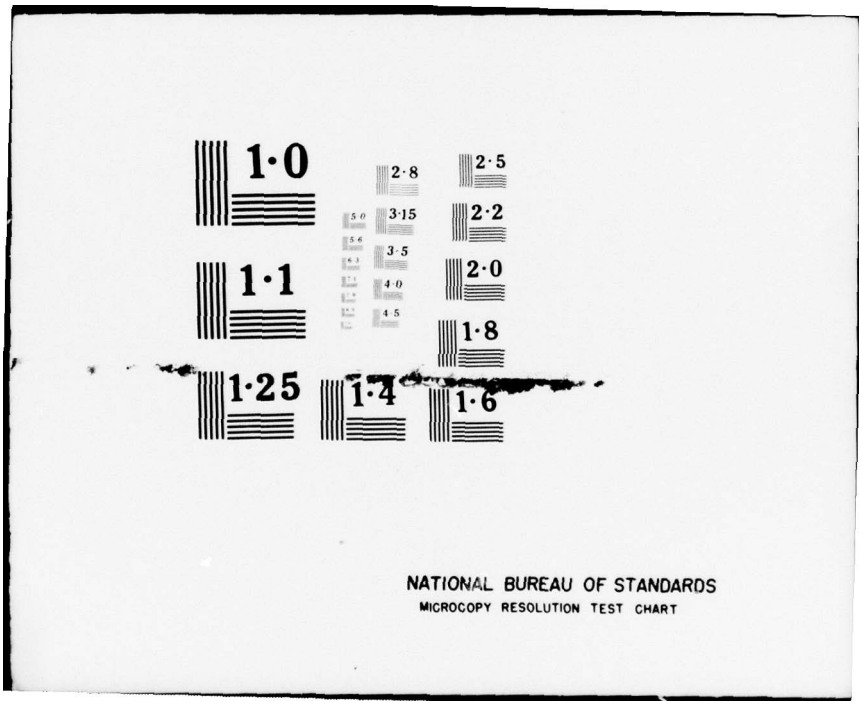
1·0
2·8
2·5
3·15
2·2
3·5
1·1
2·0
4·0
1·8
1·25
1·4
1·6
NATIONAL BUREAU OF STANDARDS
MICROCOPY RESOLUTION TEST CHART

12

LUX ET VERITAS

SYSTEMS AND INFORMATION SCIENCES

DEPARTMENT OF ENGINEERING
AND APPLIED SCIENCE

YALE UNIVERSITY

NEW HAVEN, CONNECTICUT

12

BISTATIC SURFACE SCATTERING STRENGTH

AT SHORT WAVELENGTHS

J. G. Zornig
P. M. Schultheiss
J. Snyder

Technical Report CS-9

June 1977

SECURITY CLASSIFICATION OF THIS PAGE (When Data Entered)

REPORT DOCUMENTATION PAGE	READ INSTRUCTIONS BEFORE COMPLETING FORM
1. REPORT NUMBER (14) CS-9 (9) Final rept. 1 Apr 76-31 Mar 77	2. GOVT ACCESSION NO. 3. RECIPIENT'S CATALOG NUMBER
4. TITLE (and Subtitle) (6) Bistatic Surface Scattering Strength at Short Wavelengths.	5. TYPE OF REPORT & PERIOD COVERED Technical (Final) Report 4/1/76 - 3/31/77
	6. PERFORMING ORG. REPORT NUMBER
7. AUTHOR(s) (10) John G. Zornig, Peter M. Schultheiss Jacqueline Snyder (15)	8. CONTRACT OR GRANT NUMBER(s) N00014-75-C-1014
9. PERFORMING ORGANIZATION NAME AND ADDRESS (1) Yale University New Haven, Ct. Dept. of Engrg. & Applied Science	10. PROGRAM ELEMENT, PROJECT, TASK AREA & WORK UNIT NUMBERS NRL Req. N00173-75-RQ-6410/3-14-75 8163
11. CONTROLLING OFFICE NAME AND ADDRESS Office of Naval Research Arlington, Va. 22217	12. REPORT DATE (11) June 1977
	13. NUMBER OF PAGES 89 (12) 95p.
14. MONITORING AGENCY NAME & ADDRESS (if different from Controlling Office) ONR Resident Representative 715 Broadway, 5th Floor New York, N. Y. 10003	15. SECURITY CLASS. (of this report) U
	15a. DECLASSIFICATION/DOWNGRADING SCHEDULE
16. DISTRIBUTION STATEMENT (of this Report) Approved for public release, distribution unlimited	
17. DISTRIBUTION STATEMENT (of the abstract entered in Block 20, if different from Report)	
18. SUPPLEMENTARY NOTES	
19. KEY WORDS (Continue on reverse side if necessary and identify by block number) Communication, Underwater Acoustics, Propagation, Scattering, Reverberation, Modelling, Bistatic	
20. ABSTRACT (Continue on reverse side if necessary and identify by block number) 400 987	

DD FORM 1 JAN 73 1473 EDITION OF 1 NOV 65 IS OBSOLETE
S/N 0102-014-6601

SECURITY CLASSIFICATION OF THIS PAGE (When Data Entered)

ABSTRACT

A series of measurements of the scattering strength of a wind driven water surface at 1.3 mHz have been made. The measurements have been made at 12° and 17° grazing angles, bistatic azimuths ranging from 0° to 180°, and two different surface roughness conditions. Orientations with respect to the wind over a range of 180° were used. The measurements were made with short, relatively narrow band probing signals under computer control. The data were converted to scattering strength using a flat surface reference and a compensation for beam patterns and source and receiver timing. The results of these measurements indicate that wind direction is an important factor in determining reverberation from the surface. Surface roughness was found to be important, but the scalar Rayleigh Parameter is found not to be a useful indicator of reverberation level. Grazing angle and acoustic wavelength were found to be relatively insignificant variables. The results obtained in this series of experiments indicate that present theory will not predict scattering strength accurately without a detailed knowledge of the second order spatial statistics of the surface. Efforts to obtain measurements of surface slopes of the required precision have met with very limited success but will continue.

Introduction

This report describes a series of experiments designed to investigate the reverberation properties of a rough wind-driven water surface, in particular the bistatic scattering strength, a measure of the degree to which a surface can be expected to radiate in one direction if insonified from some other direction. This particular statistic is of general importance both in the design of bistatic sonar systems and in the prediction of reverberation in a refractive ocean. The experiments described in this report were conducted in a 7.3 m. diameter, 1 m. deep water tank over which runs a fan driven wind tunnel. This apparatus has been described previously [1] and has been in use for some time. It provides a homogeneous, statistically stationary wind driven surface of known, repeatable statistics. For this particular measurement a goniometer was constructed which served as a mount for projector and hydrophone and permitted rapid and precise changes in azimuth, range, and grazing angle. This goniometer, while still only partially under remote control, has made an enormous difference in the speed and repeatability of data collection.

As in previous experiments at this facility, probing signals were generated and data were acquired by on line computer. The principal difference from earlier work is that the probing signal was narrow band rather than impulsive. This choice was made in order to obtain maximum signal to noise ratio by analog and digital filtering and to simplify the calculation of beam patterns. The form of the signal used was a single frequency carrier modulated by a cosine envelope. The purpose of the envelope was to reduce transducer transients at the

beginning and end of the pulse and, consistent with that requirement, to simplify the data reduction calculations.

Frequencies employed in this series of experiments were quite high, (1.3 mHz) for three reasons. The first two are purely practical: The greater ease of generating the desired narrow transmitter and receiver beam patterns and the generally higher scattering levels which can be expected when the surface is rough compared with the acoustical wavelength. The third, more fundamental reason was a desire to operate in a regime which permitted comparison of the experimental results with available theory. The elementary rough surface theory developed earlier [2] assumes facet-like configurations on the surface over distances at least of the order of an acoustic wavelength. It is a theory which should work best in the optical limit and the parameters chosen here at least approach that condition.

The Water Surface

Most of the data were collected at one of two surface roughnesses. They are labelled Wind 4 and Wind 5 in the tabulation. In addition one run was made at a roughness substantially smaller than these, Wind 1, in order to get an idea of the dynamic range of the data acquisition system. These standard surfaces are characterized in Figures 1-9 by their one dimensional statistics (height distribution, temporal autocorrelation, and power spectrum). These were measured using a capacitance wire probe and developmental analog detector. It is recognized, however, that one dimensional statistics cannot shed much light on the mechanism of surface reverberation. The statistic of most interest in modelling surface reverberation is thought to be on involving simultaneous measurement of surface height at spatially separated points, such as the spatial autocorrelation function, 2 dimensional PDF of surface heights, or PDF of surface slopes. The measurement of these statistics at spatial separations on the order of 1 mm. is somewhat tricky, however, and a technique for producing reliable precise results is still being developed. It is clear from the one dimensional PDF of heights that the data presented in this report were taken at "high" Rayleigh parameters. We do not belabor this issue other than to mention it because there seems to be no reason to expect a relationship between Rayleigh parameter and scattering strength as long as the former is substantially larger than unity.

The issue of realism inevitably comes up whenever scale model studies are presented. In this case it is difficult to make a conclusive argument supporting the applicability of the model to ocean

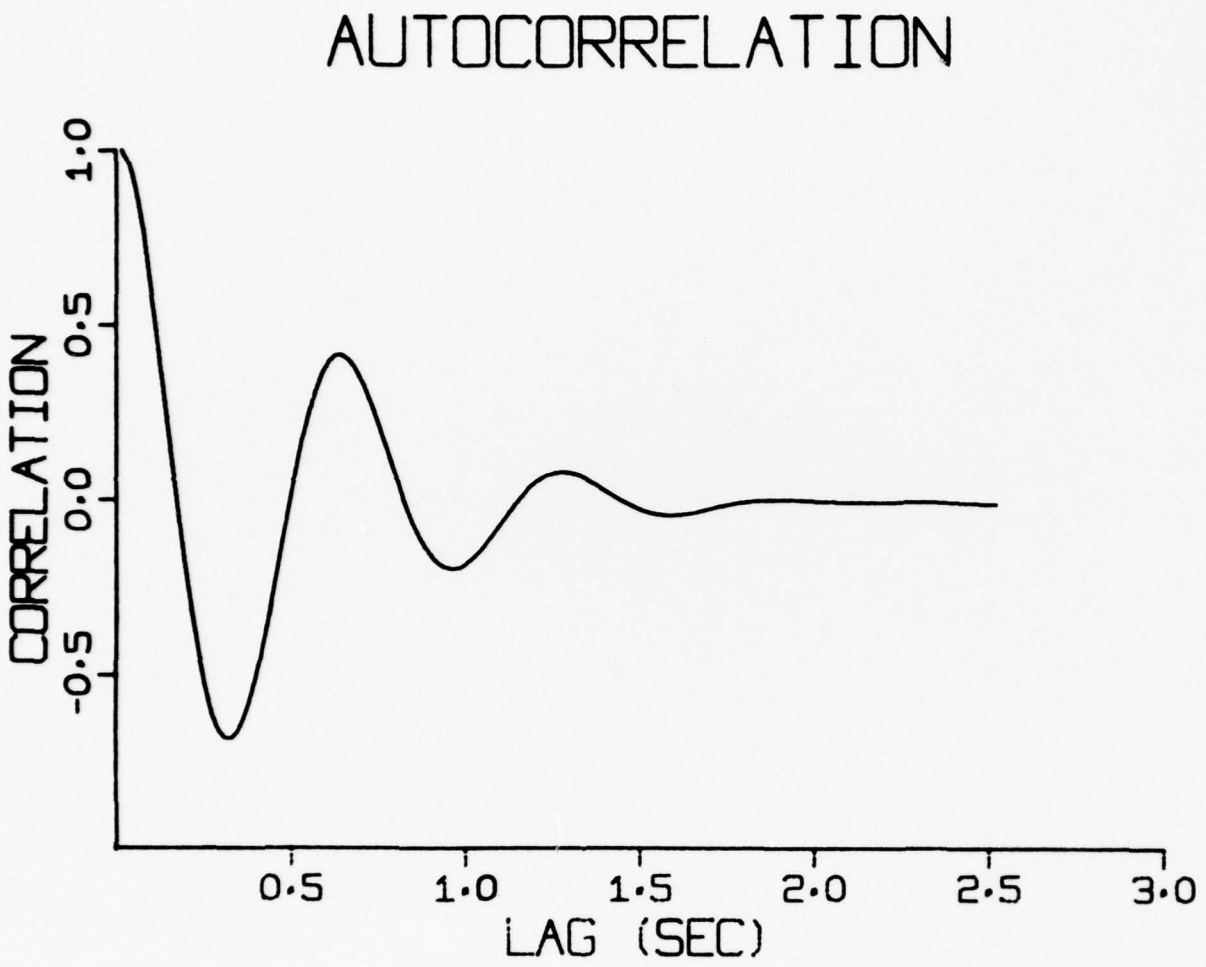

Figure 1: Temporal Auto-correlation Function, Surface due to Wind 5

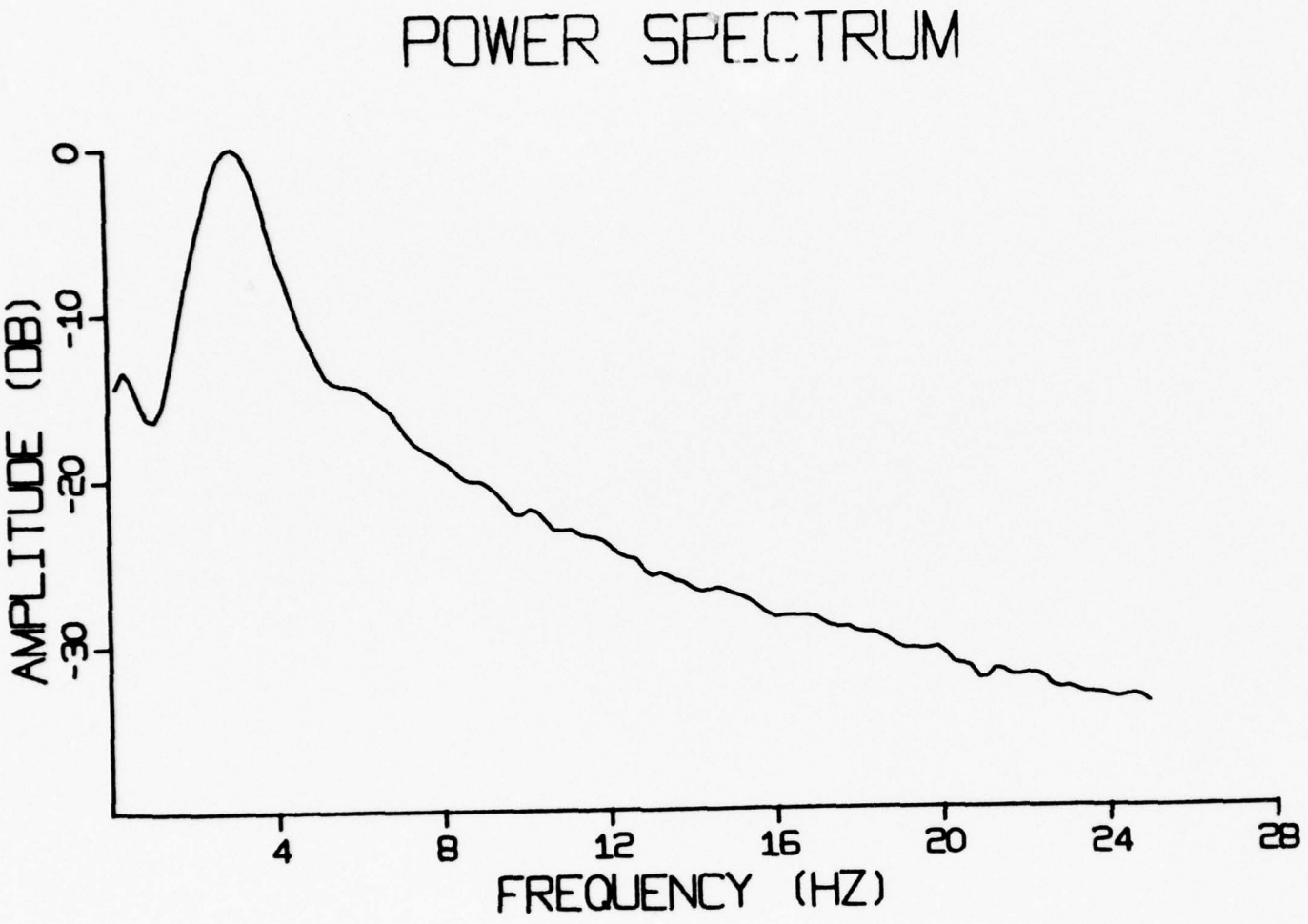

Figure 2: Power Spectrum,

Surface due to Wind 5

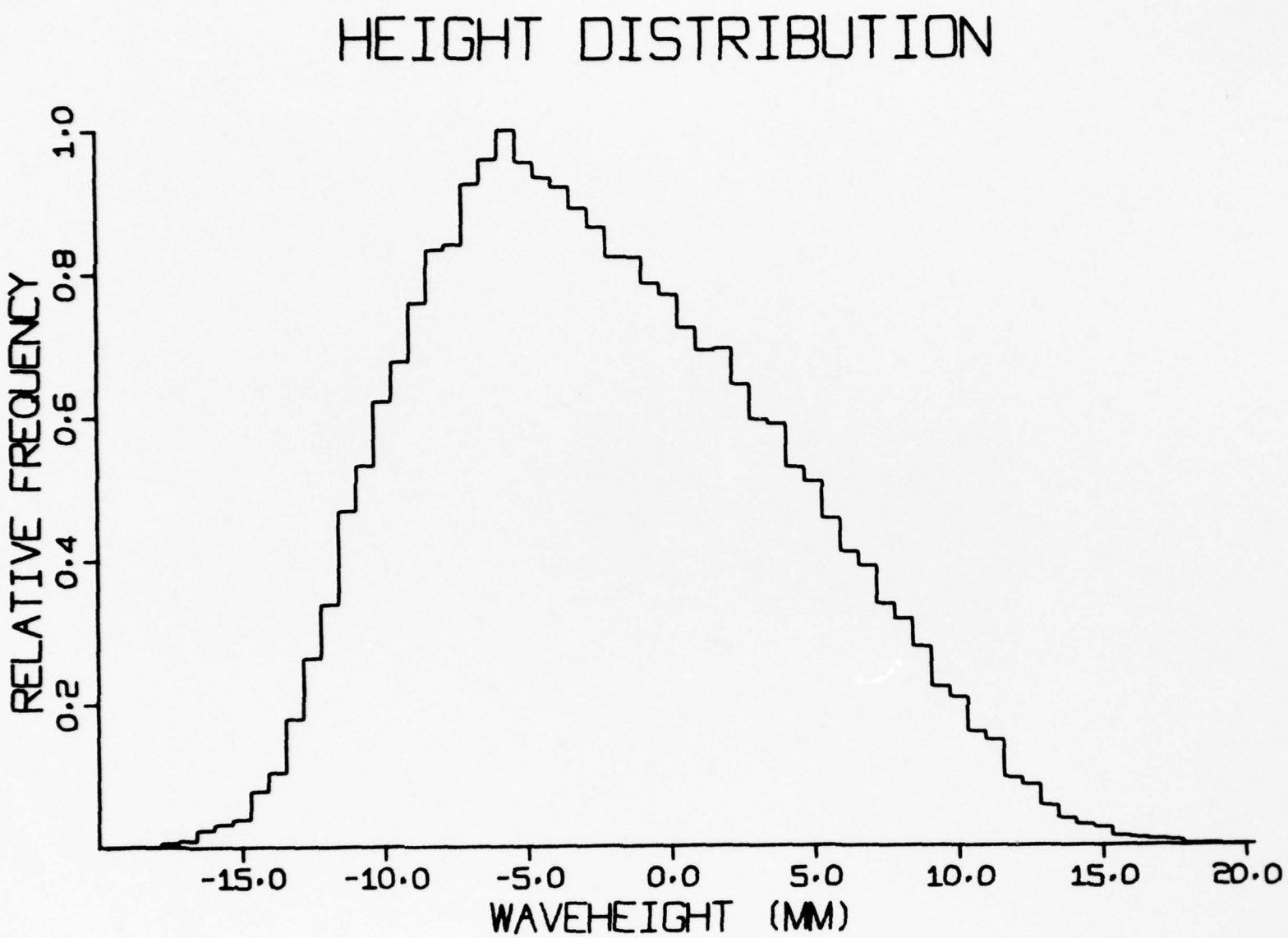

Figure 3: Surface Height Distribution, Wind 5

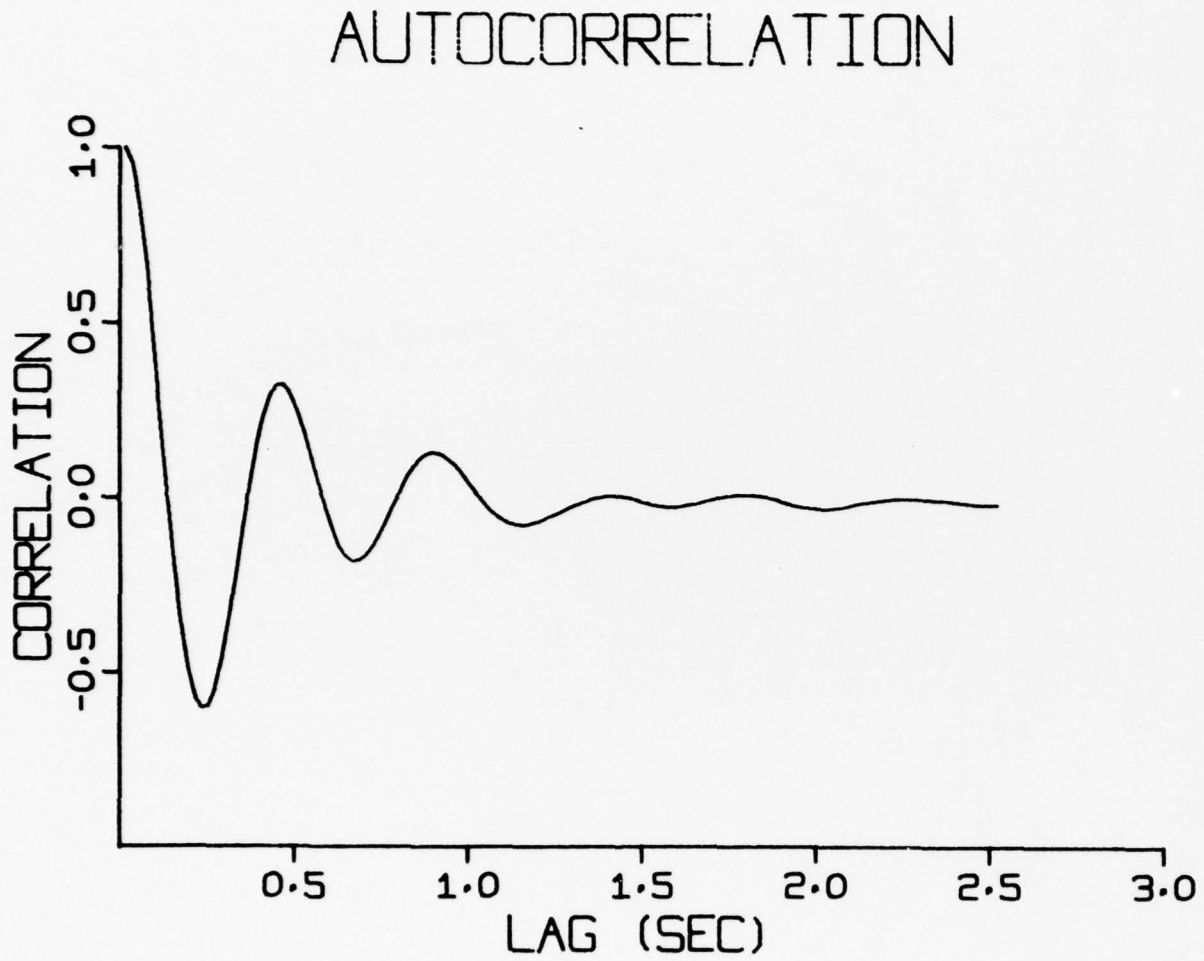

Figure 4: Temporal Auto-correlation Function, Surface due to Wind 4

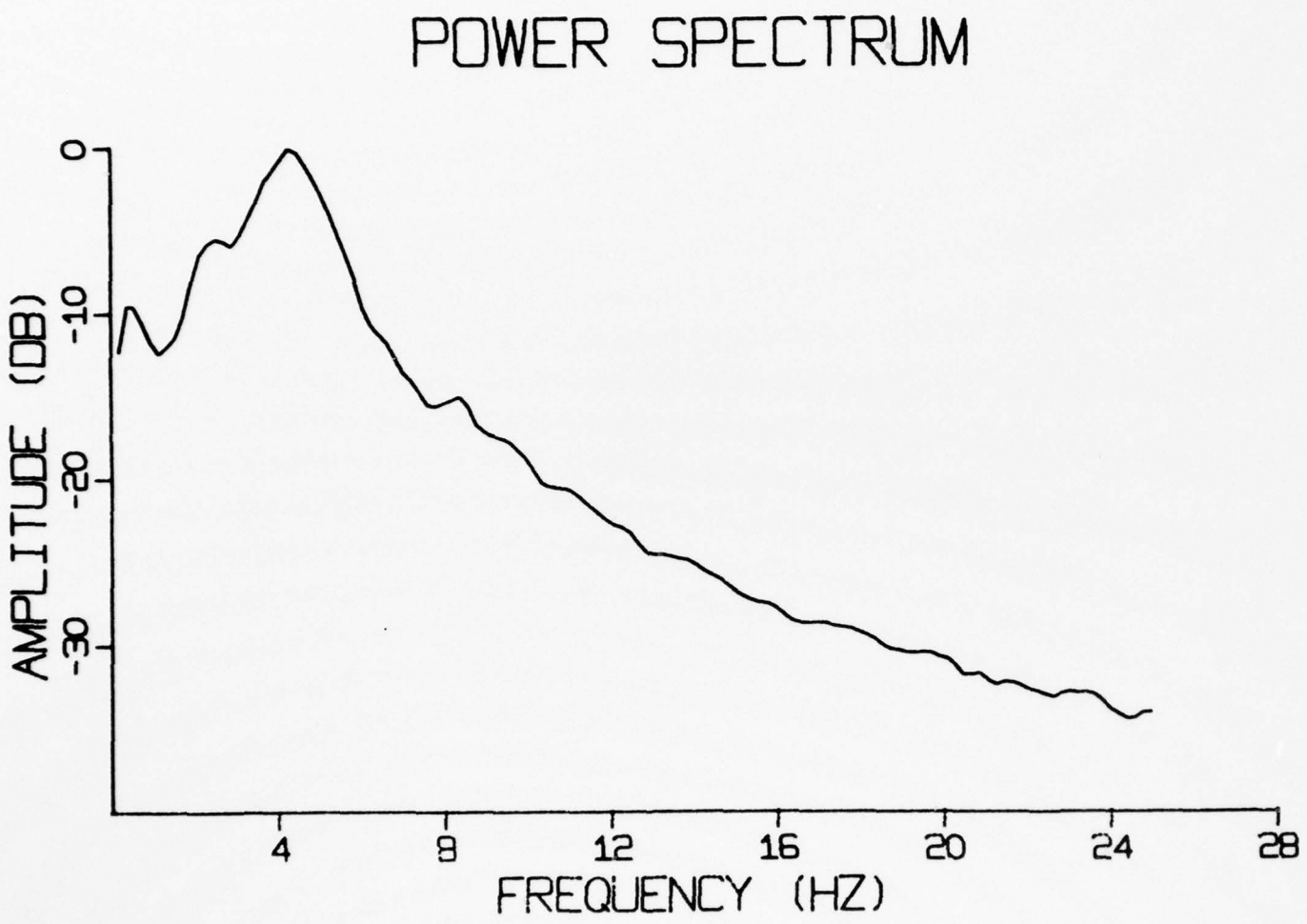

Figure 5: Power Spectrum,

Surface due to Wind 4

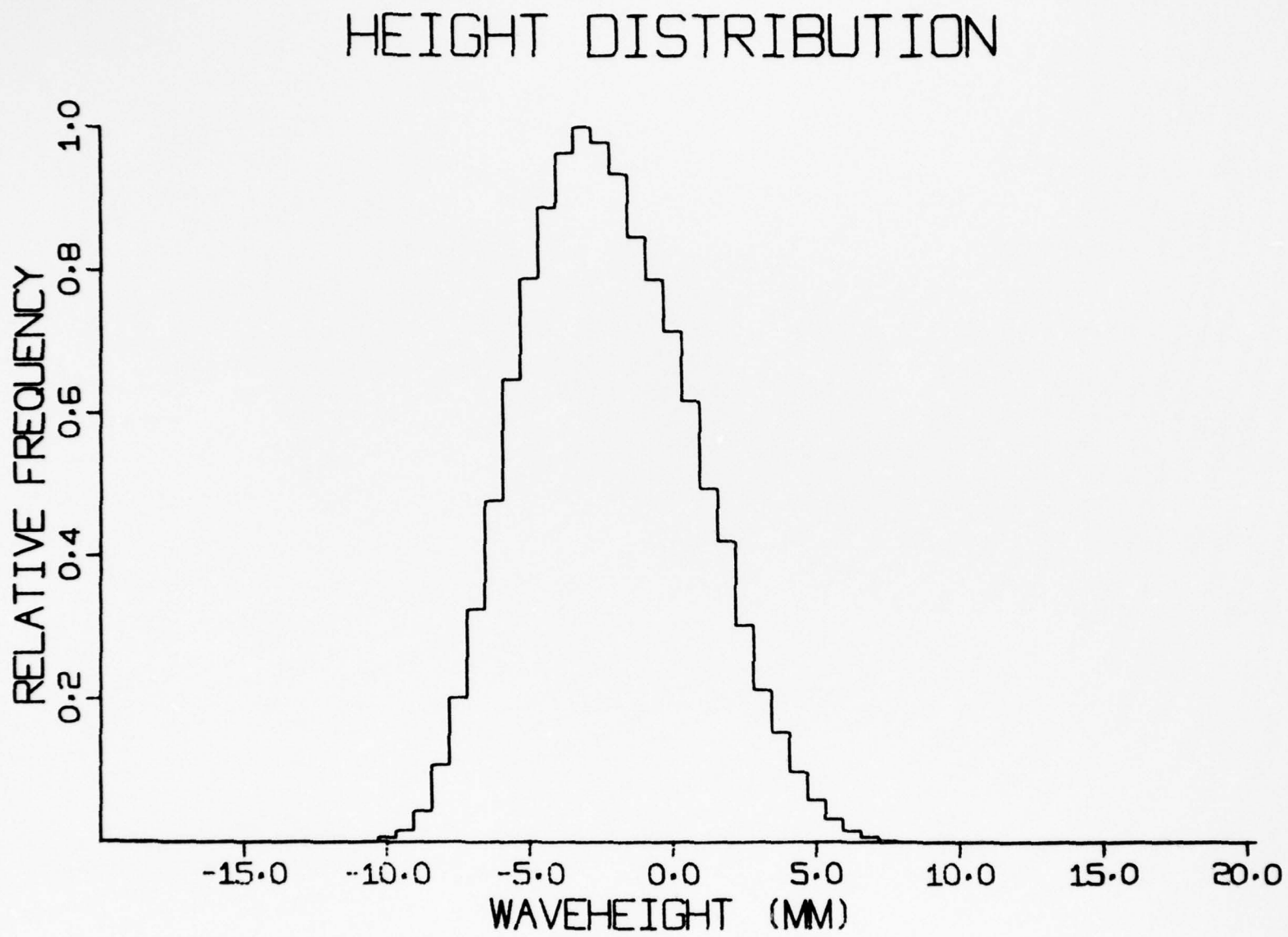

Figure 6: Surface Height Distribution, Wind 4

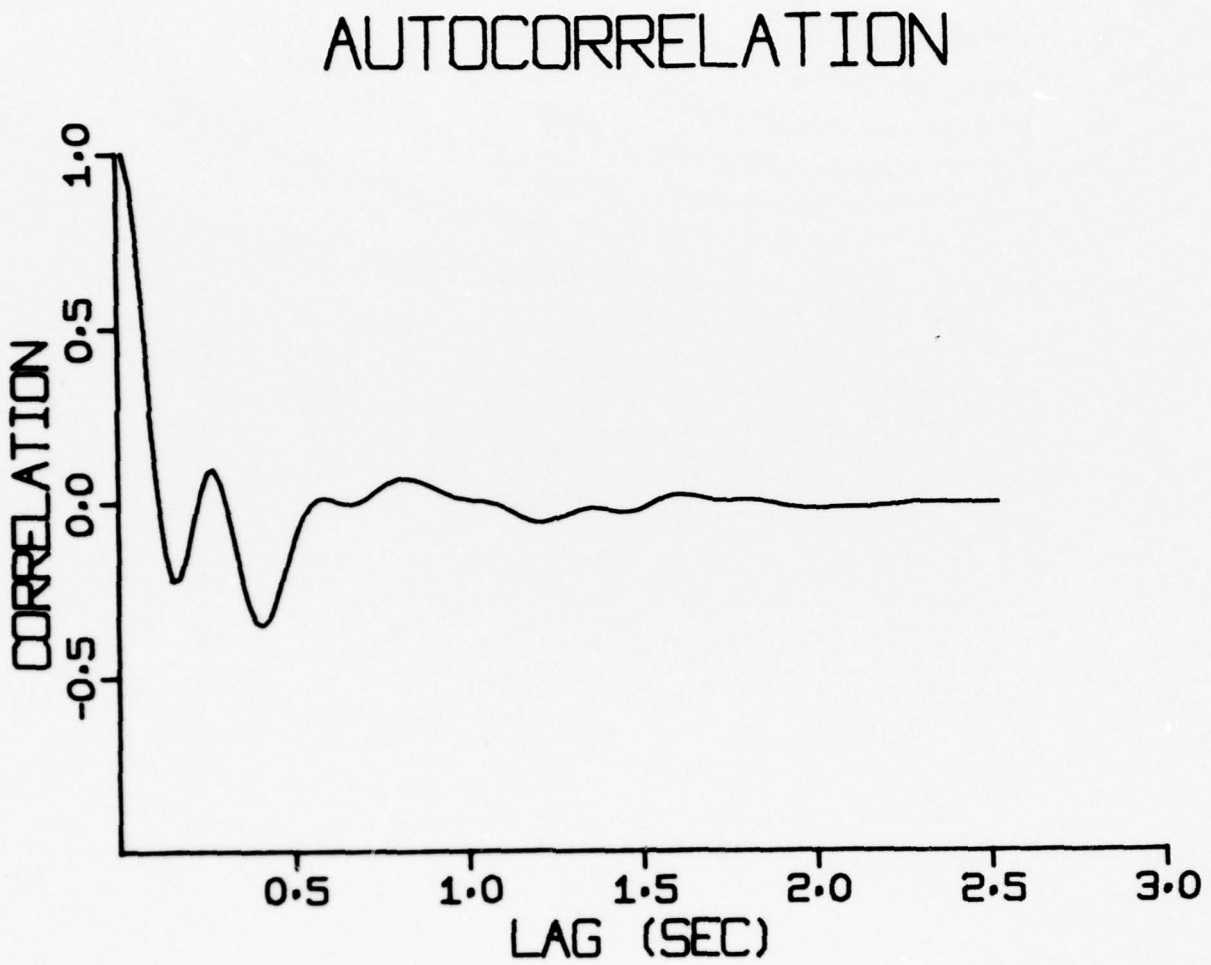

Figure 7: Temporal Auto-correlation Function, Surface due to Wind 1

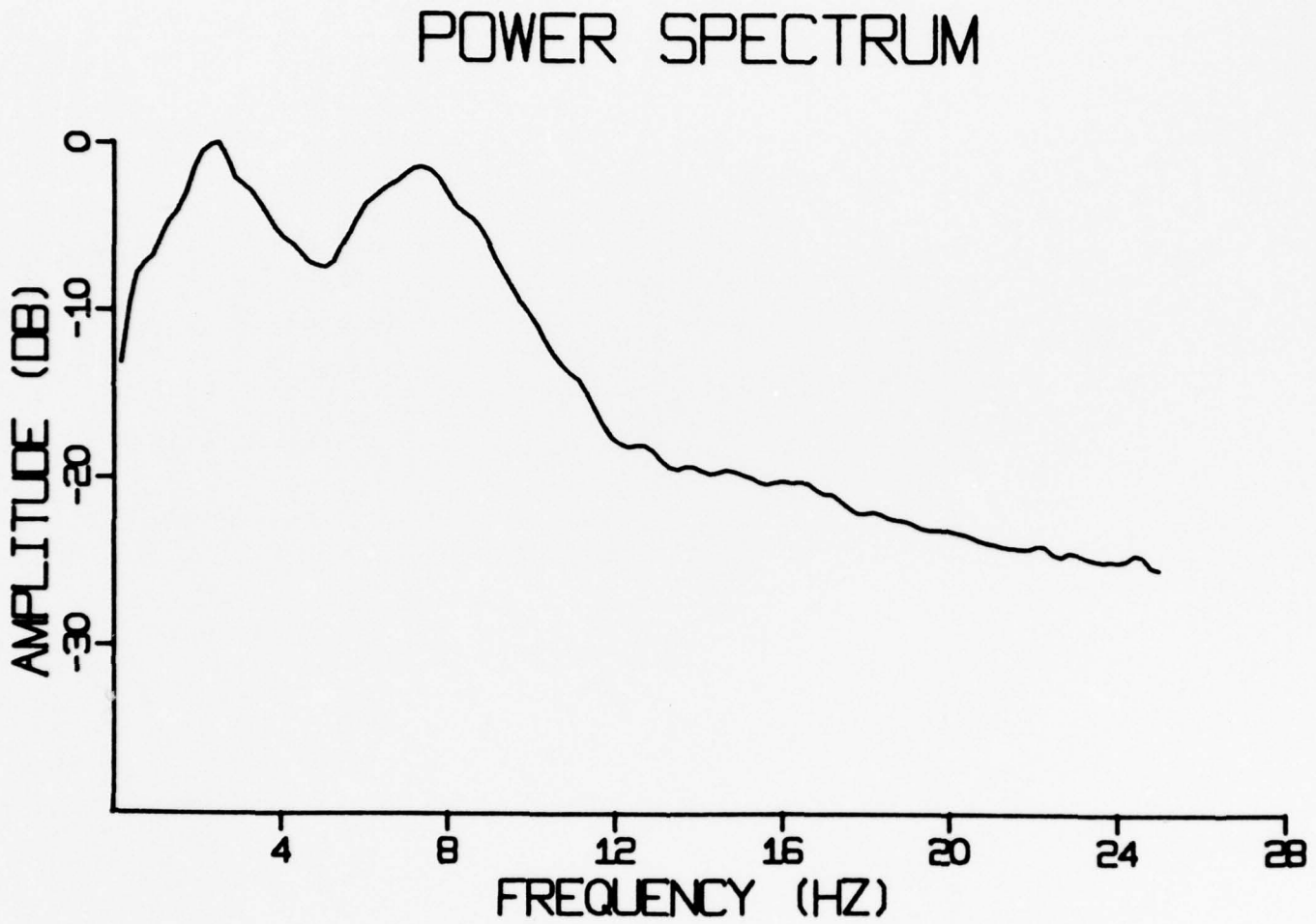

Figure 8: Power Spectrum,

Surface due to Wind 1

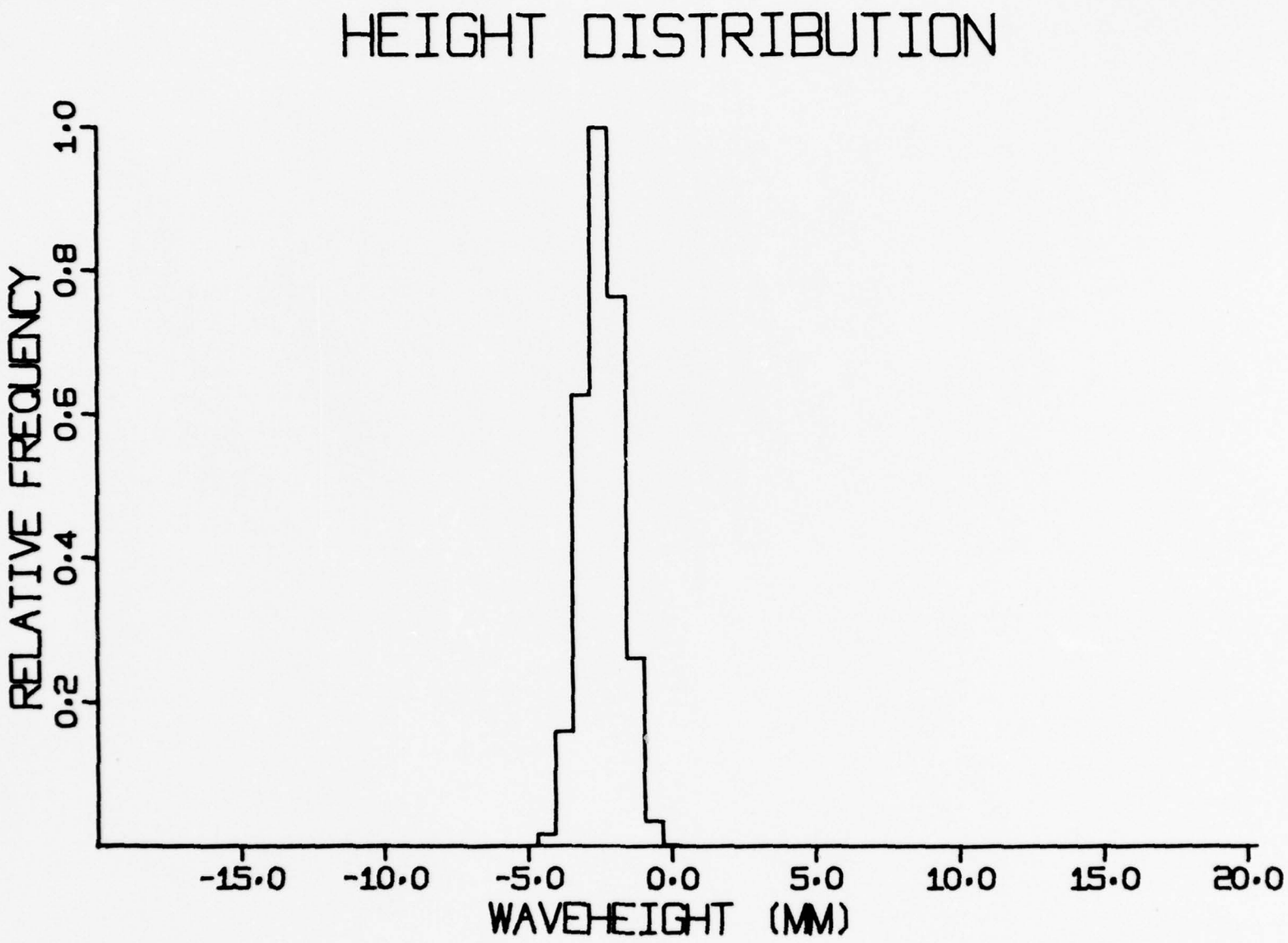

Figure 9: Surface Height Distribution, Wind 1

reverberation prediction. However, a brief inspection of the temporal one dimensional statistics shows them to be not unlike similar ocean statistics [3]. In addition the backscatter reverberation levels measured in this series of experiments are consistent with typical ocean measurements at similar grazing angles. Establishment of a more precise relationship between the model surface and the ocean surface, however, is at present not feasible due to an almost total lack of second order statistical measurements of ocean surfaces from which reverberation has been recorded.

Experimental Procedure

The geometry of the experimental configuration is shown in Fig. 10. θ_0 and θ_1 are the azimuth angles of the beam pattern axes of the projector and receiver respectively. These are measured relative to the wind direction. Similarly ψ_0 and ψ_1 are the grazing angles measured from the horizontal and r_0, r_1 are the ranges from the transducers to an origin on the surface chosen as the point at which the beam pattern axes intersect.

Data were acquired using the apparatus depicted in Fig. 11 by the following procedure:

1) With a smooth surface (no wind) a narrowband probing signal was generated by direct digitization under program control. This signal was amplified and applied to the projector. The signal consisted of a carrier of 1.3 mHz coherently cosine modulated with an envelope duration of 179.2 μsec. (Fig. 12.) The receiver was placed at $\theta_1 = \theta_0 - 180°$, $\psi_1 = \psi_0$ (i.e. on the specularly reflected ray defined by the projector axis), and the receiver acquisition window (time gate) was adjusted so that the received pulse was centered in the window (Fig. 13).

2) A large number of pulses were digitized and the results used to calculate an estimate of average received reference power, P_{ref}, according to

$$P_{ref} = \frac{1}{N} \sum_{n=1}^{N} \sum_{k=k_1}^{k_2} \sum_{i=1}^{256} |S_n(t_i) e^{-j2\pi ki/256}|^2 \qquad (1)$$

This estimate was stable to within .1 dB.

3) At this point the receiver was moved in grazing angle if necessary and the fan was turned on. After the surface had become statisti-

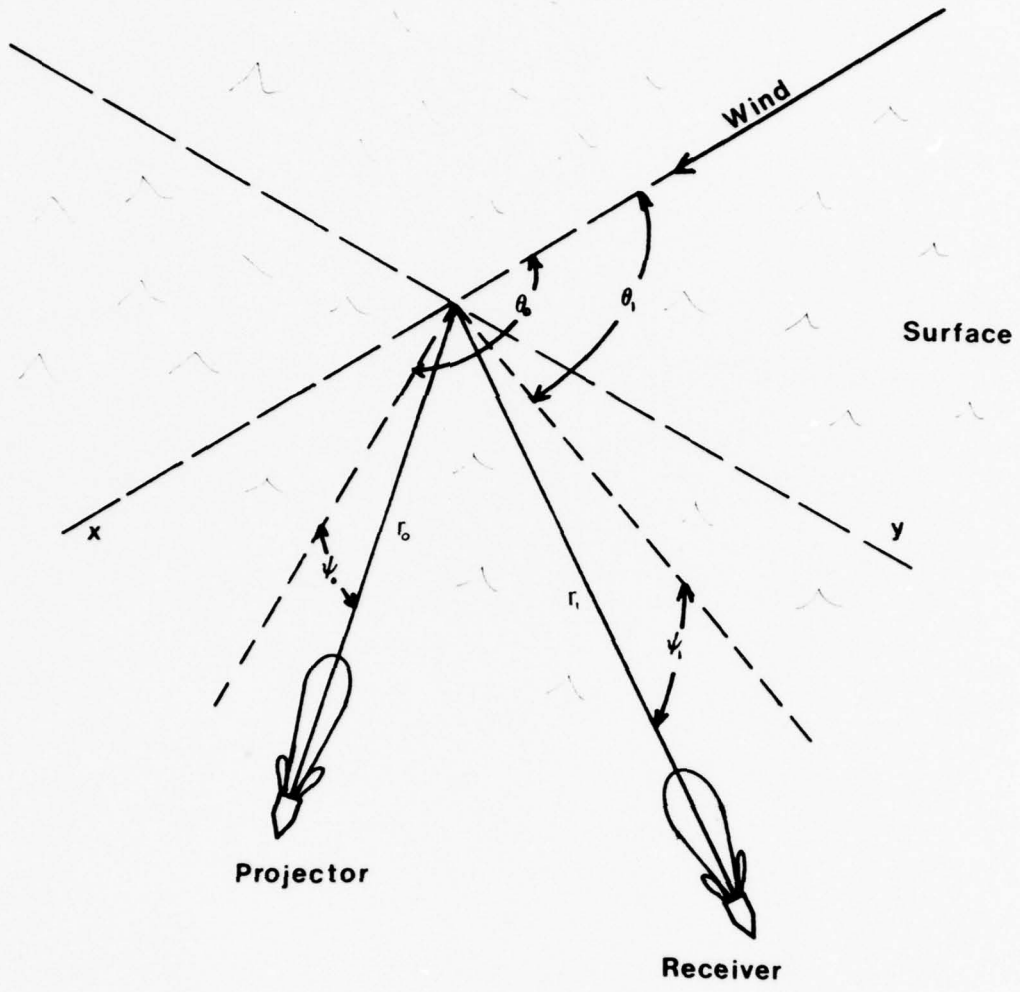

Figure 10: Experimental Geometry

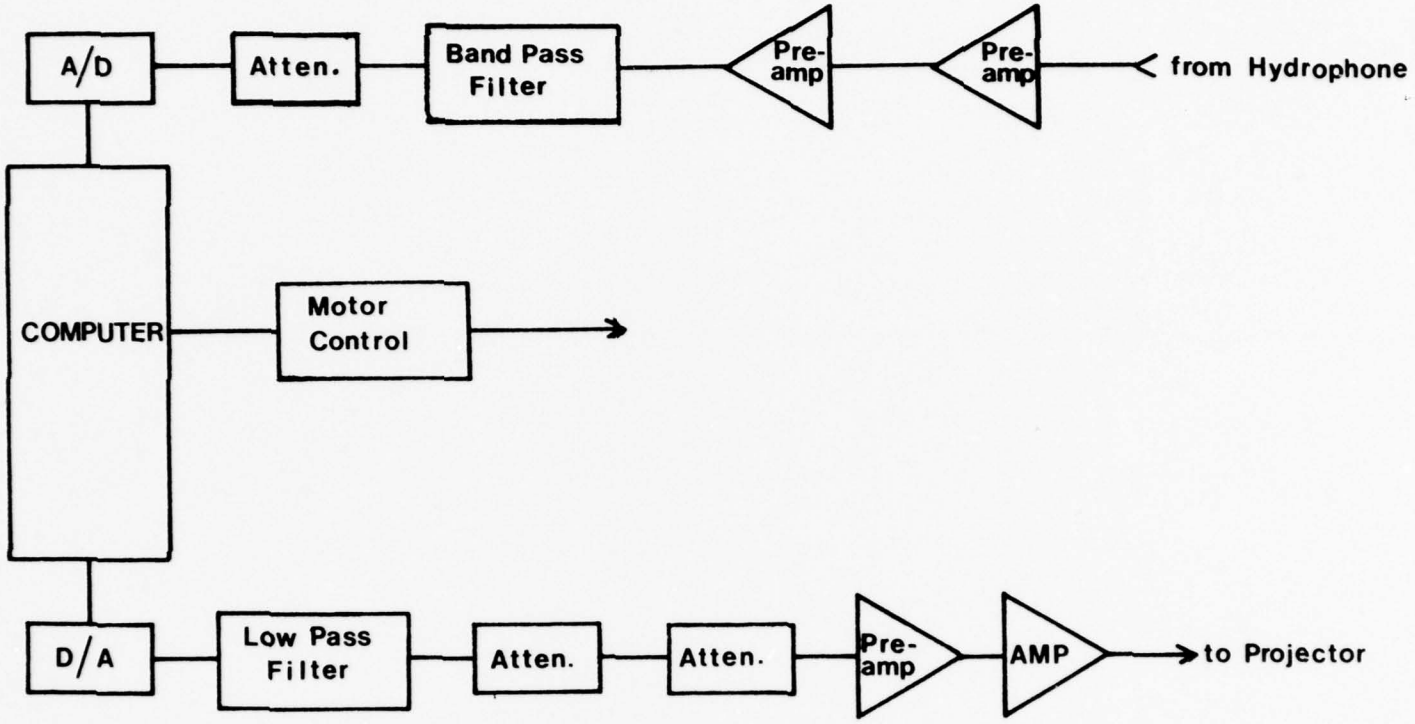

Figure 11: Data Acquisition Apparatus

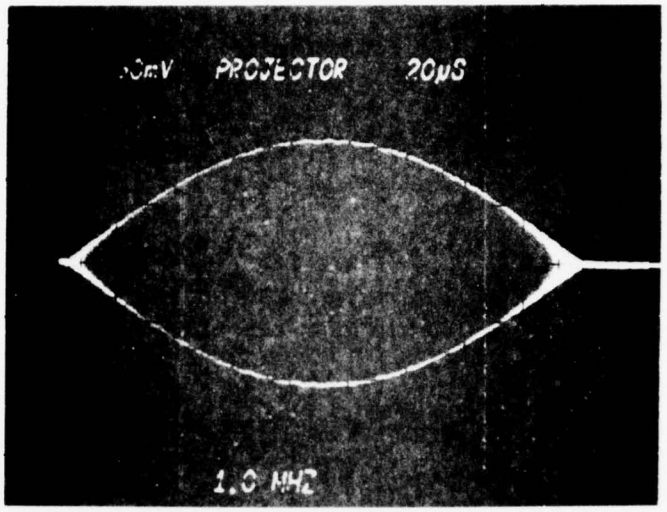

Figure 12: 1.3 mHZ Cosine Envelope Probing Pulse

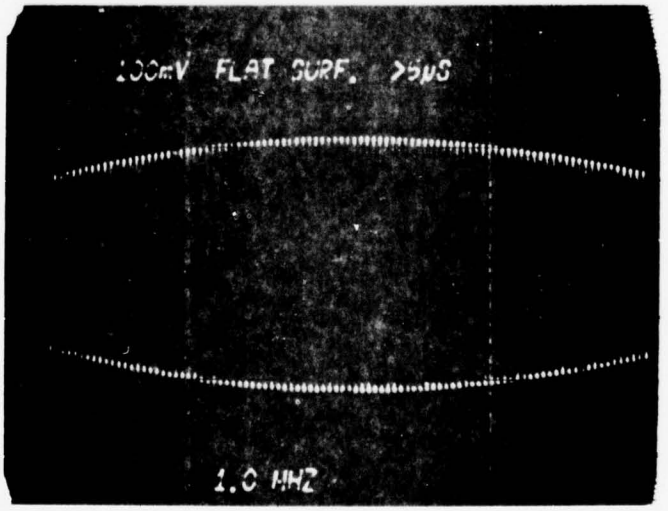

Figure 13: Flat surface received signal

cally stable (3 min.), between 512 and 2048 pulses were digitized at 100 ms. intervals for each of 19 azimuthal receiver orientations (Fig. 14). These digitized responses were transformed, filtered and averaged just as before (1) to obtain the average scattered power, P_{scat}, at each azimuth.

4) The values of P_{scat} and P_{ref} were used to obtain an estimate of the surface scattering strength for each geometry by use of the expression

$$S(\theta_0,\psi_0,\theta_1,\psi_1) = 10 \log \frac{P_{scat}}{P_{ref}} - 10 \log \Delta A + 20 \log \frac{r_0}{1+r_0} \qquad (2)$$

This expression is derived in the next section.

5) Steps 1) through 4) were repeated at a variety of projector locations, winds, grazing angles, and one other carrier frequency (1.1 mHz).

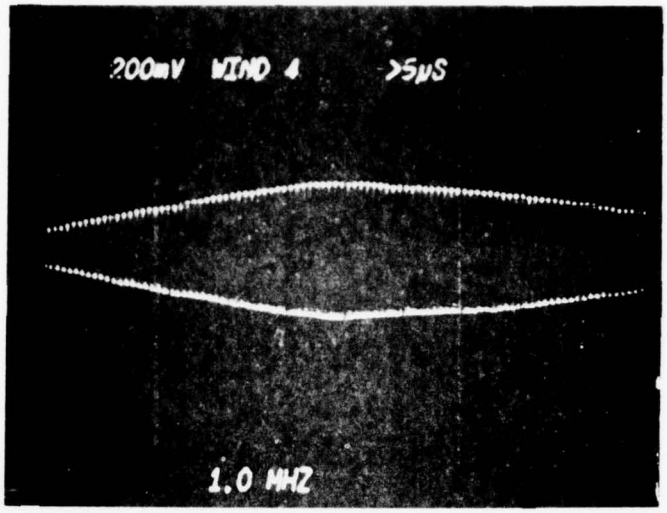

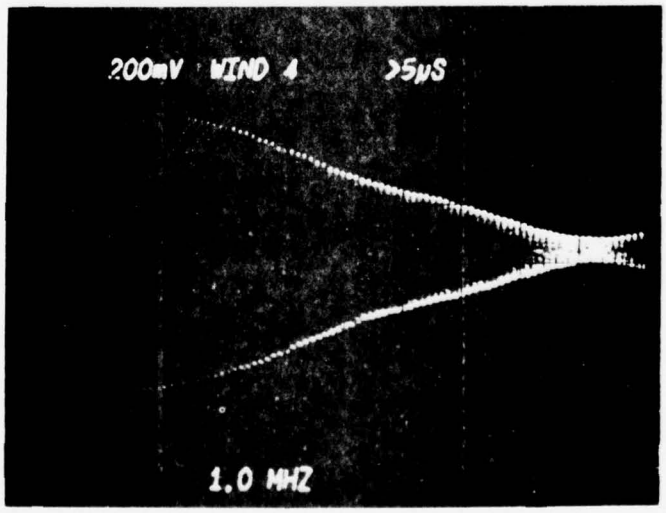

Figure I4: Sample rough surface reverberation

Scattering Strength

Reverberation from rough surfaces is commonly characterized by the scattering strength of the surface defined as:

$$S(\theta_0,\theta_1,\psi_0,\psi_1) = 10 \log \frac{I_1(\theta_1,\psi_1)}{I_0(\theta_0,\psi_0)\Delta A} \tag{3}$$

$I_0(\theta_0,\psi_0)$ is the intensity of the sound wave incident on the surface measured relative to a surface perpendicular to the direction of propagation. $I_1(\theta_1,\psi_1)$ is the intensity of the far field reverberation caused by a unit area ΔA uniformly insonified at intensity $I_0(\theta_0,\psi_0)$ measured at a distance and reduced to an equivalent intensity at one yard. This definition has been used by Urick [4] and Brown and Saenger [5] and is commonly accepted.

In this series of experiments the data produced consist of a set of measurements of P_{ref} and P_{scat} as defined earlier. The measured values of P_{scat}, however, were due to a distinctly non uniform insonification of the surface. In order to obtain the scattering strength from the data a conversion from laboratory power measurements and parameters to the quantities I_1, I_0 and ΔA was performed based on the following:

1) I_0 was obtained from P_{ref} by the following:

$$I_0(\theta_0,\psi_0) = k_1 P_{ref} \frac{(r_1 + r_0)^2}{r_0} \tag{4}$$

where k_1 is the net conversion coefficient of the receiver hydrophone.

2) I_1 was obtained from P_{scat} in a similar way. However, the exact form of the conversion depends upon the spreading law governing

propagation from the surface to the receiver. It is commonly assumed and has been verified by ocean measurements at wavelengths greater than 1 cm that spreading from the surface is spherical around an origin near the surface. In that case the conversion has the form

$$I_1(\theta_1,\psi_1) = k_1 P_{scat} r_1^2 \tag{5}$$

If, however, the acoustic wavelength is shorter than the curvatures of the surface, the interaction becomes that of reflection from small flat facets. In that case, the spreading law remains the same as that of the incident field and the conversion has the form:

$$I_1(\theta_1,\psi_1) = k_1 P_{scat} \frac{r_0 + r_1}{r_0 + 1}^2 \tag{6}$$

Schooley [6] has presented evidence that radii of curvature as small as 1 mm. are extremely rare in wind driven surfaces. This suggested that for the wavelengths used in these experiments (6) might be more nearly valid. As a check on the spreading law, a series of runs at several azimuths were performed. The experiments were conducted with r_1, varying by a factor of 3 to see if there was any dependence of P_{scat}/P_{ref} on r_1 other than that due to the change in insonified area. The results of this series showed no substantial dependence and certainly nothing like the r_1^2 dependence to be expected from (5). Therefore for this series of experiments (6) was used in the computation of scattering strength.

3) ΔA is obtained from the geometry, beam patterns, and timing of the experiment. In the apparatus, the surface is non-uniformly insonified by a projector having a beam pattern projection

$$B_p(x,y;\theta_0,\psi_0,r_0) = I_p(x,y;\theta_0,\psi_0,r_0)/I_p(0,0) \qquad (7)$$

where x,y are horizontal coordinates of a point on the surface. $B_p(x,y)$ is the normalized intensity distribution on the surface as a result of a projector located at $[\theta_0,\psi_0,r_0]$. Similarly the hydrophone is variably sensitive to sound radiated from the surface according to a beam pattern, $B_h(x,y;\theta_1,\psi_1,r_1)$. In addition, for any point on the surface other than the origin a differential path delay exists which shifts any reflection out of the center of the receiver time gate. These three effects give rise to an effective insonification function $\Phi(x,y)$ on the surface which represents the attenuation, compared to reflection from the origin, imposed by the apparatus on reflections occurring at each point on the surface. The validity of this construct is only dependent on a condition of small surface roughness with respect to the dimensions of the insonified region. The effective insonification is defined as

$$\Phi(x,y;\theta_0,\psi_0,r_0,\theta_1,\psi_1,r_0) = B_p(x,y;\theta_0,\psi_0,r_0)B_h(x,y;\theta_1,\psi_1,r_1)\int_0^{T_R} \hat{S}(t-T_D(x,y) + \frac{T_S - T_R}{2})dt \qquad (8)$$

where

$\hat{S}(t)$ is the normalized signal envelope

$T_D(x,y)$ is the differential path delay referred to the specular path, i.e. $T_D(0,0) = 0$

T_R is the duration of the receiver gate

T_S is the duration of $S(t)$

The term $(T_S - T_R)/2$ accounts for the centering of $S(t)$ in the receiver gate. Suppose that the area of significant power in Φ is small enough so that scattering coefficient, absorbtion and spreading loss are approximately uniform over this area. Then it is possible to find a uniformly insonified area, ΔA, on the surface which would produce reverberation of equal level

$$\Delta A = \iint_S \Phi(x,y;\theta_0,\psi_0,r_0,\theta_1,\psi_1,r_1)\,dxdy/\Phi(0,0) \tag{9}$$

Examples of $\Phi(x,y)$ are shown in Figures 15-17 for several geometries. The actual computation of ΔA is difficult analytically and so was carried out numerically for each geometry.

Having obtained I_0, I_1, and ΔA, the computation of scattering strength follows from (3), (4), and (6).

$$S(\theta_0,\psi_0,\theta_1,\psi_1) = 10 \log \frac{k_1 P_{scat} \left(\frac{r_0 + r_1}{r_0 + r_1}\right)^2}{k_1 P_{ref} \left(\frac{r_1 + r_0}{r_0}\right)^2} \tag{10}$$

$$= \log P_{scat} - 10 \log P_{ref} - 10 \log \Delta A + 20 \log \frac{r_0}{r_0 + 1} \tag{11}$$

As was mentioned above the last term in this expression represents the attenuation due to spreading from the surface to the 1 yard standard measurement distance.

We note that the normal definition of scattering strength is only independent of the units chosen if spreading from surface to receiver is proportional to r_1^2. If the spreading law is otherwise, the change

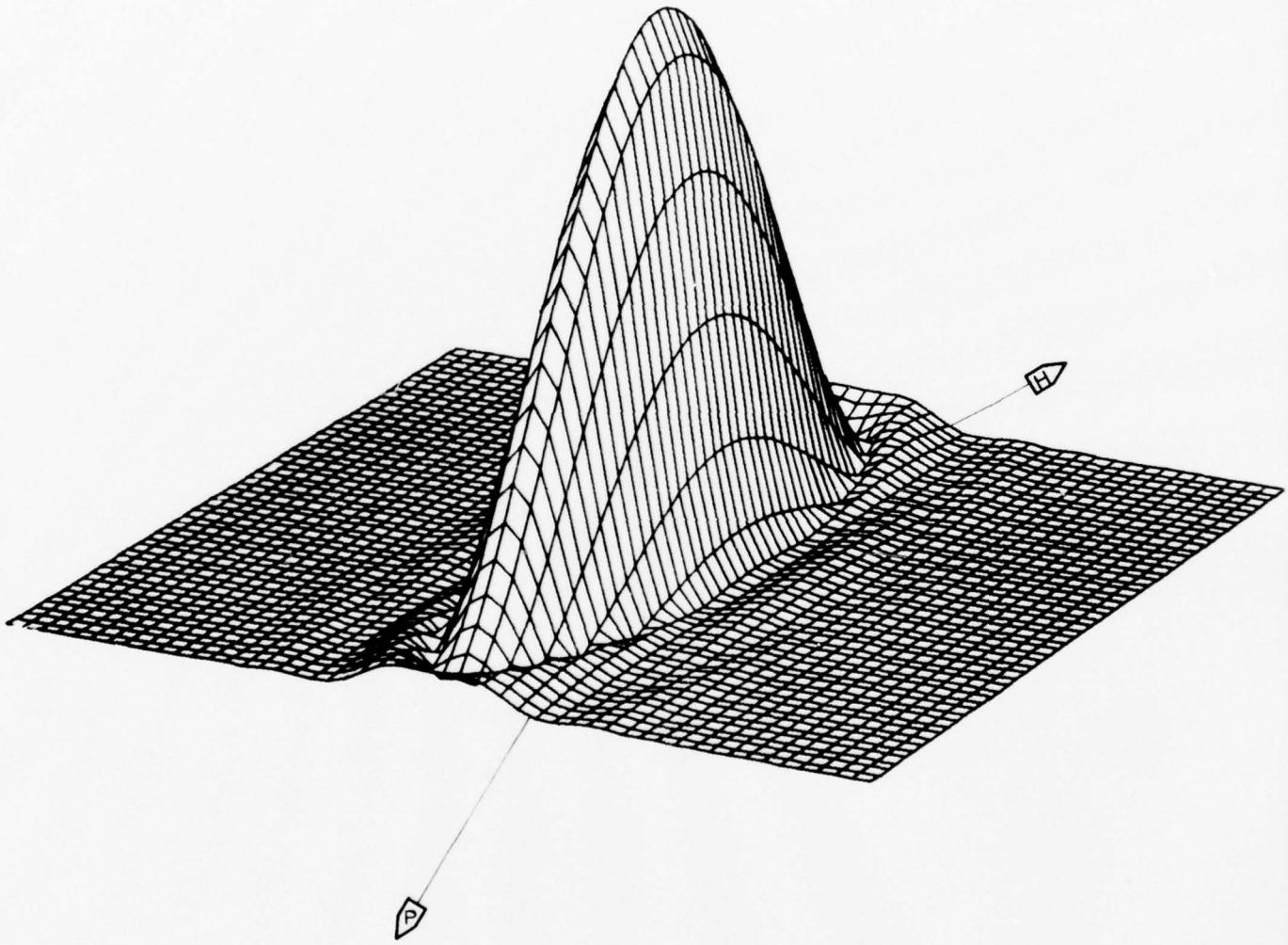

12° 12° 180°

Figure 15: Effective Insonification Function, $\psi_0 = \psi_1 = 12°$, $\theta_0 - \theta_1 = 180°$

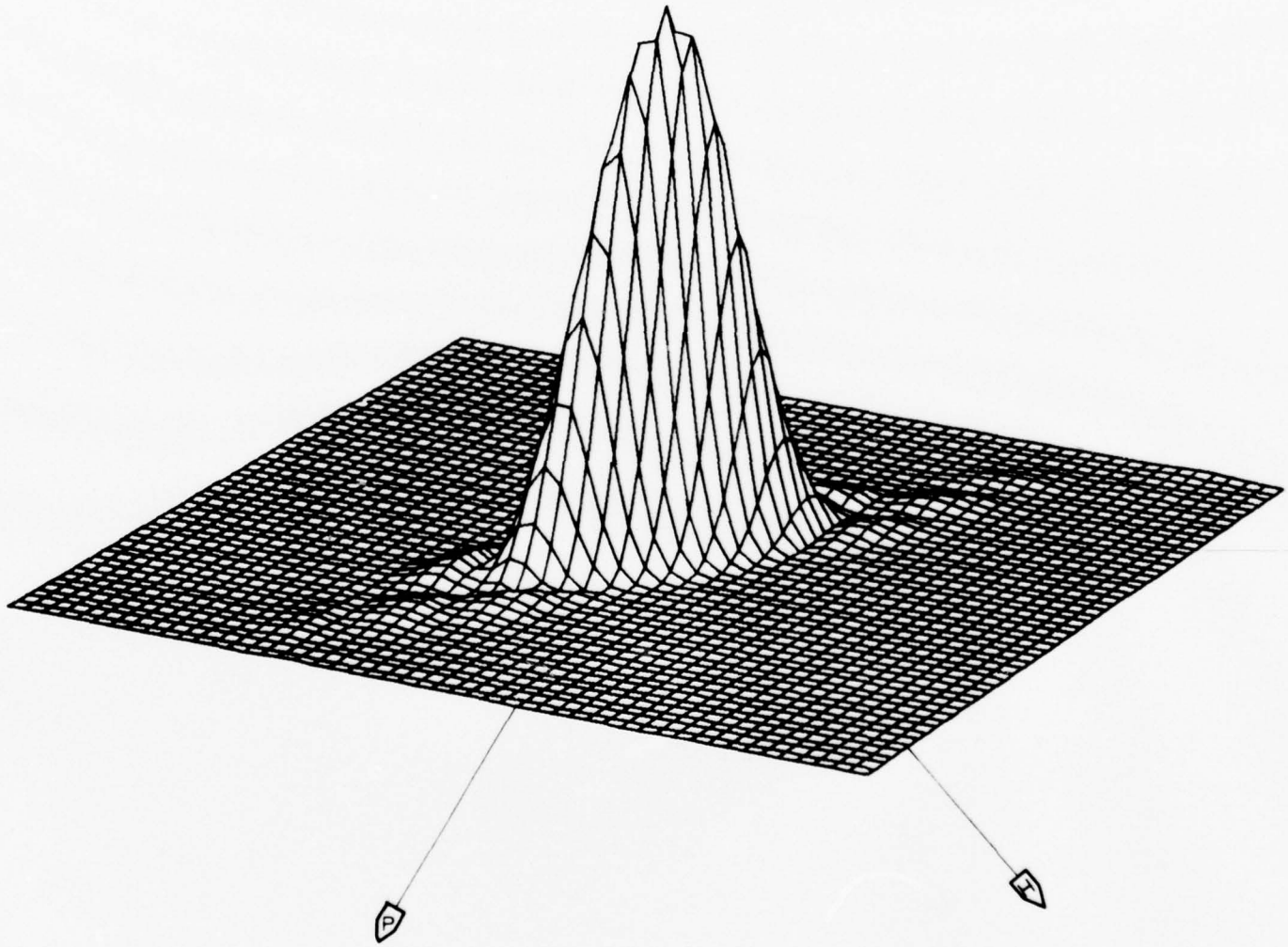

Figure 16: Effective Insonification Function, $\psi_0 = \psi_1 = 12°$, $\theta_0 - \theta_1 = 120°$

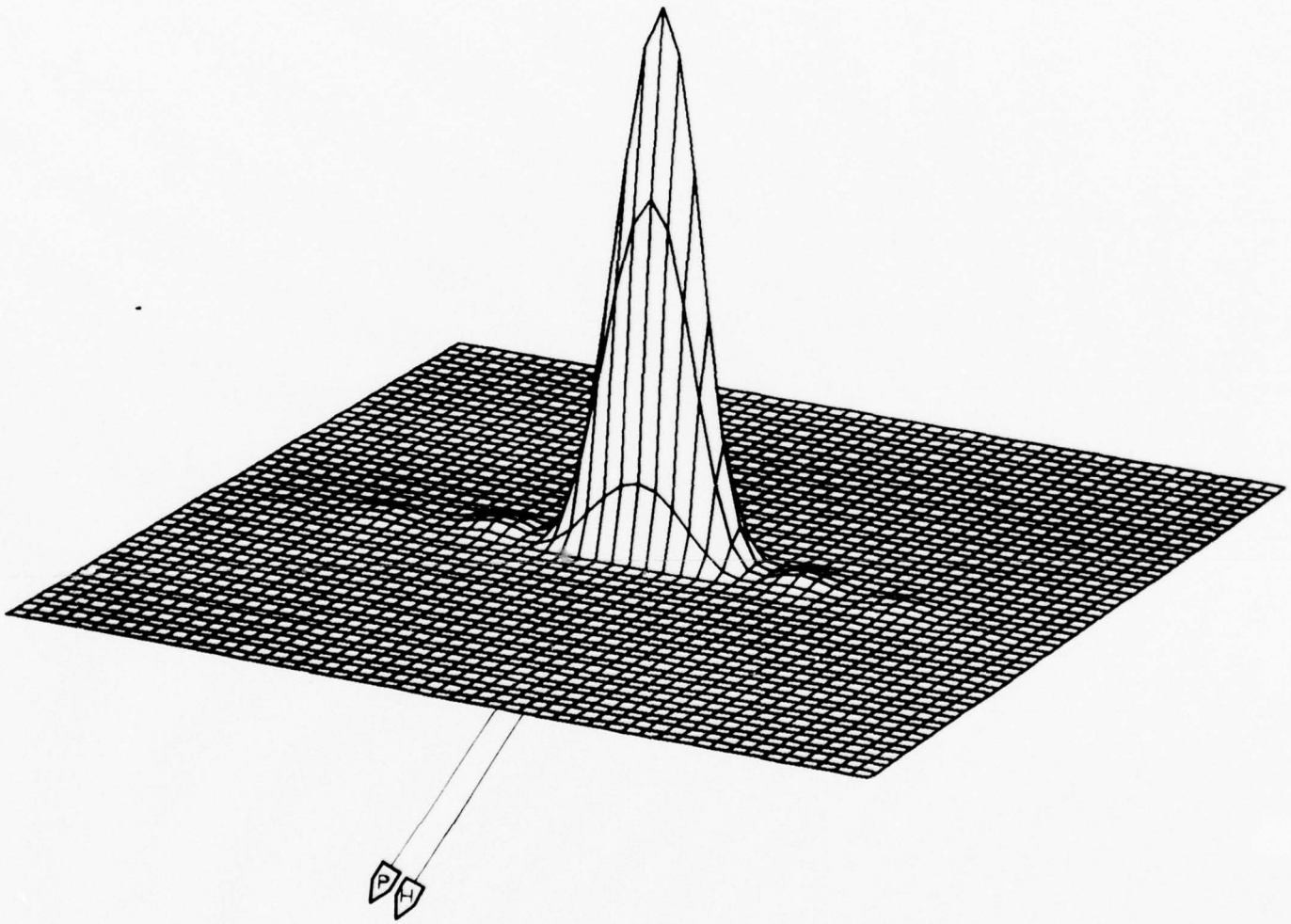

Figure 17: Effective Insonification Function, $\psi_0 = \psi_1 = 12°$, $\theta_0 - \theta_1 = 0°$

in ΔA produced by a change of units is not compensated for by an equivalent change in the adjustment for receiver range. This unfortunate aspect of the definition of scattering strength, while probably not of great importance in ocean applications, should be kept in mind whenever short wavelengths are used.

Experimental Results

The experimental measurements of scattering strength are presented as Appendices A. and B. Each figure represents a scan in azimuth of the receiver hydrophone for a particular set of geometrical parameters other than θ_1 and a fixed wind speed. The plots of scattering strength given in App. A. are supplemented by tabulations of the same data given in App. B.

Except for two cases the azimuthal scans were taken at 10° degree increments over a range of 180°. An estimate of the statistical uncertainty in the data is indicated by error bars. The residual system noise mapped onto scattering strength coordinates is of course variable as a function of system geometry. The worst case noise, however, is never more than -80 dB. equivalent scattering strength. The system noise is due primarily to electrical noise in the preamplifier. These data may be grouped into 5 sets of 5 scans each, plus two single runs taken as system checks. Each set consists of a scan in azimuth of the receiver for each of 5 projector angles ranging from facing downwind (360°) to facing upwind (180°). The parameters for the 5 sets are summarized in the appendices.

The general appearance of the results is rather uniform across sets. As one would expect the scattering strength falls off rapidly from a peak at $\theta_0 - \theta_1 = 180°$. At approximately $\theta_0 - \theta_1 = 120°$ a plateau is reached which then rises or falls depending on the orientation with respect to the wind as the bistatic azimuthal angle decreases. The most striking feature of the results is this dependence on wind direction. Both the form and magnitude of the dependence on bi-

static angle is a function of wind direction. In the case $\theta_0 = 270°$, for example, scattering strength decreases with decreasing bistatic angle to a minimum of backscatter. At $\theta_0 = 315°$, on the other hand, the minimum is at roughly $\theta_0 - \theta_1 = 90°$ and there is a strong increase in scattering strength as the receiver approaches the projector. For a fixed geometry the scattering strength was observed to vary as much as 25 dB with wind direction.

In addition to the basic 5 sets of measurements, two scans were made to investigate sensitivity to wind speed and acoustic frequency. The first of these, shown as Fig. A-26, is a scan made to verify that a small change in incident acoustic wavelength produces no change in observed scattering strength. Comparison with Fig. A-2 shows that this is the case. The second (Fig. A-27) was a scan at a very low value of roughness to verify that scattering strength continues to fall off as a function of surface roughness. In this case the reverberation at other than near-forward bistatic angles was too low to be accurately measured.

As a result of these experiments a number of specific observations have been compiled.

1) Scattering strength is strongly dependent on wind direction. As was pointed out above the way in which this dependence manifests itself is somewhat complex. However, in general it can be said that for a given grazing angle and incident acoustic wavelength, the wind driven surface scatters much more strongly upwind than downwind. Crosswind scattering is only slightly weaker than downwind.

2) In general scattering strengths measured for equal values of

$(\theta_0 + \theta_1)/2$ are equal. This observation is consistent with the idea that the mechanism of scattering is facet reflection in that the orientation of the normal to a facet for best reflection from θ_0 to θ_1 is $(\theta_0 + \theta_1)/2$. This observation together with the first tends to suggest a model of the surface constructed in terms of a distribution of facet sizes and orientations. Such a model is not presently available.

3) Over the range of grazing angles observed (12° - 17°) scattering strength is not a strong function of grazing angle. This is consistent with ocean measurements indicating that backscattering strength does not fall off rapidly until grazing angles below 10° are encountered. This observation tends to indicate that the probability density of slopes or of significant facet occurrence is relatively smoothly varying. As yet no slopes of the requisite values have been measured directly.

4) Asymetry in receiver and projector grazing angles had little or no effect on measured scattering strength. It was to be expected that the mixed grazing angle cases, (12°, 17°) and (17°, 12°) would resemble quite closely those at equal grazing angles.

5) At the wavelengths at which this series of experiments was performed scattering strength is not a strong function of acoustic wavelength. This observation is based on a comparison of Fig. A-2 and Fig. A-26 and is consistent with the quasi-optical notion of reflection from facets. It is interesting that the agreement of these two runs was nearly exact in spite of a substantial difference in the value of ΔA used in the computation of scattering strength.

6) Scattering strength is a strong function of surface roughness. Except for near-forward orientation of the receiver, the scattering strengths observed at Wind 5, Figures A-21 to A-25 are generally in excess of 10 dB higher than those observed at Wind 4. The change in roughness in this case was produced by an increase in local wind speed. This tends to produce an increase in RMS waveheight due to chop or sea as opposed to swell. Therefore it would be dangerous to make general conclusions about the nature of the dependence of scattering strength on roughness in the ocean on the basis of this observation alone.

7) At a very low wind speed (Wind 1) the scattering strength at bistatic angles less than 120° became unobservable. The point of performing the scan at Wind 1 (Figure A-27) was to demonstrate that scattering strength at such low wind speeds was extremely low. No other conclusions are drawn from this data.

It is evident from the above that the Rayleigh parameter alone is not sufficient to predict surface scattering strength. This commonly used scalar index of apparent surface roughness is a function of acoustic wavelength, RMS waveheight, and grazing angle. From the above observations it is evident that bistatic scattering strength at high frequencies, while certainly a function of waveheight, is not strongly dependent on either acoustic wavelength or grazing angle. Indeed, it seems reasonable to expect that it is not directly a function of RMS waveheight, but of some second order spatial statistic such as RMS slope, slope PDF, or correlation distance.

Discussion

The experiments reported here have dealt with the spatial variation of surface scattering strength at high frequencies. As pointed out in the introduction, a primary reason for the choice of high frequencies was the opportunity to check the results with available theory. This objective has not yet been reached. The basic conclusion of the theory developed in [2] is that scattering levels for any set of bistatic angles depends on the existence of surface facets oriented properly for the reflection of energy from projector to receiver. If the surface is Gaussian in two dimensions (which has frequently been assumed) it is a simple matter to relate the surface slope probability density (also Gaussian) to the RMS waveheight. For the case of back scatter and upwind transmission one finds specifically

$$\frac{\text{Back scattered power}}{\text{Forward scattered power}} = e^{-\frac{\cot^2 \psi_0}{2S^2}} \qquad (12)$$

where S^2 is the mean square slope of the surface in the wind direction. Even with the roughest surface used in the experiments (or imaginable in practice) this yields backscatter levels many orders of magnitude below those observed. There is a great deal of evidence (both from ocean and model tank measurements) that the one dimensional distribution, while not precisely Gaussian, is at least reasonably close to Gaussian. Much less is known about the two dimensional surface statistics and drastic deviations from Gaussian behavior can at least not be ruled out on the basis of existing evidence. Perhaps more fundamentally, it is becoming clear that scattering depends critically

on small features of the surface (which generate locally high slopes) but whose effect on the probability density could be very minor. Direct measurements of slope statistics are therefore essential and a program towards that end has been initiated. Initial measurements with the newly constructed slope probe are encouraging to the extent that they indicate much higher probabilities for relatively large values of slope than one would have anticipated from the Gaussian model. However, they have not yielded positive probabilities for slopes of the order of magnitude which would be required to generate backscatter. This is not surprising if one considers the levels of probability involved. Even under the roughest surface conditions backscattering strength is of the order of -30 db. Even if the scattering mechanism is precisely the facet-like reflection postulated by the theory, only a minute fraction of the surface would have to exhibit the proper orientation at any given instant in order to account for the scattered power actually observed. At the particular location of the slope probe the occurrance of the required slope will therefore be a very rare event indeed and one which has not so far been observed. Efforts to obtain reliable slope measurements in this difficult region will certainly continue. Even if they prove unsuccessful, it should be possible to check theory against experiment by working at somewhat larger grazing angles (perhaps 30°) where the required slopes are much smaller (and hence more probable) so that the collection of meaningful slope statistics should not be excessively difficult.

From the practical point of view, looking towards ocean applications, one is of course less interested in the optical limit of fre-

quencies than in signals with wavelengths comparable to or larger than the surface roughness. Plans for the next series of measurements call for the use of frequencies of the order of 200 KHz or less, hence wavelengths of the order of 1 cm. Transducers suitable for use in that frequency range are available and they will be installed when planned experiments with the high frequency transducers have been completed.

References

1. J. G. Zornig and J. F. McDonald, "Direct Measurement of Surface-Scatter Channel Coherence by Impulse Probing," J. Acoust. Soc. Am. 55, 1205-1211 (1974).

2. P. M. Schultheiss, J. Snyder, H. Tung and J. Zornig, "Acoustic Scattering from a Wind Driven Water Surface," Final Report under ONR Contract N00014-75-C-1014, Dept. of E. & A. S., Yale U. (1976).

3. C. L. Bretschneider, "A One-Dimensional Gravity Wave Spectrum," in Ocean Wave Spectra, Proceedings of a Conference (Prentice-Hall, 1963) p. 41.

4. R. J. Urick, "Principles of Underwater Sound for Engineers," (McGraw-Hill, 1967) pp. 188-189.

5. M. V. Brown and R. A. Saenger, "Bistatic Backscattering of Low-Frequency Underwater Sound from the Ocean Surface," J. Acoust. Soc. Amer. 52, 944-960 (1972).

6. A. H. Schooley, "Curvature Distributions of Wind-Created Water Waves," Trans. Amer. Geo. Un. 36, (1955), p. 273-278.

Appendix A: Scattering Strength Plots

This appendix contains 27 plots of scattering strength vs. receiver azimuth measured as described in the text. The fixed parameters are annotated on the top right of each plot. Statistical uncertainty in the measurements is estimated to be roughly as indicated by the error bars. The effect of system noise is in no case greater than an equivalent scattering strength of -80 dB. The first 25 figures of this appendix are organized according to the following scheme:

Figure A-	Wind #	Projector Grazing Angle	Receiver Grazing Angle
1 - 5	4	12°	12°
6 - 10	4	17°	17°
11 - 15	4	12°	17°
16 - 20	4	17°	12°
20 - 25	5	12°	12°

Each group of 5 figures consists of a repetition of the basic 180° scan in receiver azimuth for each of 5 projector azimuths (180°, 225°, 270°, 315°, 360°).

Figure 26 is a repetition of the geometry of Figure 2 at a carrier frequency of 1.1 mHz.

Figure 27 is a repetition of the geometry of Figure 3 at Wind 2.

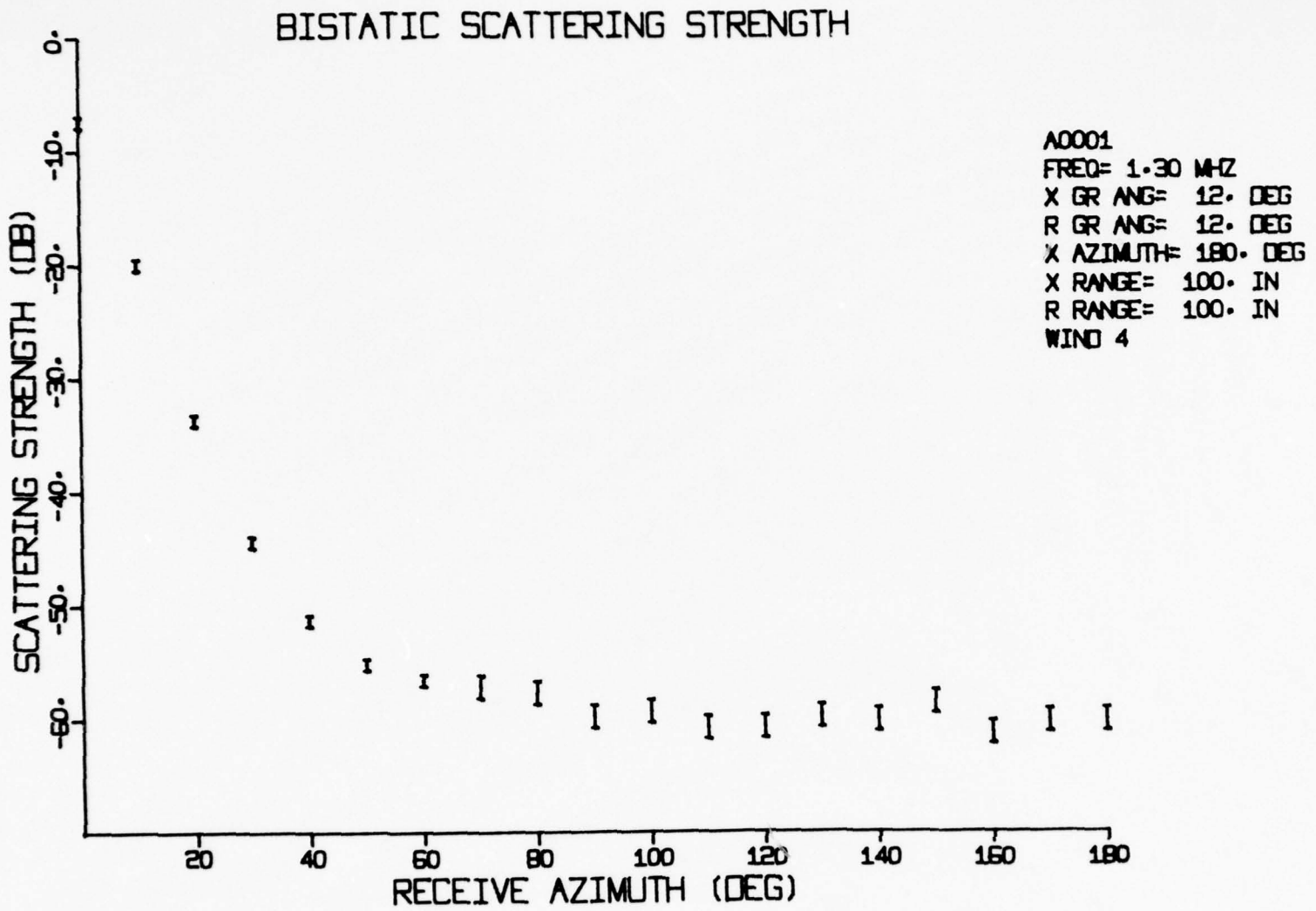
BISTATIC SCATTERING STRENGTH
A0001
FREQ= 1.30 MHZ
X GR ANG= 12. DEG
R GR ANG= 12. DEG
X AZIMUTH= 180. DEG
X RANGE= 100. IN
R RANGE= 100. IN
WIND 4
SCATTERING STRENGTH (DB)
0.
-10.
-20.
-30.
-40.
-50.
-60.
20
40
60
80
100
120
140
160
180
RECEIVE AZIMUTH (DEG)

Figure A-1

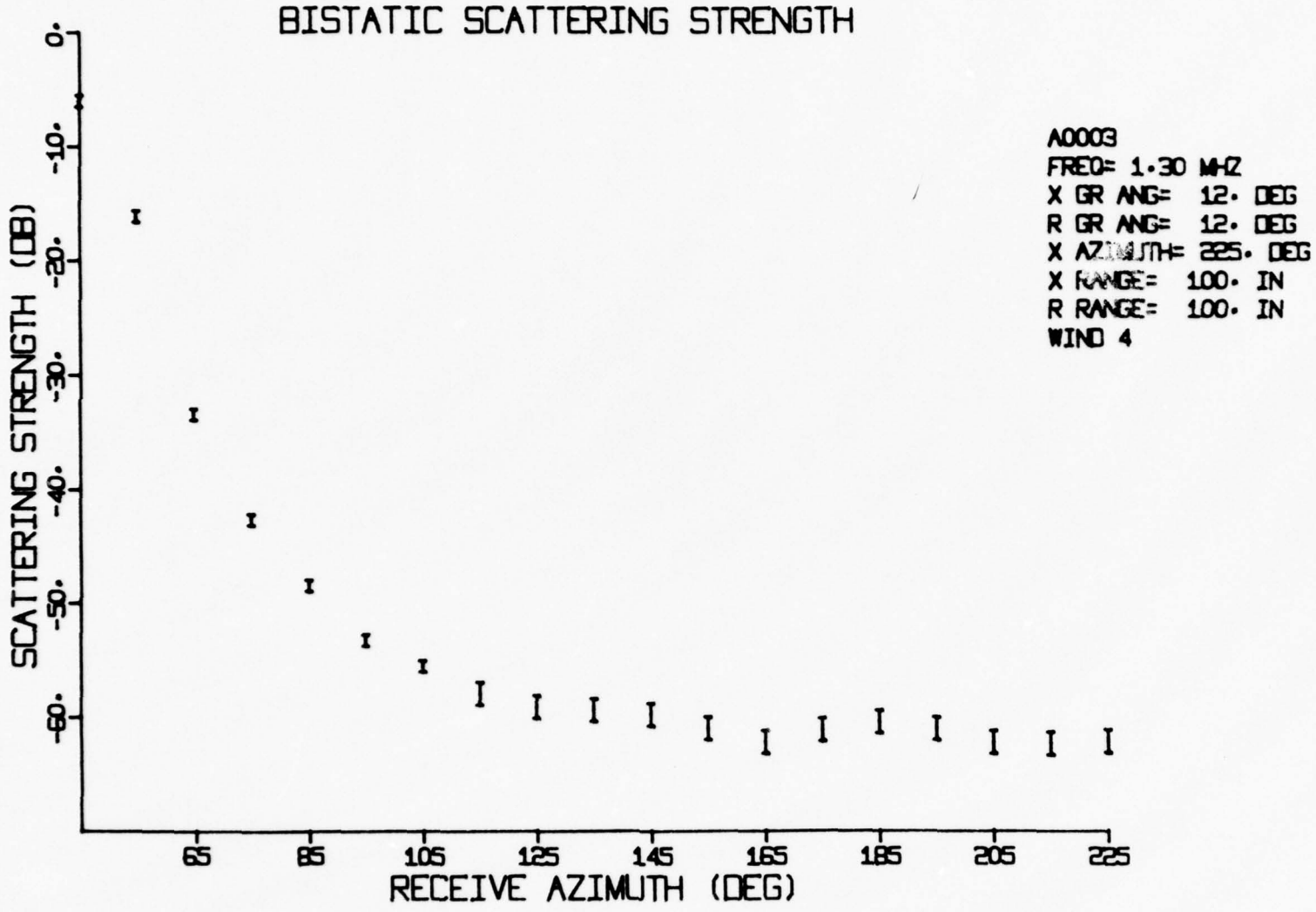
BISTATIC SCATTERING STRENGTH
A0003
FREQ= 1.30 MHZ
X GR ANG= 12. DEG
R GR ANG= 12. DEG
X AZIMUTH= 225. DEG
X RANGE= 100. IN
R RANGE= 100. IN
WIND 4
SCATTERING STRENGTH (DB)
0.
-10.
-20.
-30.
-40.
-50.
-60.
65
85
105
125
145
165
185
205
225
RECEIVE AZIMUTH (DEG)

Figure A-2

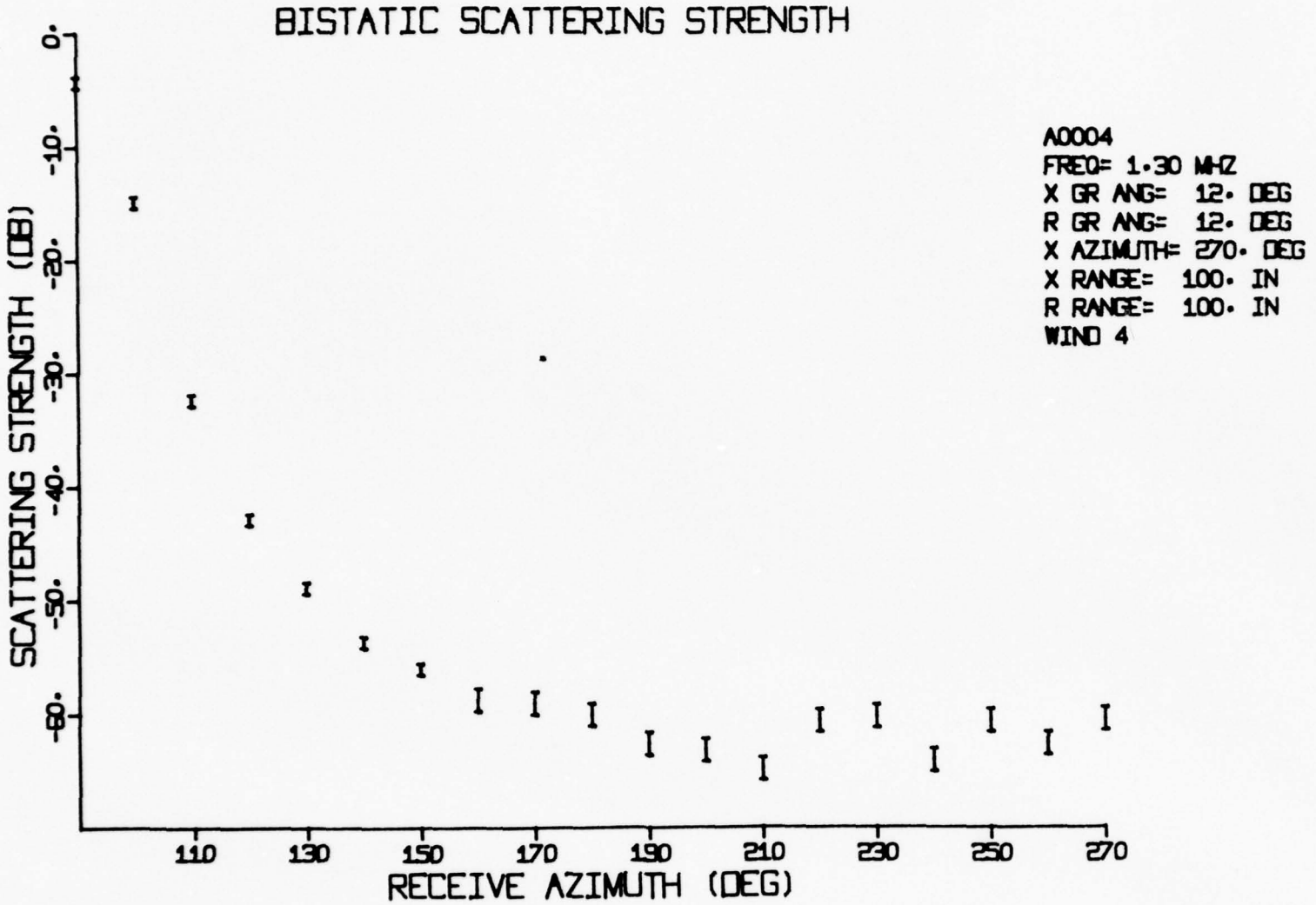
BISTATIC SCATTERING STRENGTH
A0004
FREQ= 1.30 MHZ
X GR ANG= 12. DEG
R GR ANG= 12. DEG
X AZIMUTH= 270. DEG
X RANGE= 100. IN
R RANGE= 100. IN
WIND 4
SCATTERING STRENGTH (DB)
0.
-10.
-20.
-30.
-40.
-50.
-60.
110
130
150
170
190
210
230
250
270
RECEIVE AZIMUTH (DEG)

Figure A-3

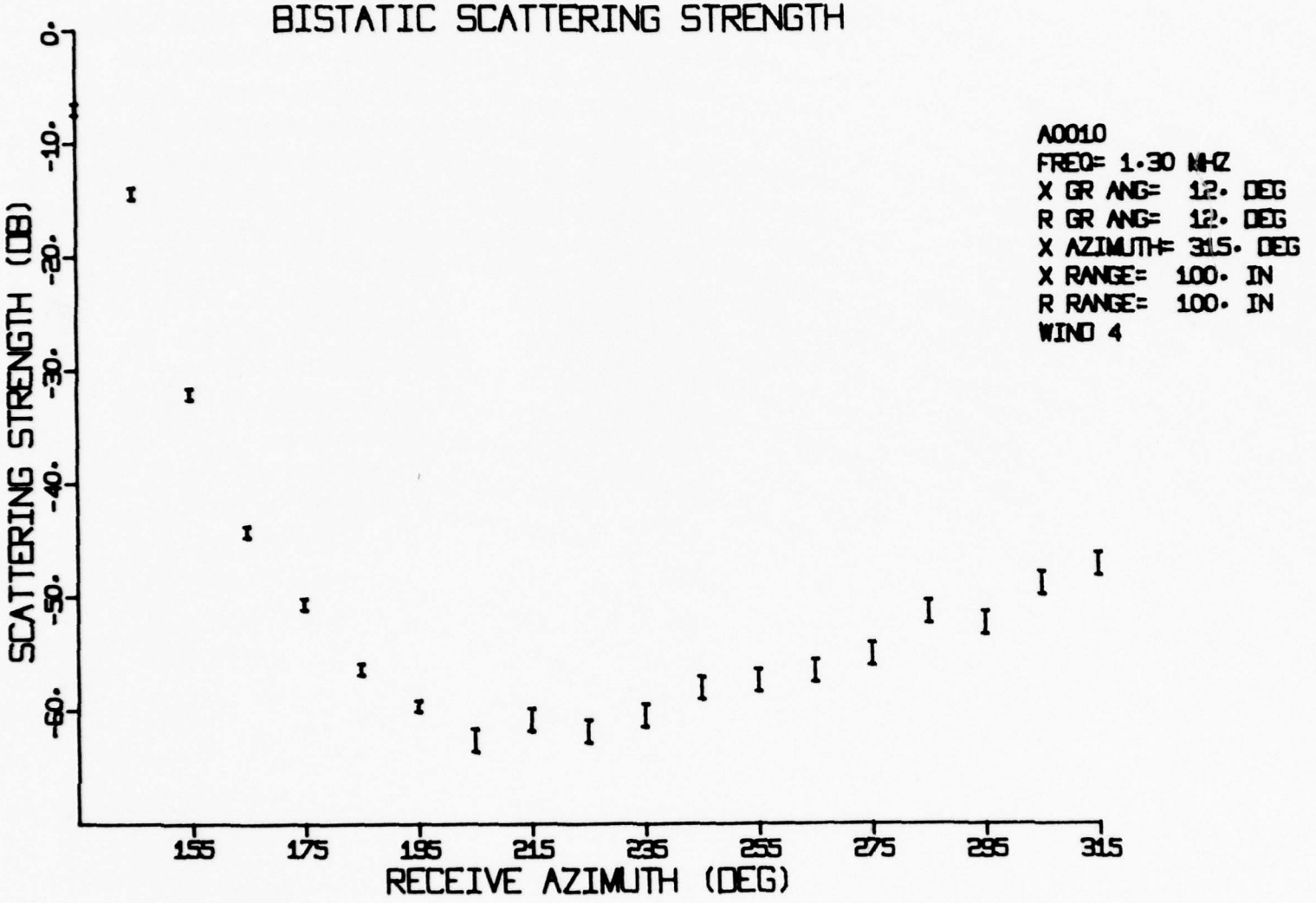
BISTATIC SCATTERING STRENGTH
A0010
FREQ= 1.30 MHZ
X GR ANG= 12. DEG
R GR ANG= 12. DEG
X AZIMUTH= 315. DEG
X RANGE= 100. IN
R RANGE= 100. IN
WIND 4
SCATTERING STRENGTH (DB)
0.
-10.
-20.
-30.
-40.
-50.
-60.
155
175
195
215
235
255
275
295
315
RECEIVE AZIMUTH (DEG)

Figure A-4

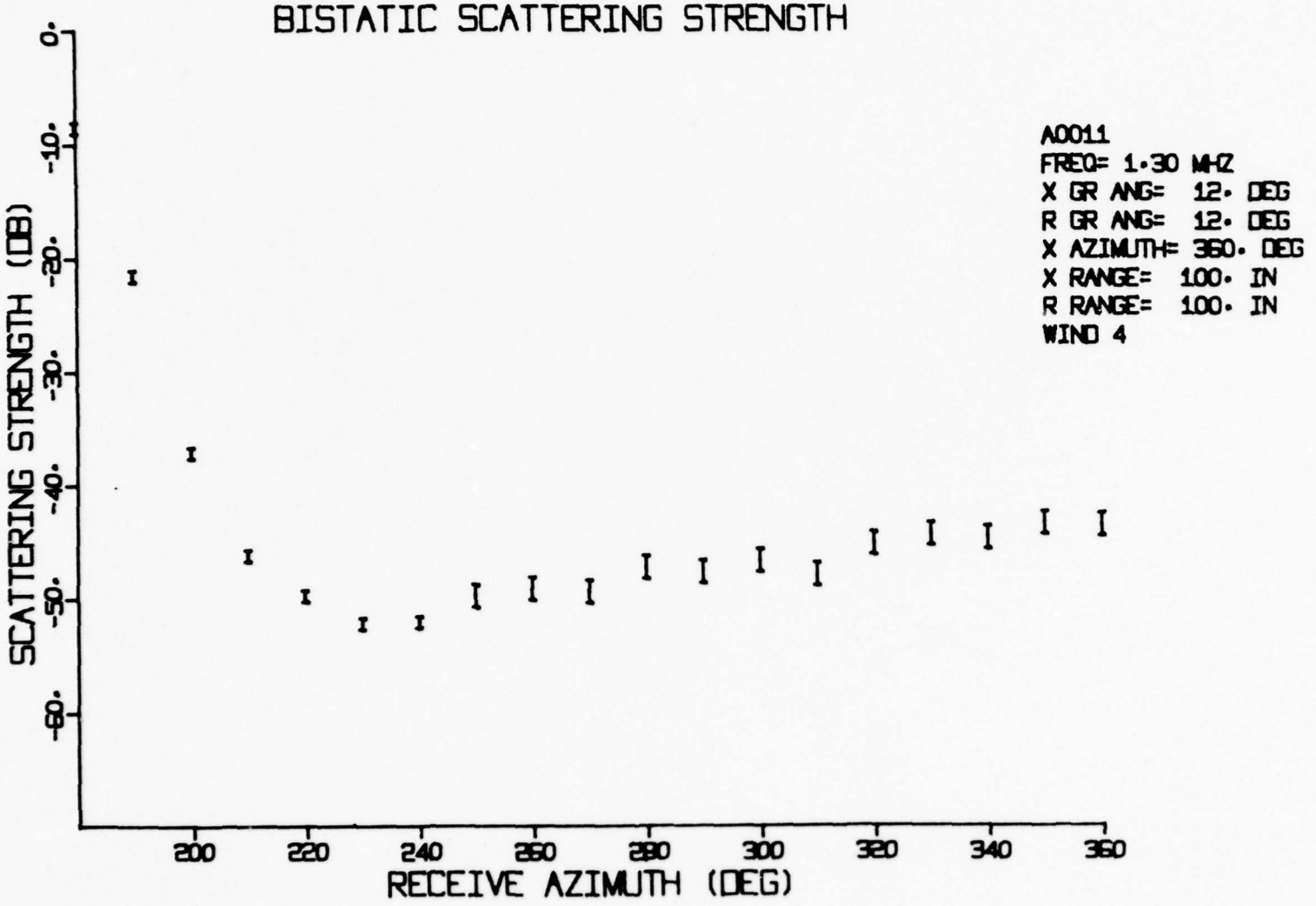
BISTATIC SCATTERING STRENGTH
A0011
FREQ= 1.30 MHZ
X GR ANG= 12. DEG
R GR ANG= 12. DEG
X AZIMUTH= 360. DEG
X RANGE= 100. IN
R RANGE= 100. IN
WIND 4
SCATTERING STRENGTH (DB)
0.
-10.
-20.
-30.
-40.
-50.
-60.
200
220
240
260
280
300
320
340
360
RECEIVE AZIMUTH (DEG)

Figure A-5

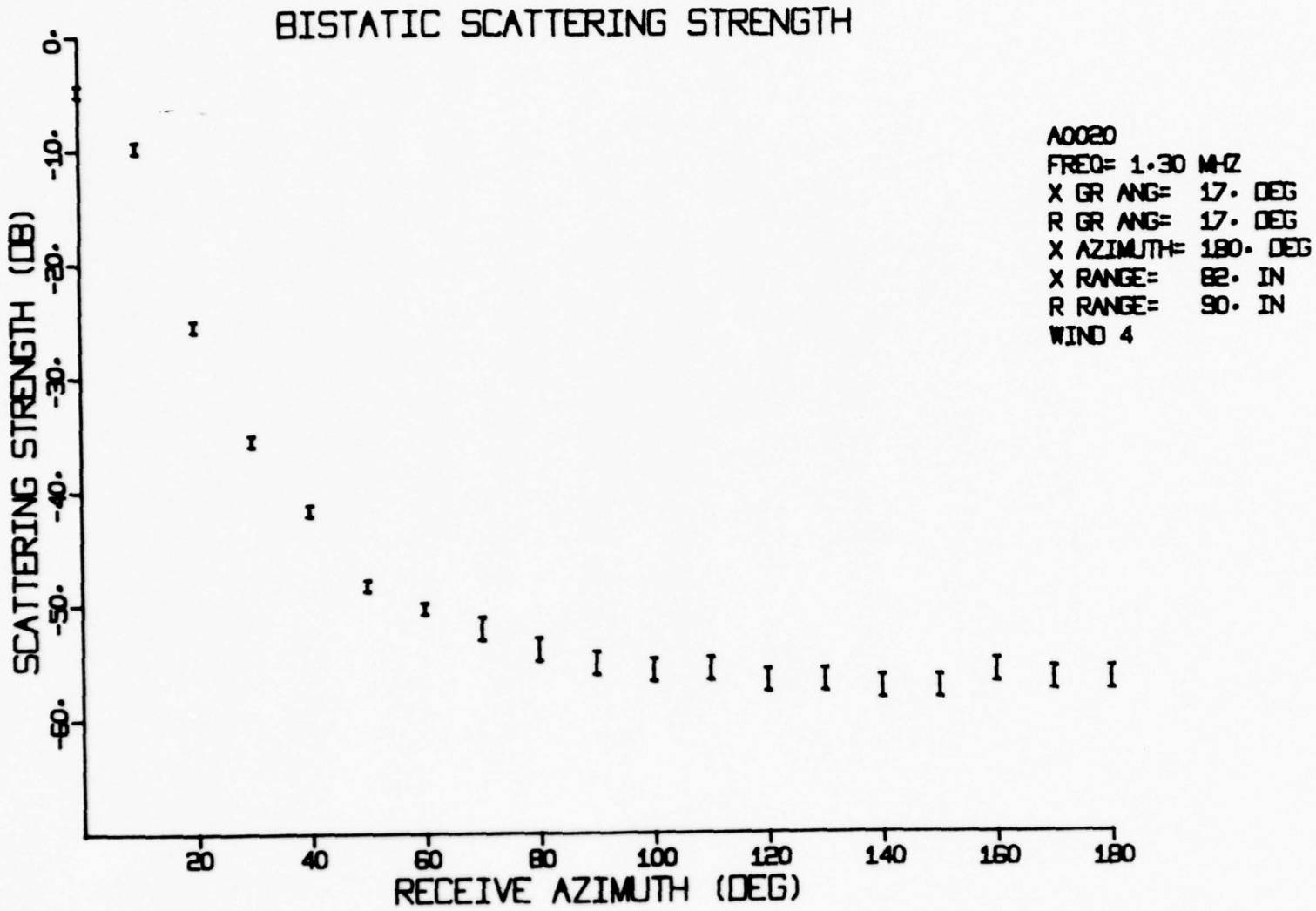
BISTATIC SCATTERING STRENGTH
A0020
FREQ= 1.30 MHZ
X GR ANG= 17. DEG
R GR ANG= 17. DEG
X AZIMUTH= 180. DEG
X RANGE= 82. IN
R RANGE= 90. IN
WIND 4
SCATTERING STRENGTH (DB)
0.
-10.
-20.
-30.
-40.
-50.
-60.
20
40
60
80
100
120
140
160
180
RECEIVE AZIMUTH (DEG)

Figure A-6

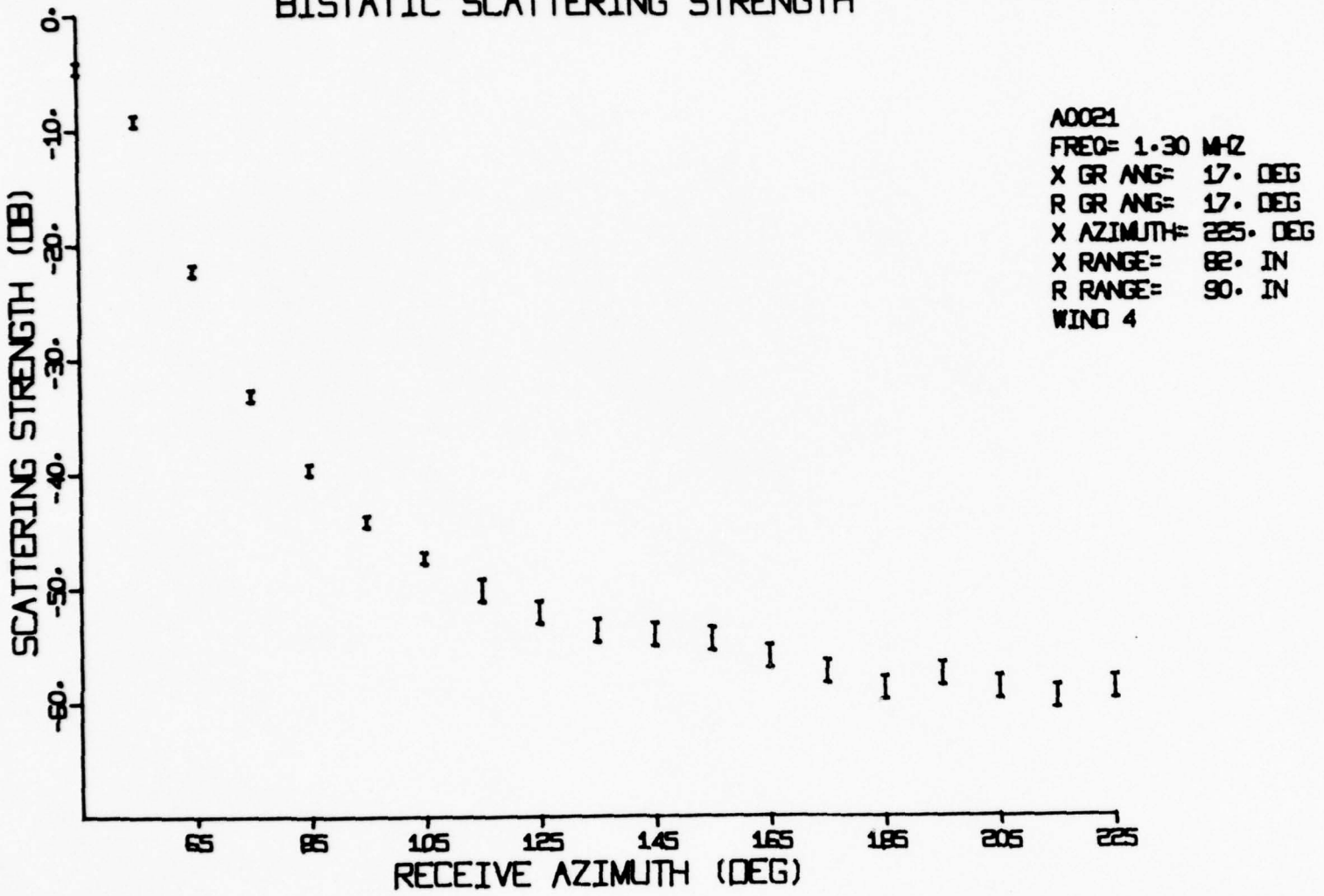
BISTATIC SCATTERING STRENGTH
SCATTERING STRENGTH (DB)
0.
-10.
-20.
-30.
-40.
-50.
-60.
65
85
105
125
145
165
185
205
225
RECEIVE AZIMUTH (DEG)
A0021
FREQ= 1.30 MHZ
X GR ANG= 17. DEG
R GR ANG= 17. DEG
X AZIMUTH= 225. DEG
X RANGE= 82. IN
R RANGE= 90. IN
WIND 4

Figure A-7

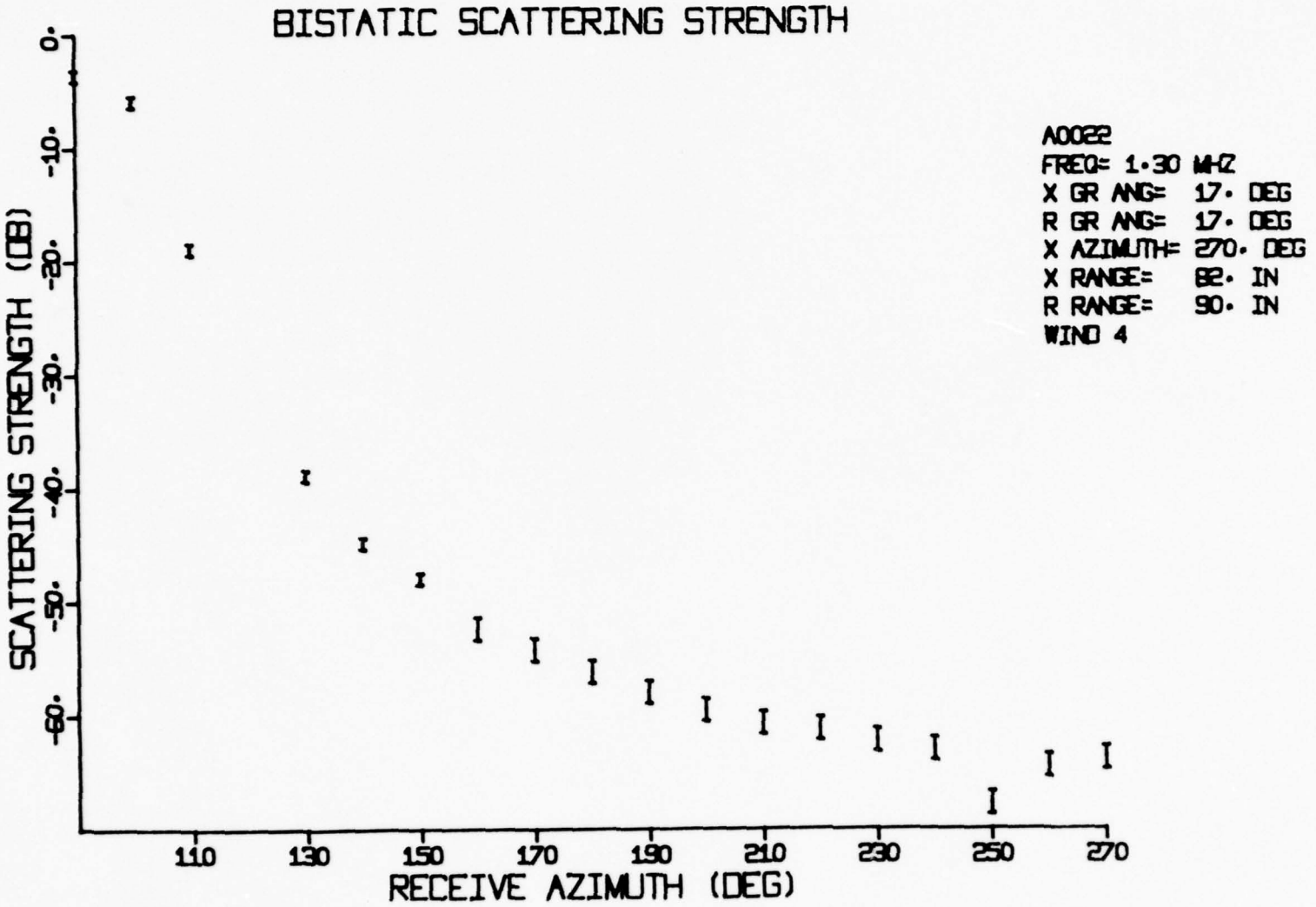
BISTATIC SCATTERING STRENGTH
A0022
FREQ= 1.30 MHZ
X GR ANG= 17. DEG
R GR ANG= 17. DEG
X AZIMUTH= 270. DEG
X RANGE= 82. IN
R RANGE= 90. IN
WIND 4
SCATTERING STRENGTH (DB)
0.
-10.
-20.
-30.
-40.
-50.
-60.
110
130
150
170
190
210
230
250
270
RECEIVE AZIMUTH (DEG)

Figure A-8

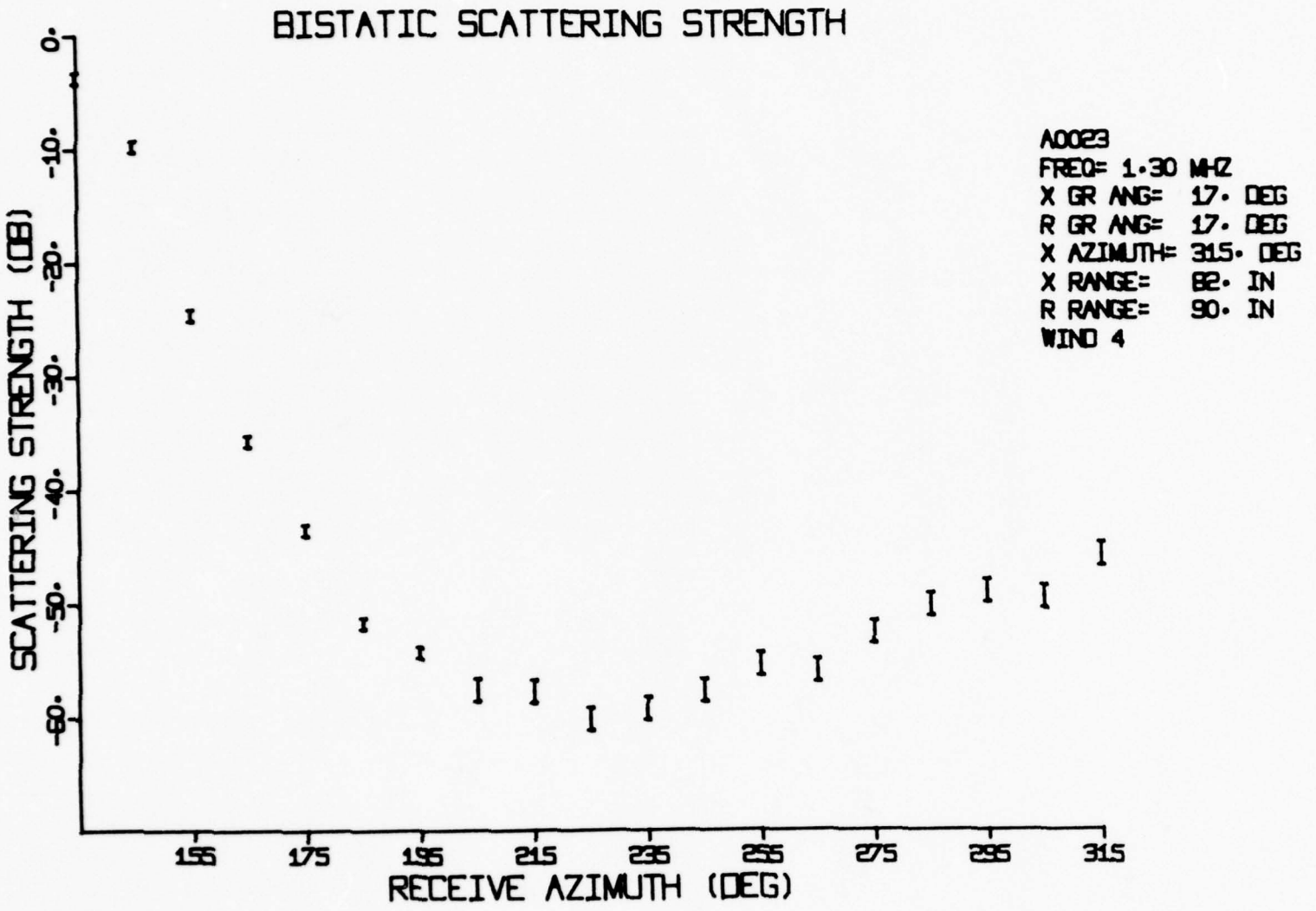
BISTATIC SCATTERING STRENGTH
A0023
FREQ= 1.30 MHZ
X GR ANG= 17. DEG
R GR ANG= 17. DEG
X AZIMUTH= 315. DEG
X RANGE= 82. IN
R RANGE= 90. IN
WIND 4
SCATTERING STRENGTH (DB)
0.
-10.
-20.
-30.
-40.
-50.
-60.
155
175
195
215
235
255
275
295
315
RECEIVE AZIMUTH (DEG)

Figure A-9

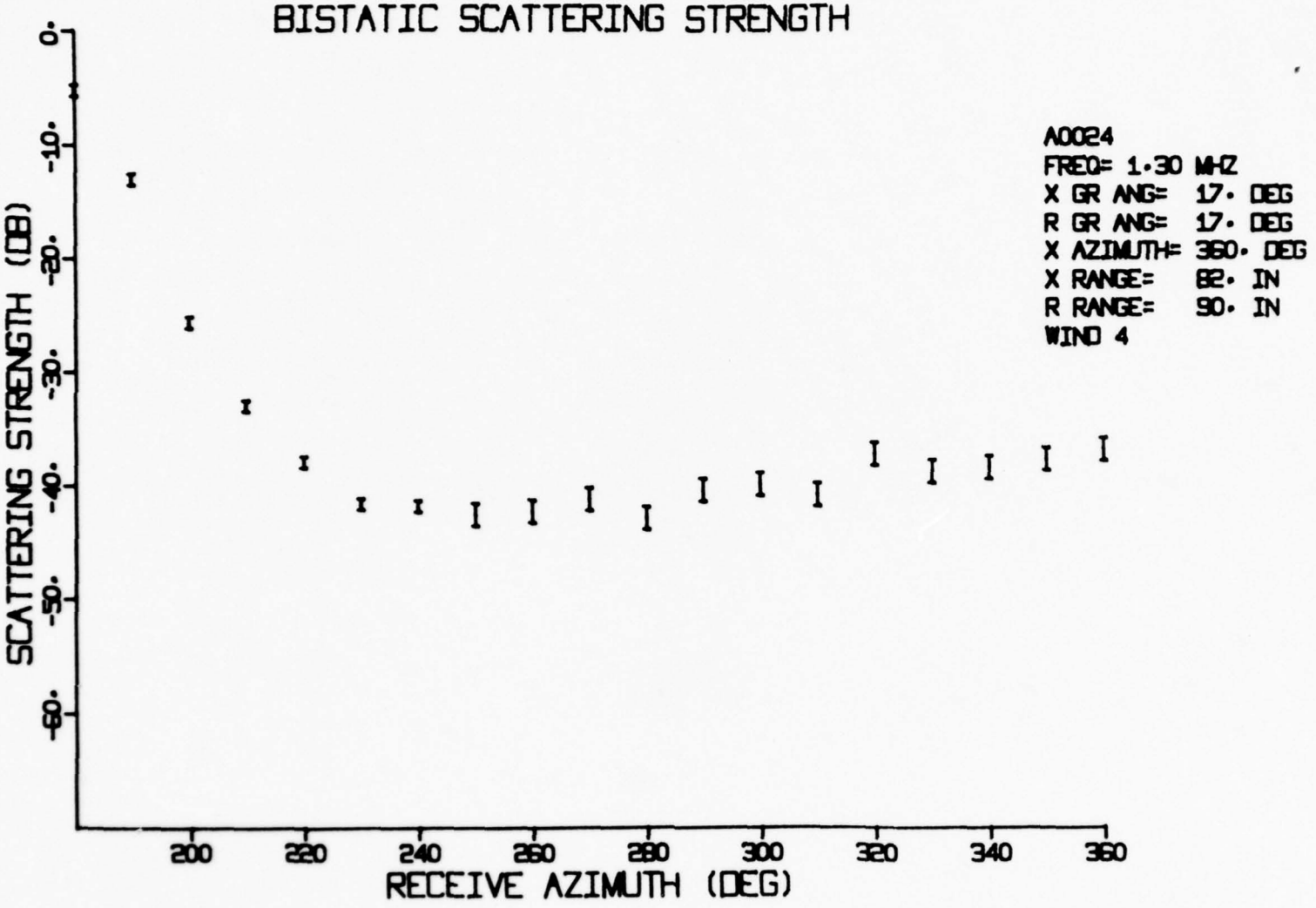
BISTATIC SCATTERING STRENGTH
A0024
FREQ= 1.30 MHZ
X GR ANG= 17. DEG
R GR ANG= 17. DEG
X AZIMUTH= 360. DEG
X RANGE= 82. IN
R RANGE= 90. IN
WIND 4
SCATTERING STRENGTH (DB)
0.
-10.
-20.
-30.
-40.
-50.
-60.
200
220
240
260
280
300
320
340
360
RECEIVE AZIMUTH (DEG)

Figure A-10

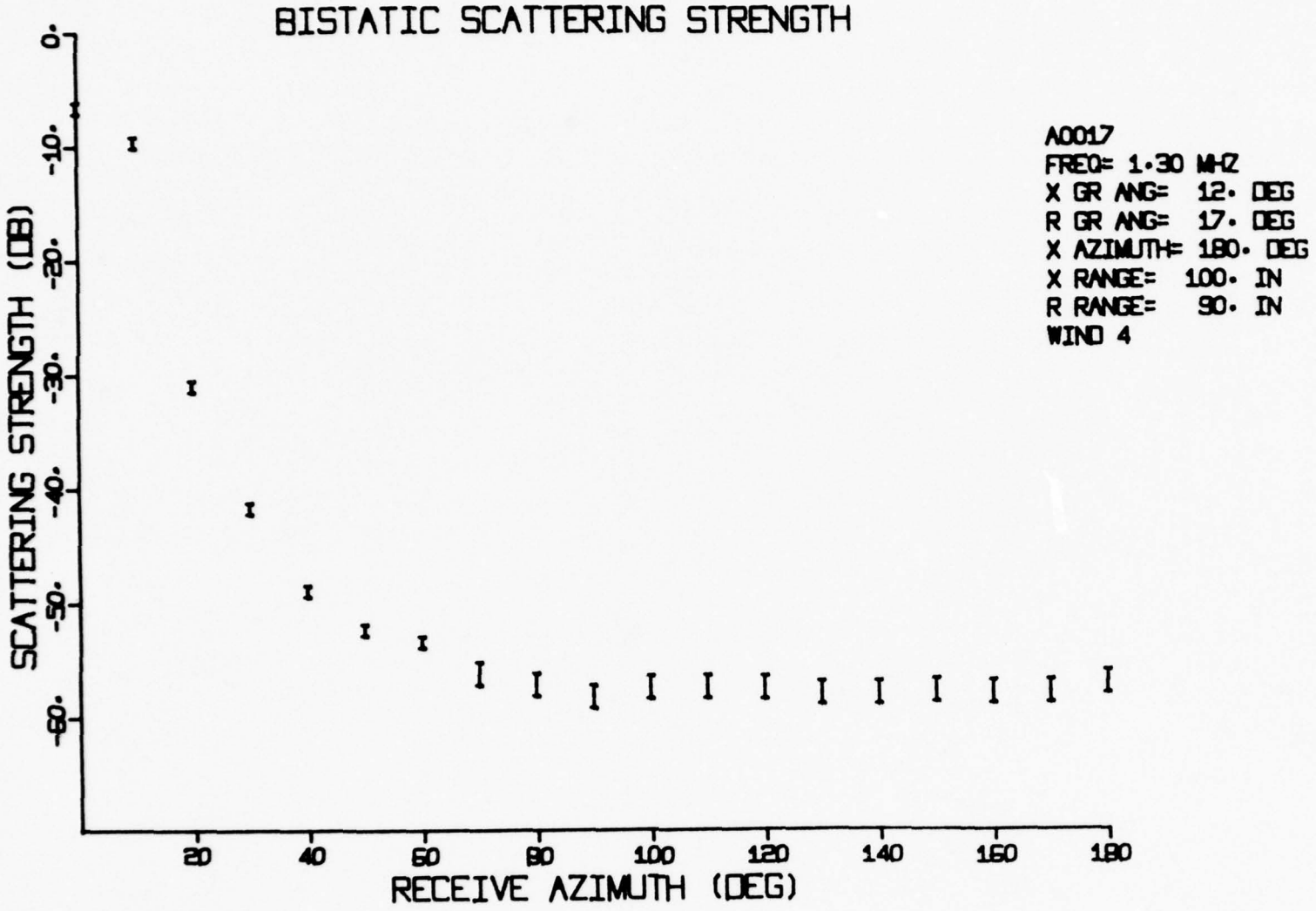
BISTATIC SCATTERING STRENGTH
A0017
FREQ= 1.30 MHZ
X GR ANG= 12. DEG
R GR ANG= 17. DEG
X AZIMUTH= 180. DEG
X RANGE= 100. IN
R RANGE= 90. IN
WIND 4
SCATTERING STRENGTH (DB)
0.
-10.
-20.
-30.
-40.
-50.
-60.
20
40
60
80
100
120
140
160
180
RECEIVE AZIMUTH (DEG)

Figure A-11

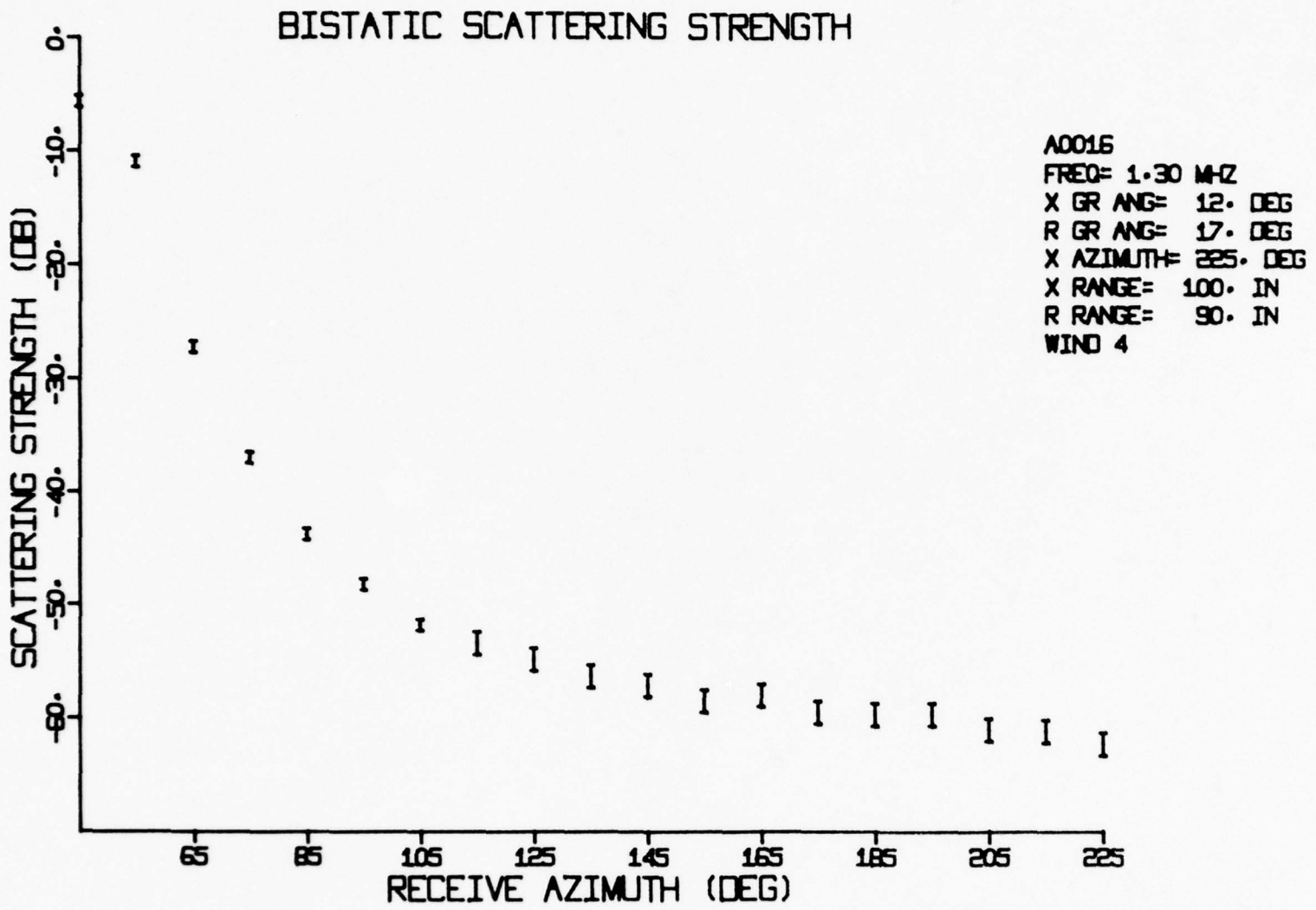
BISTATIC SCATTERING STRENGTH
A0016
FREQ= 1.30 MHZ
X GR ANG= 12. DEG
R GR ANG= 17. DEG
X AZIMUTH= 225. DEG
X RANGE= 100. IN
R RANGE= 90. IN
WIND 4
SCATTERING STRENGTH (DB)
0.
-10.
-20.
-30.
-40.
-50.
-60.
65
85
105
125
145
165
185
205
225
RECEIVE AZIMUTH (DEG)

Figure A-12

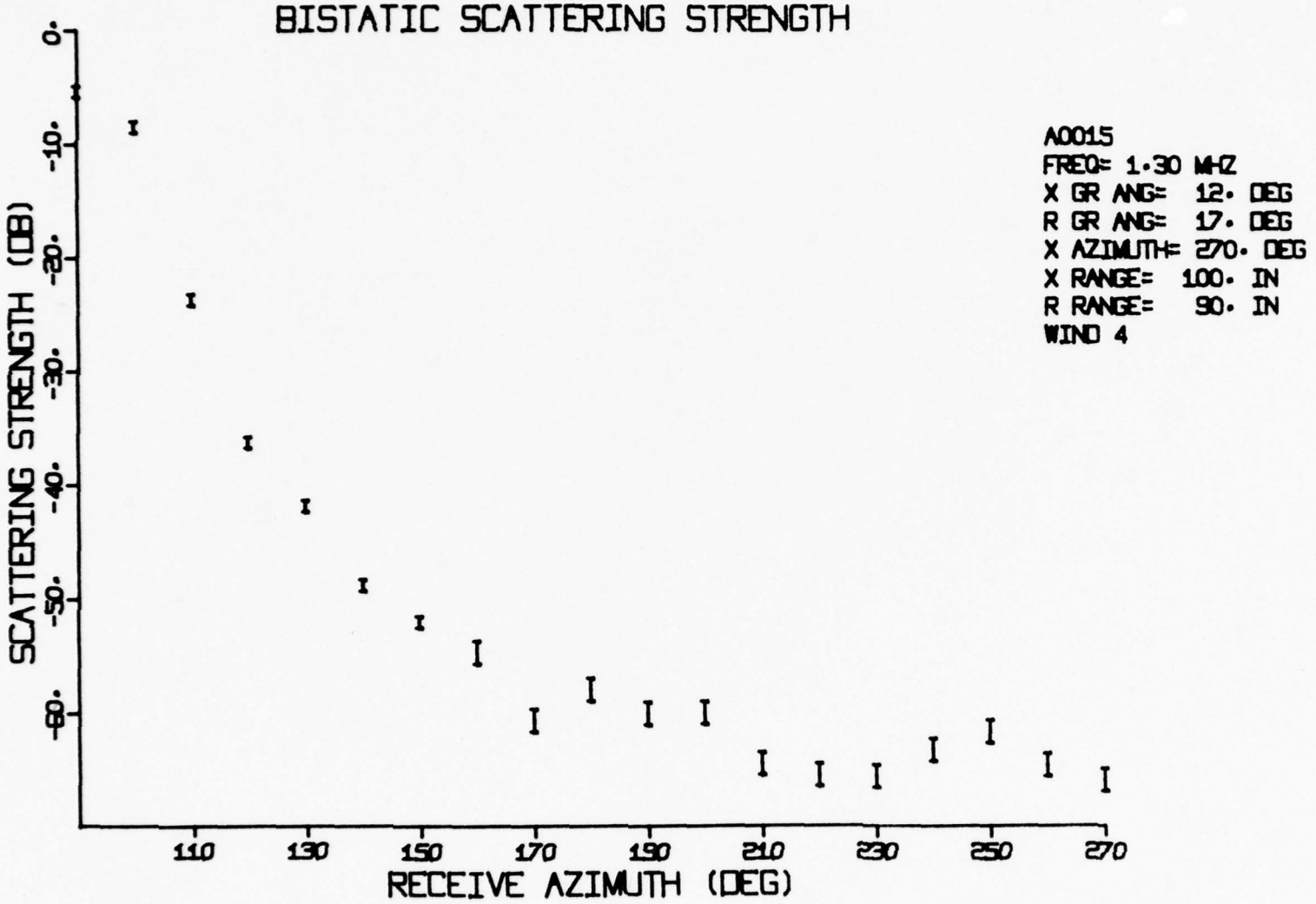
BISTATIC SCATTERING STRENGTH
A0015
FREQ= 1.30 MHZ
X GR ANG= 12. DEG
R GR ANG= 17. DEG
X AZIMUTH= 270. DEG
X RANGE= 100. IN
R RANGE= 90. IN
WIND 4
SCATTERING STRENGTH (DB)
0.
-10.
-20.
-30.
-40.
-50.
-60.
110
130
150
170
190
210
230
250
270
RECEIVE AZIMUTH (DEG)

Figure A-13

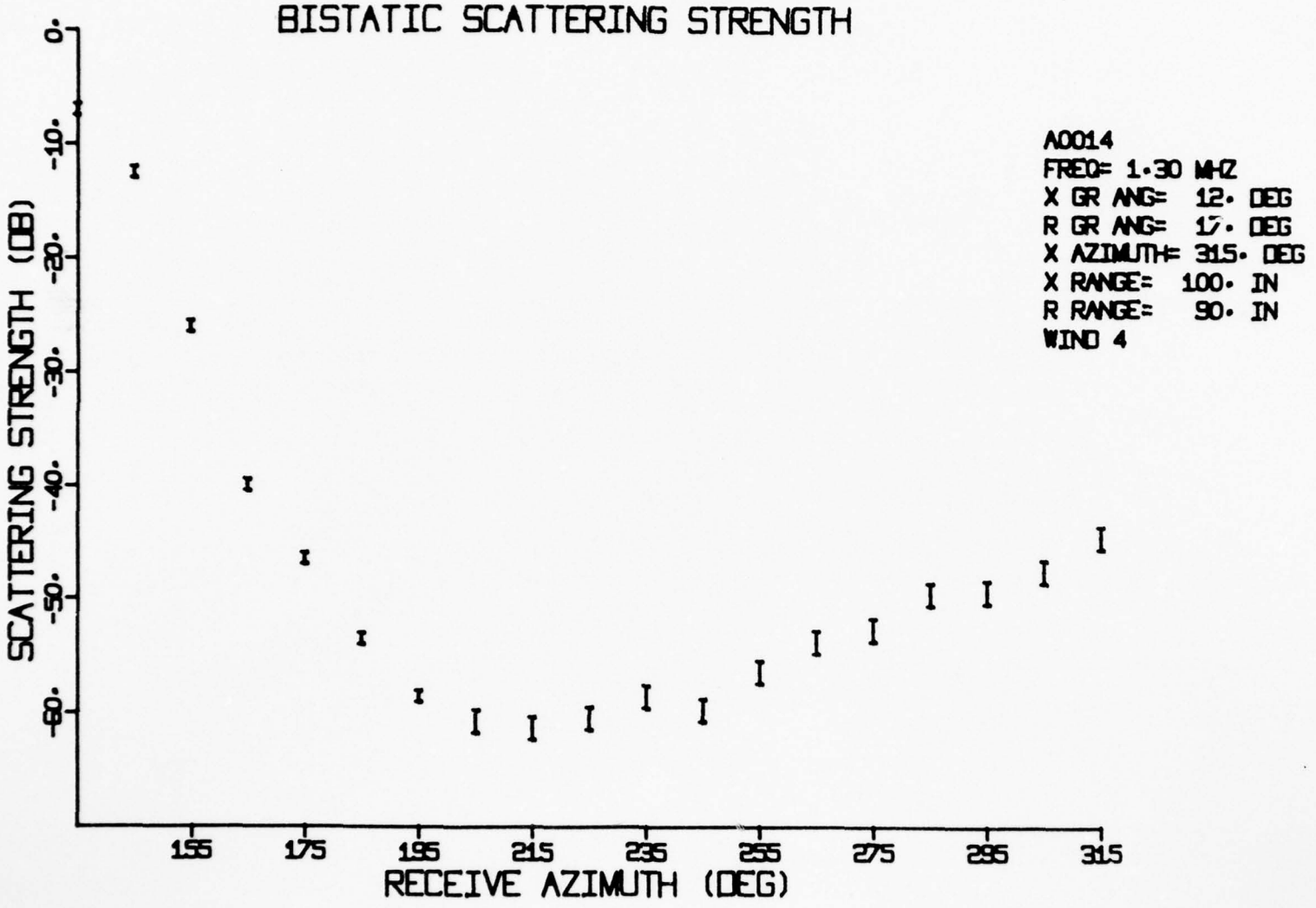
BISTATIC SCATTERING STRENGTH
A0014
FREQ= 1.30 MHZ
X GR ANG= 12. DEG
R GR ANG= 17. DEG
X AZIMUTH= 315. DEG
X RANGE= 100. IN
R RANGE= 90. IN
WIND 4
SCATTERING STRENGTH (DB)
0.
-10.
-20.
-30.
-40.
-50.
-60.
155
175
195
215
235
255
275
295
315
RECEIVE AZIMUTH (DEG)

Figure A-14

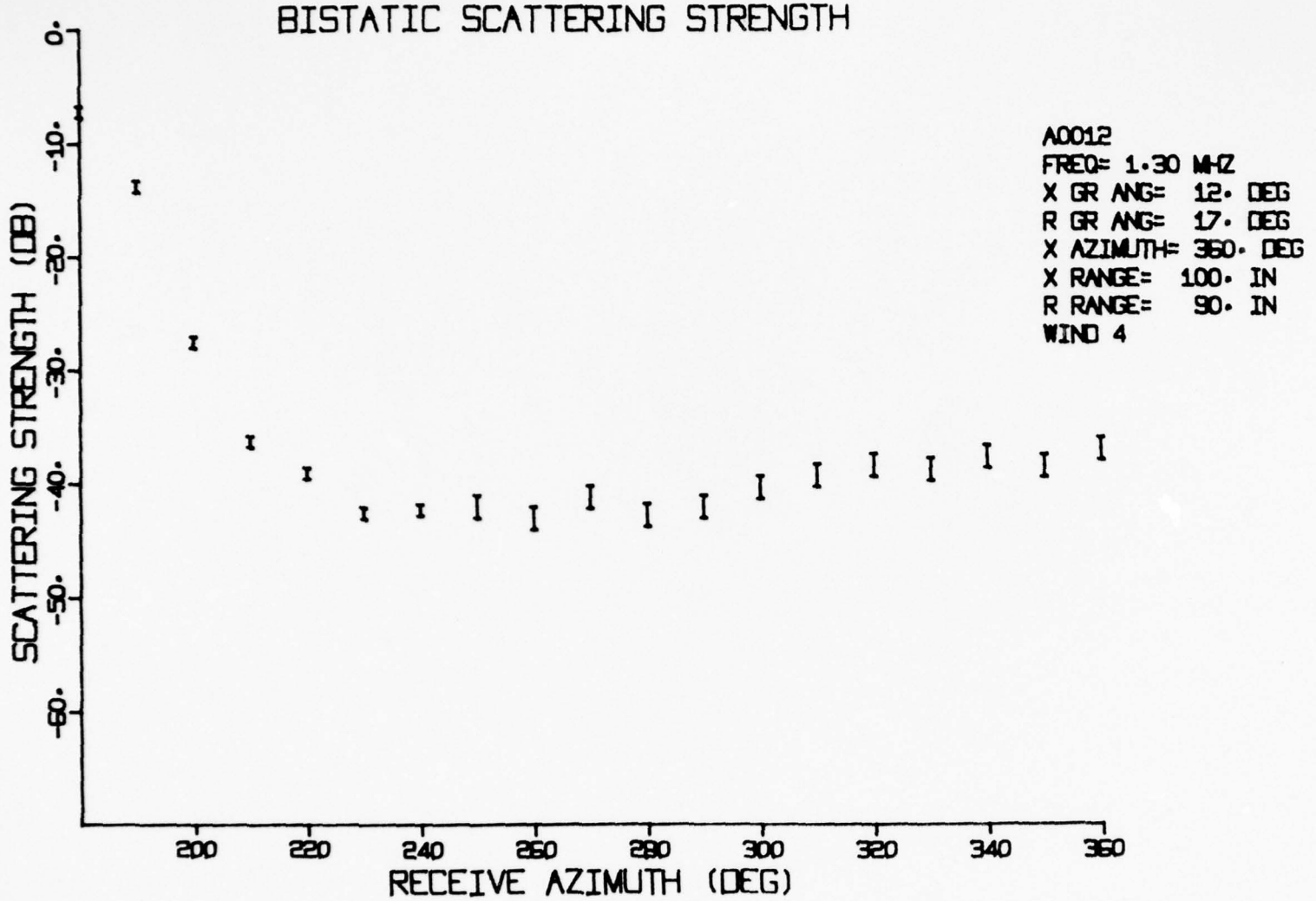
BISTATIC SCATTERING STRENGTH
A0012
FREQ= 1.30 MHZ
X GR ANG= 12. DEG
R GR ANG= 17. DEG
X AZIMUTH= 360. DEG
X RANGE= 100. IN
R RANGE= 90. IN
WIND 4
SCATTERING STRENGTH (DB)
0.
-10.
-20.
-30.
-40.
-50.
-60.
200
220
240
260
280
300
320
340
360
RECEIVE AZIMUTH (DEG)

Figure A-15

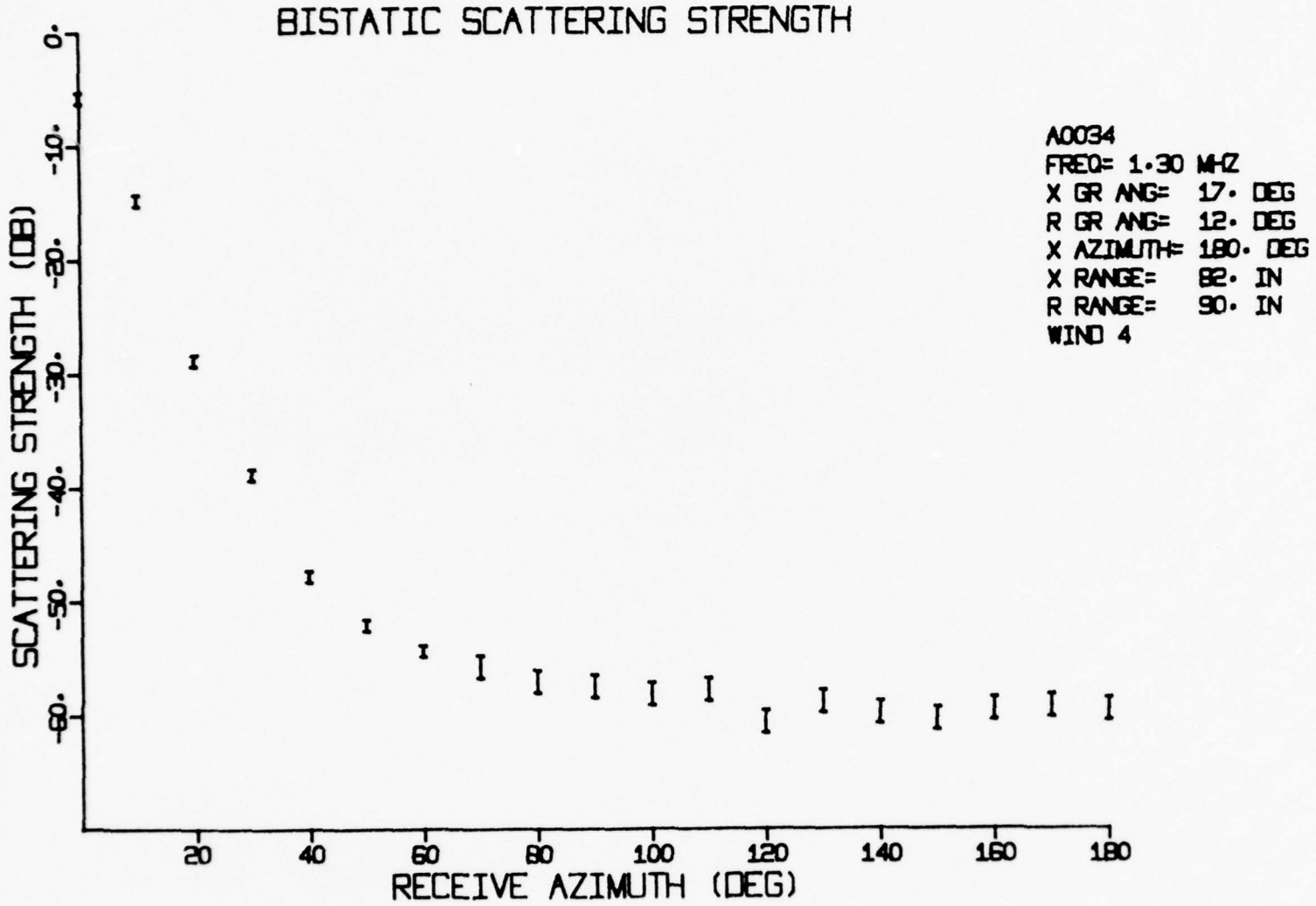
BISTATIC SCATTERING STRENGTH
A0034
FREQ= 1.30 MHZ
X GR ANG= 17. DEG
R GR ANG= 12. DEG
X AZIMUTH= 180. DEG
X RANGE= 82. IN
R RANGE= 90. IN
WIND 4
SCATTERING STRENGTH (DB)
0.
-10.
-20.
-30.
-40.
-50.
-60.
20
40
60
80
100
120
140
160
180
RECEIVE AZIMUTH (DEG)

Figure A-16

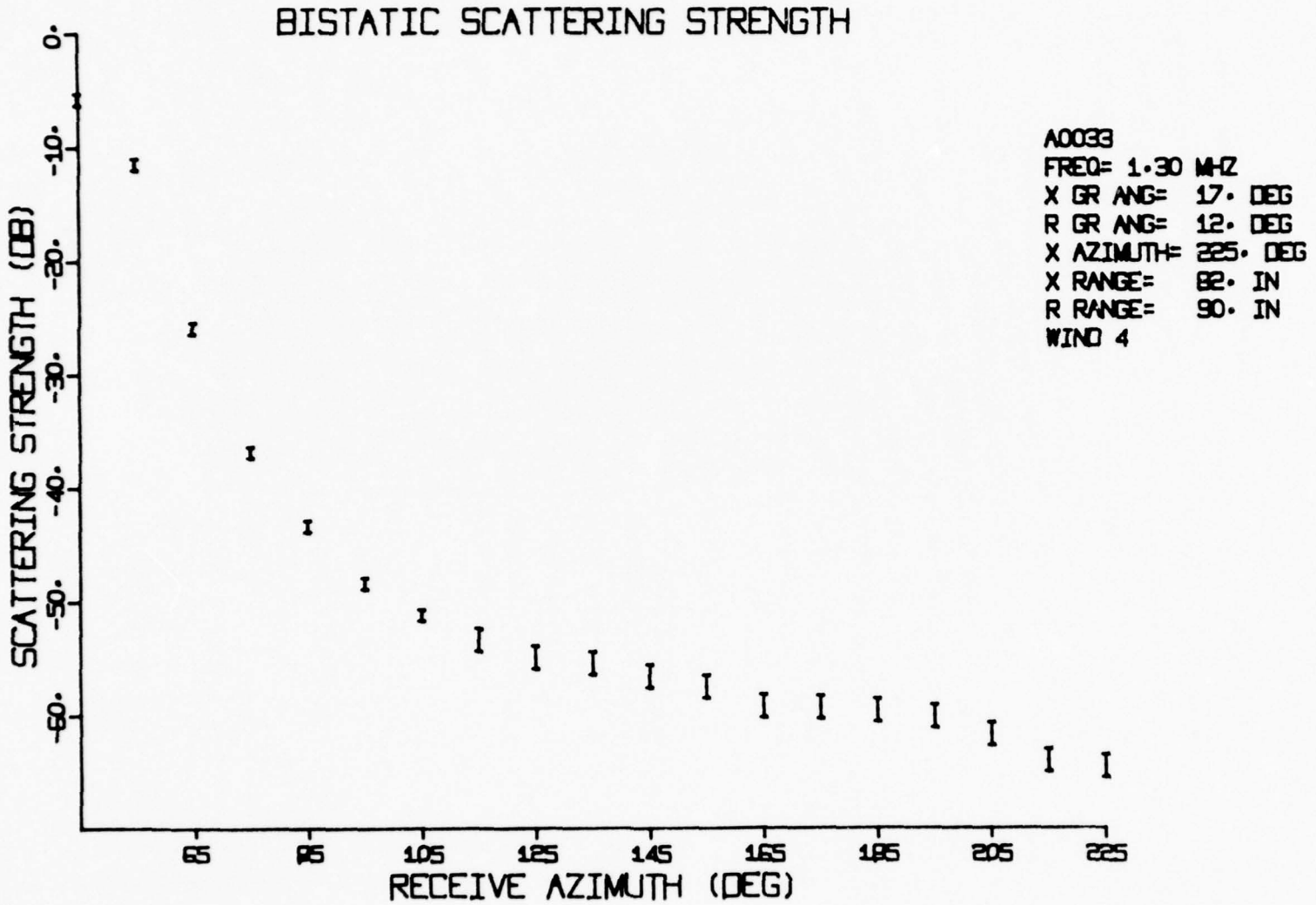
BISTATIC SCATTERING STRENGTH
A0033
FREQ= 1.30 MHZ
X GR ANG= 17. DEG
R GR ANG= 12. DEG
X AZIMUTH= 225. DEG
X RANGE= 82. IN
R RANGE= 90. IN
WIND 4
SCATTERING STRENGTH (DB)
0.
-10.
-20.
-30.
-40.
-50.
-60.
65
85
105
125
145
165
185
205
225
RECEIVE AZIMUTH (DEG)

Figure A-17

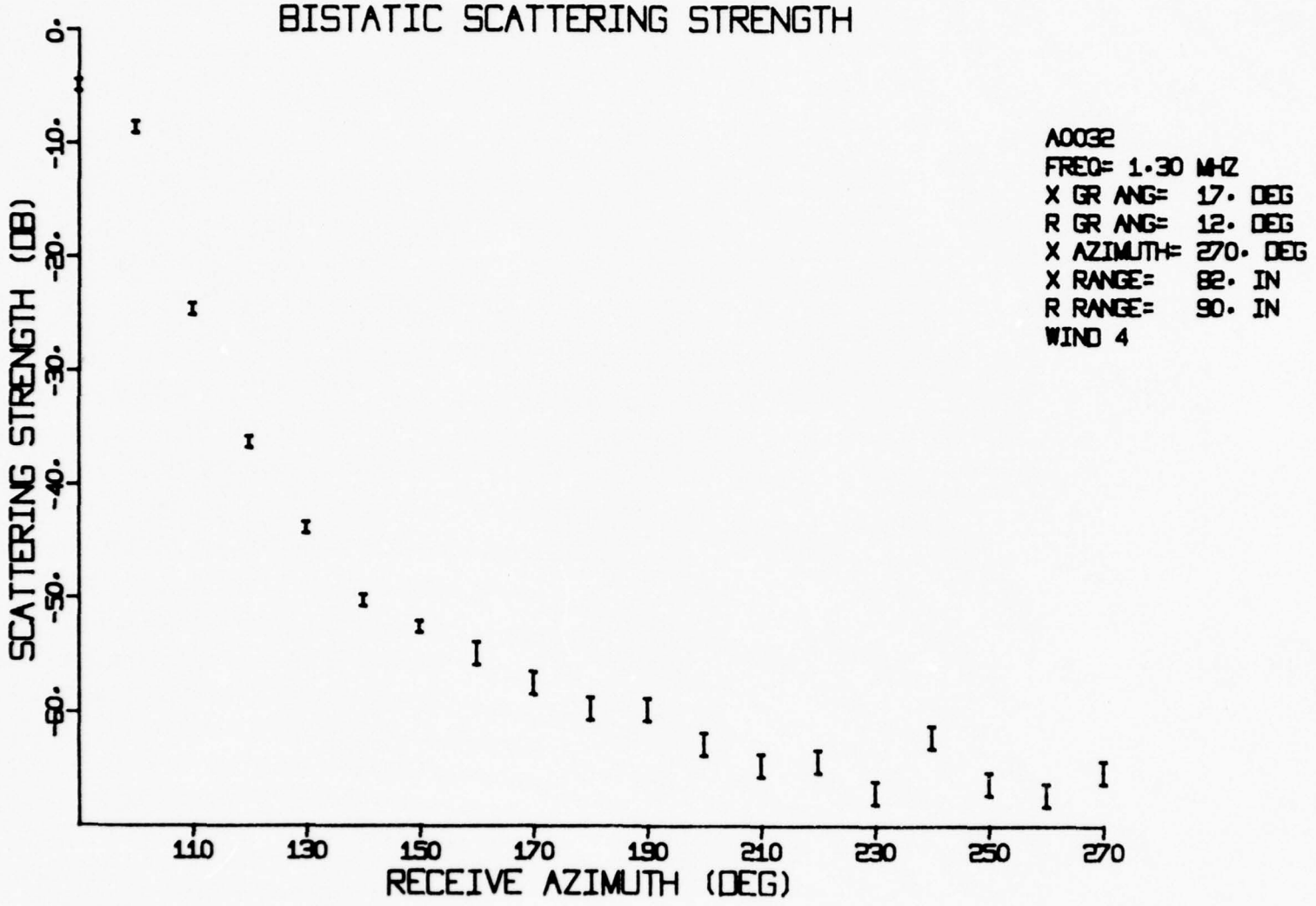
BISTATIC SCATTERING STRENGTH
A0032
FREQ= 1.30 MHZ
X GR ANG= 17. DEG
R GR ANG= 12. DEG
X AZIMUTH= 270. DEG
X RANGE= 82. IN
R RANGE= 90. IN
WIND 4
SCATTERING STRENGTH (DB)
0.
-10.
-20.
-30.
-40.
-50.
-60.
110
130
150
170
190
210
230
250
270
RECEIVE AZIMUTH (DEG)

Figure A-18

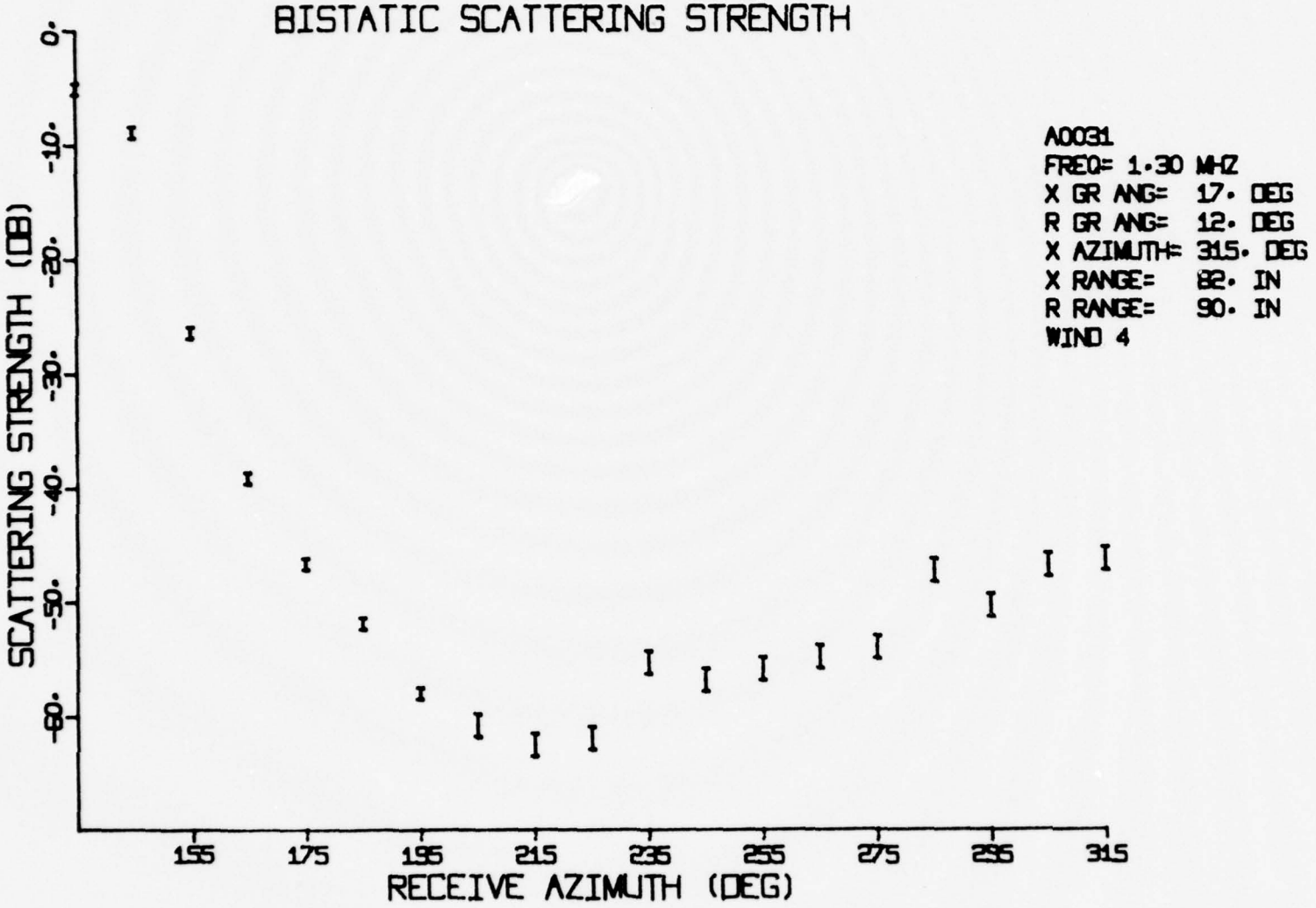
BISTATIC SCATTERING STRENGTH
A0031
FREQ= 1.30 MHZ
X GR ANG= 17. DEG
R GR ANG= 12. DEG
X AZIMUTH= 315. DEG
X RANGE= 82. IN
R RANGE= 90. IN
WIND 4
SCATTERING STRENGTH (DB)
0.
-10.
-20.
-30.
-40.
-50.
-60.
155
175
195
215
235
255
275
295
315
RECEIVE AZIMUTH (DEG)

Figure A-19

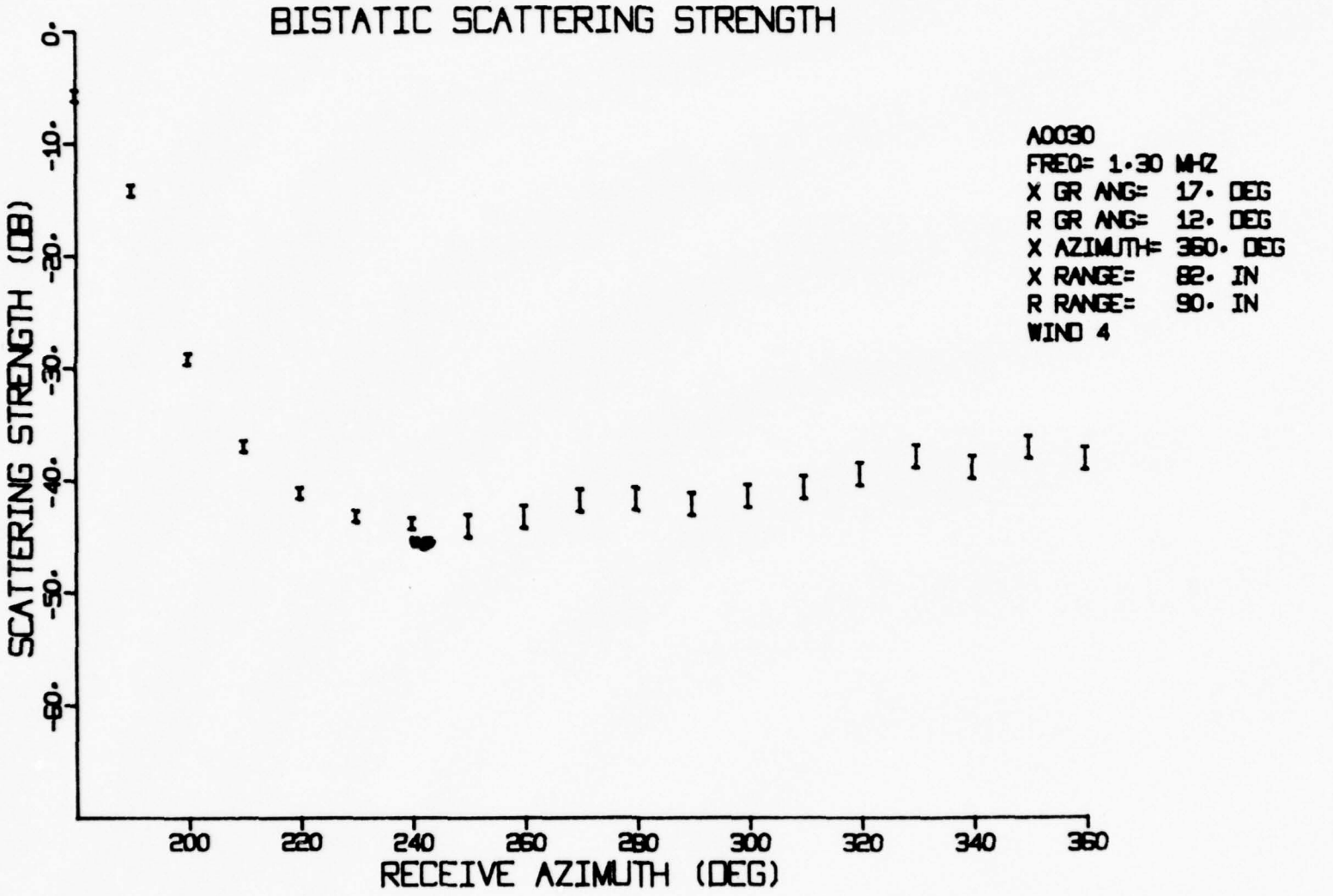
BISTATIC SCATTERING STRENGTH
A0030
FREQ= 1.30 MHZ
X GR ANG= 17. DEG
R GR ANG= 12. DEG
X AZIMUTH= 360. DEG
X RANGE= 82. IN
R RANGE= 90. IN
WIND 4
SCATTERING STRENGTH (DB)
0.
-10.
-20.
-30.
-40.
-50.
-60.
200
220
240
260
280
300
320
340
360
RECEIVE AZIMUTH (DEG)

Figure A-20

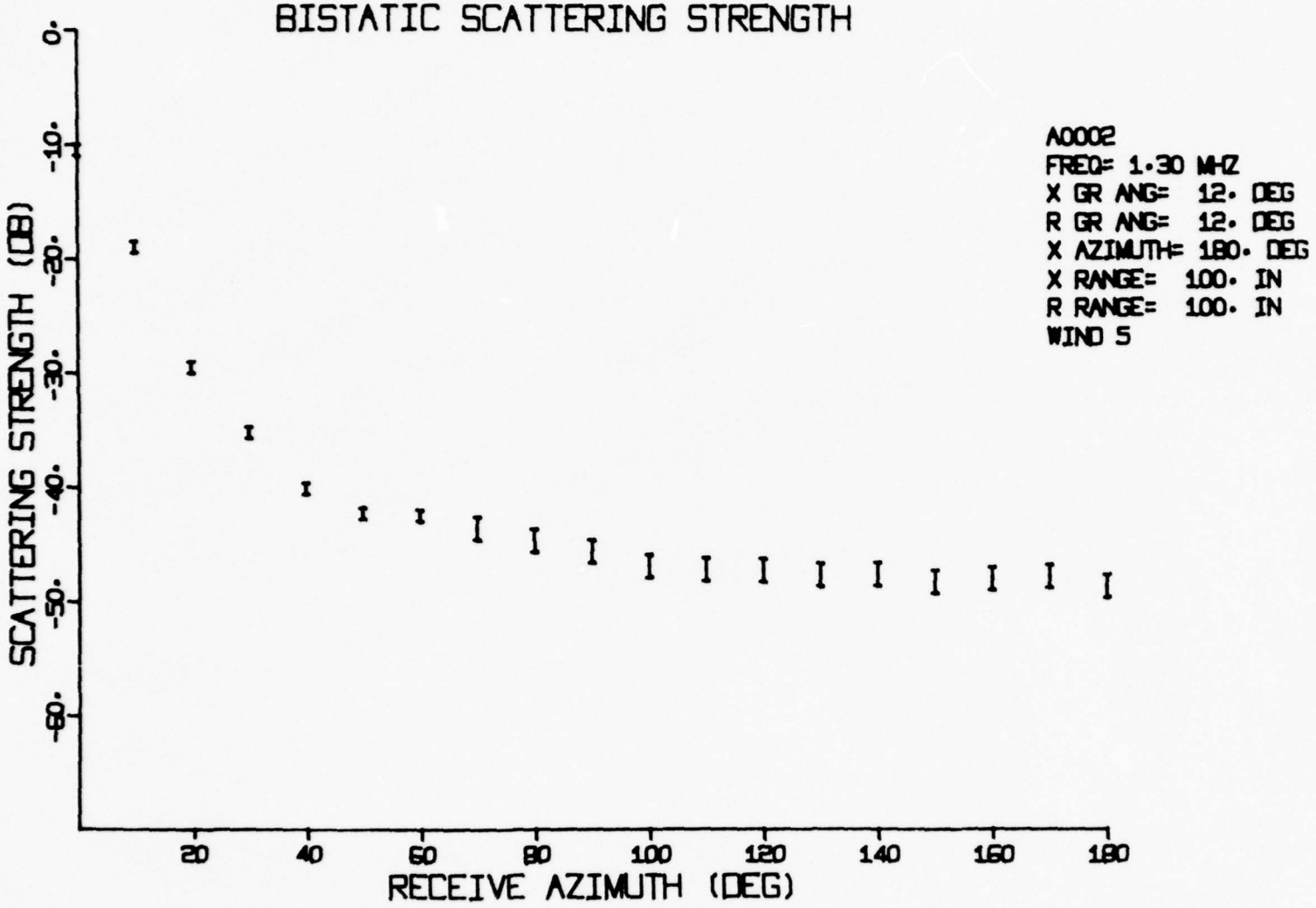
BISTATIC SCATTERING STRENGTH
A0002
FREQ= 1.30 MHZ
X GR ANG= 12. DEG
R GR ANG= 12. DEG
X AZIMUTH= 180. DEG
X RANGE= 100. IN
R RANGE= 100. IN
WIND 5
SCATTERING STRENGTH (DB)
0.
-10.
-20.
-30.
-40.
-50.
-60.
20
40
60
80
100
120
140
160
180
RECEIVE AZIMUTH (DEG)

Figure A-21

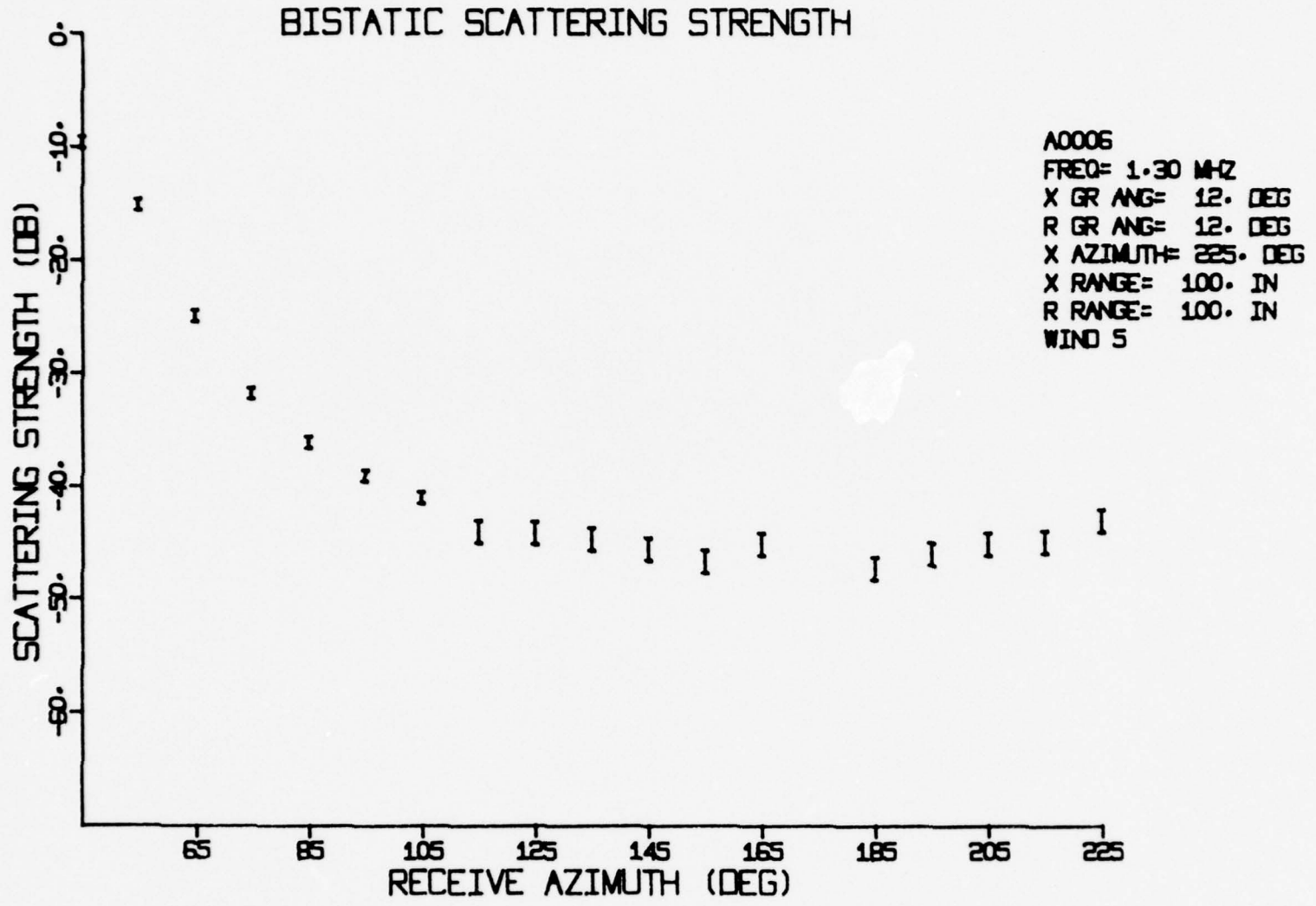
BISTATIC SCATTERING STRENGTH
A0006
FREQ= 1.30 MHZ
X GR ANG= 12. DEG
R GR ANG= 12. DEG
X AZIMUTH= 225. DEG
X RANGE= 100. IN
R RANGE= 100. IN
WIND 5
SCATTERING STRENGTH (DB)
0.
-10.
-20.
-30.
-40.
-50.
-60.
65
85
105
125
145
165
185
205
225
RECEIVE AZIMUTH (DEG)

Figure A-22

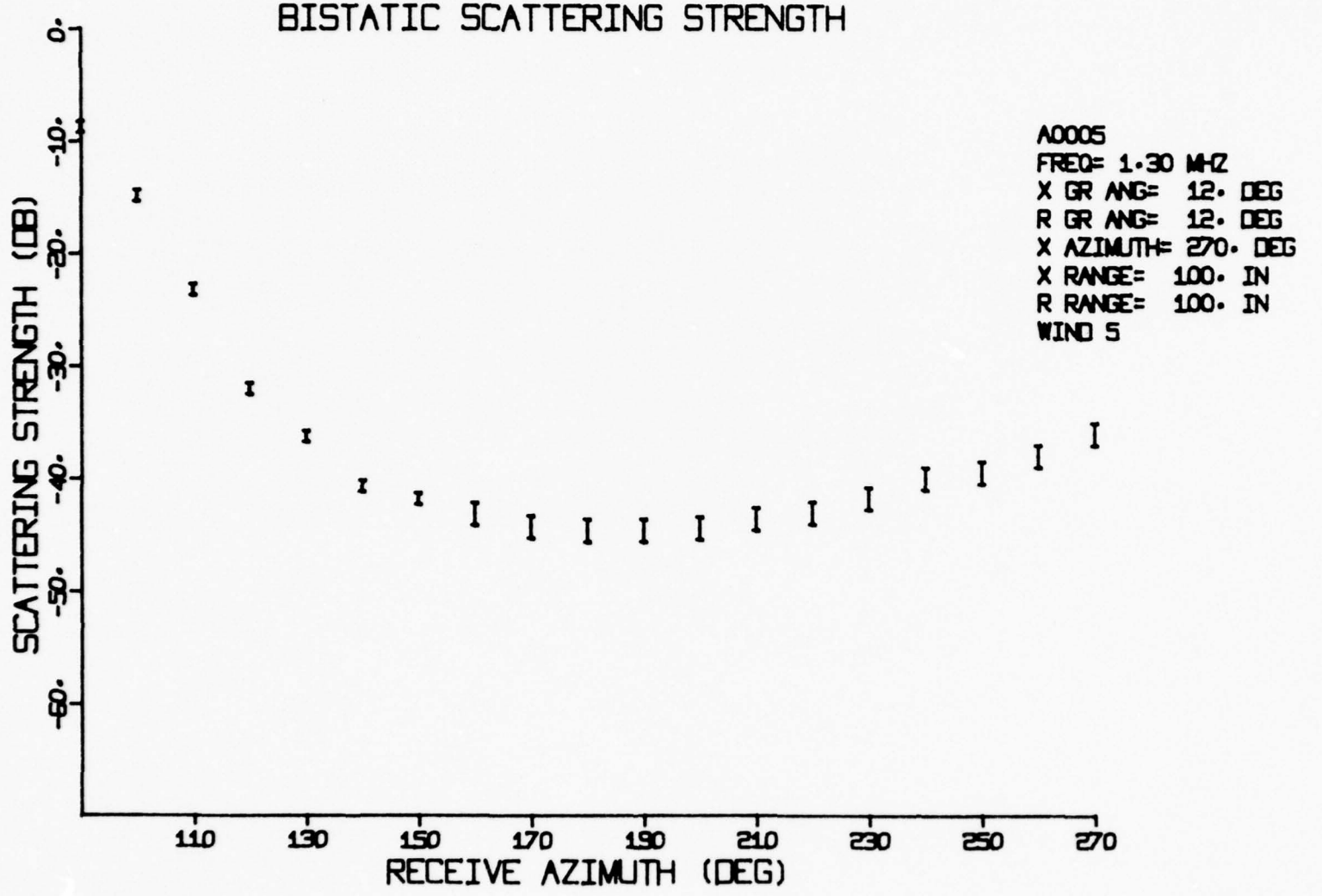
BISTATIC SCATTERING STRENGTH
A0005
FREQ= 1.30 MHZ
X GR ANG= 12. DEG
R GR ANG= 12. DEG
X AZIMUTH= 270. DEG
X RANGE= 100. IN
R RANGE= 100. IN
WIND 5
SCATTERING STRENGTH (DB)
0.
-10.
-20.
-30.
-40.
-50.
-60.
110
130
150
170
190
210
230
250
270
RECEIVE AZIMUTH (DEG)

Figure A-23

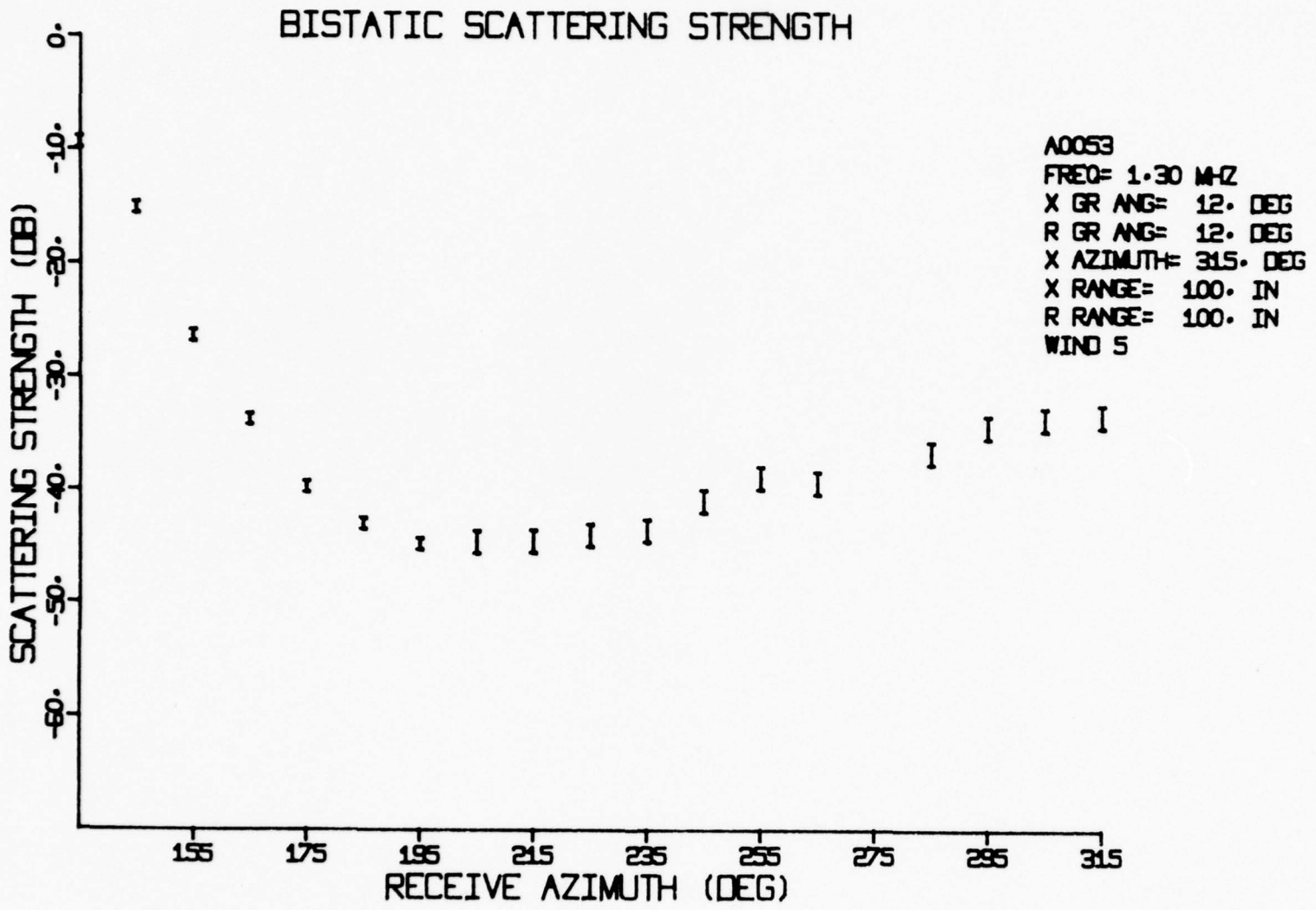
BISTATIC SCATTERING STRENGTH
A0053
FREQ= 1.30 MHZ
X GR ANG= 12. DEG
R GR ANG= 12. DEG
X AZIMUTH= 315. DEG
X RANGE= 100. IN
R RANGE= 100. IN
WIND 5
SCATTERING STRENGTH (DB)
0.
-10.
-20.
-30.
-40.
-50.
-60.
155
175
195
215
235
255
275
295
315
RECEIVE AZIMUTH (DEG)

Figure A-24

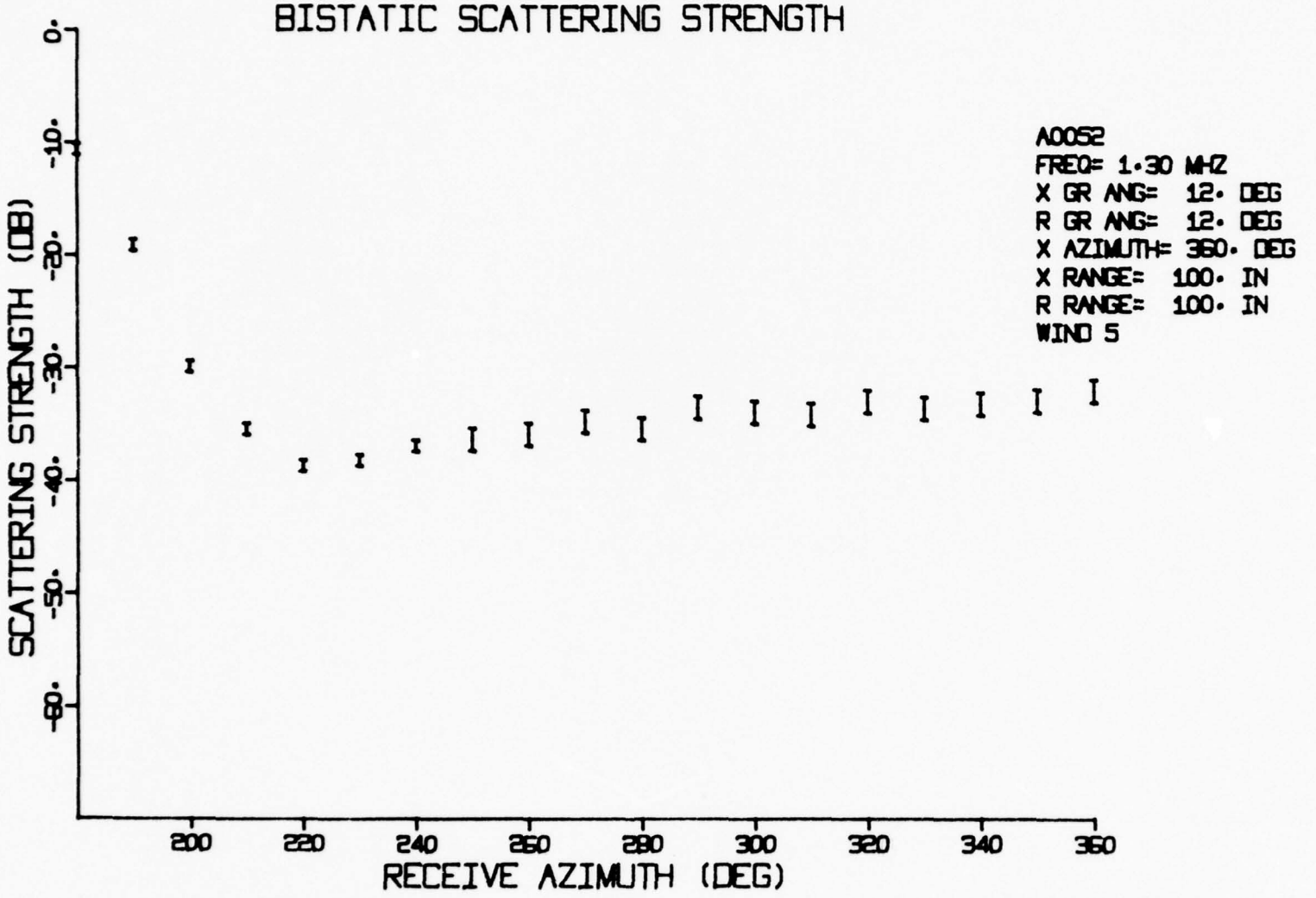
BISTATIC SCATTERING STRENGTH
A0052
FREQ= 1.30 MHZ
X GR ANG= 12. DEG
R GR ANG= 12. DEG
X AZIMUTH= 360. DEG
X RANGE= 100. IN
R RANGE= 100. IN
WIND 5
SCATTERING STRENGTH (DB)
0.
-10.
-20.
-30.
-40.
-50.
-60.
200
220
240
260
280
300
320
340
360
RECEIVE AZIMUTH (DEG)

Figure A-25

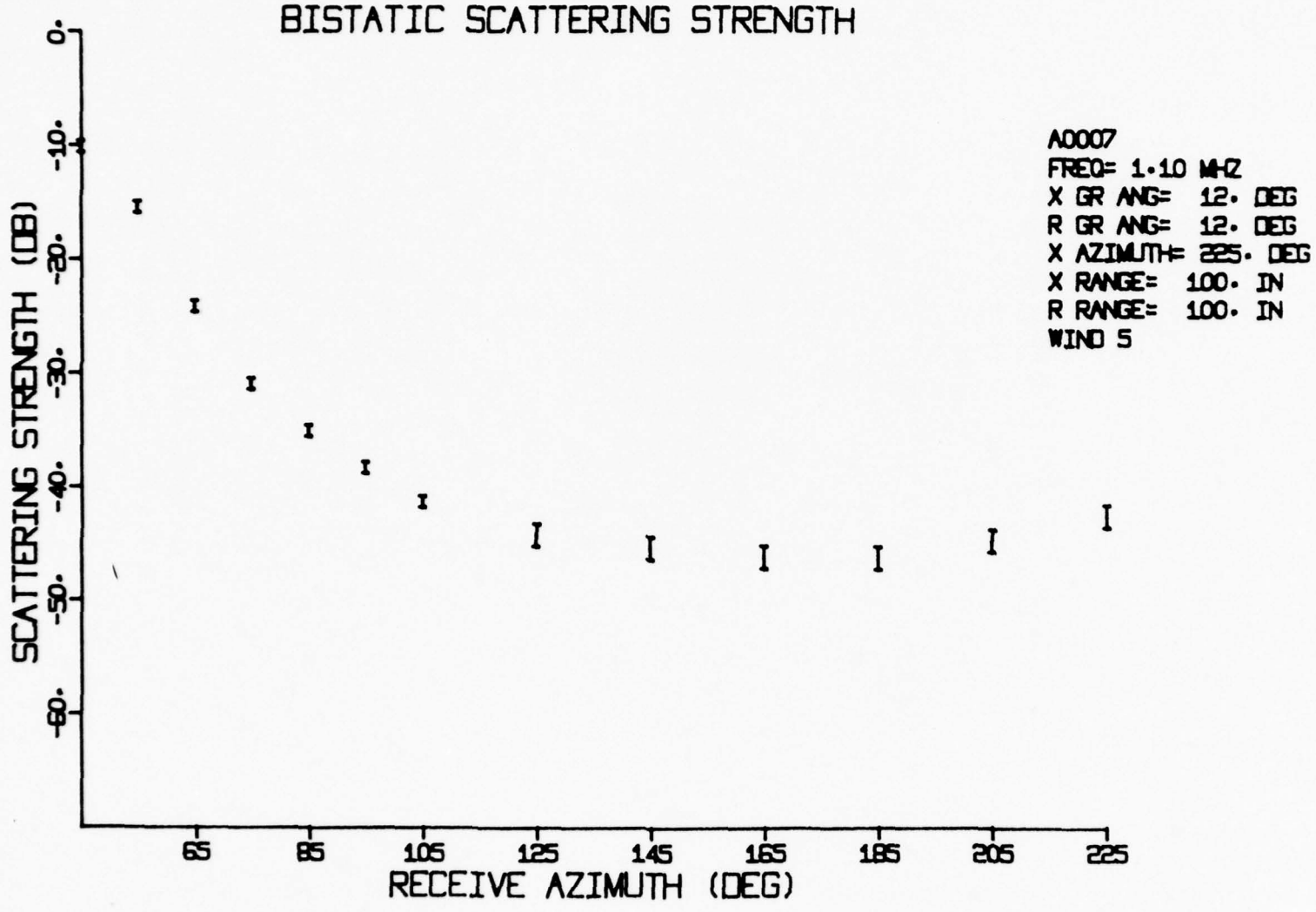
BISTATIC SCATTERING STRENGTH
A0007
FREQ= 1.10 MHZ
X GR ANG= 12. DEG
R GR ANG= 12. DEG
X AZIMUTH= 225. DEG
X RANGE= 100. IN
R RANGE= 100. IN
WIND 5
SCATTERING STRENGTH (DB)
0.
-10.
-20.
-30.
-40.
-50.
-60.
65
85
105
125
145
165
185
205
225
RECEIVE AZIMUTH (DEG)

Figure A-26

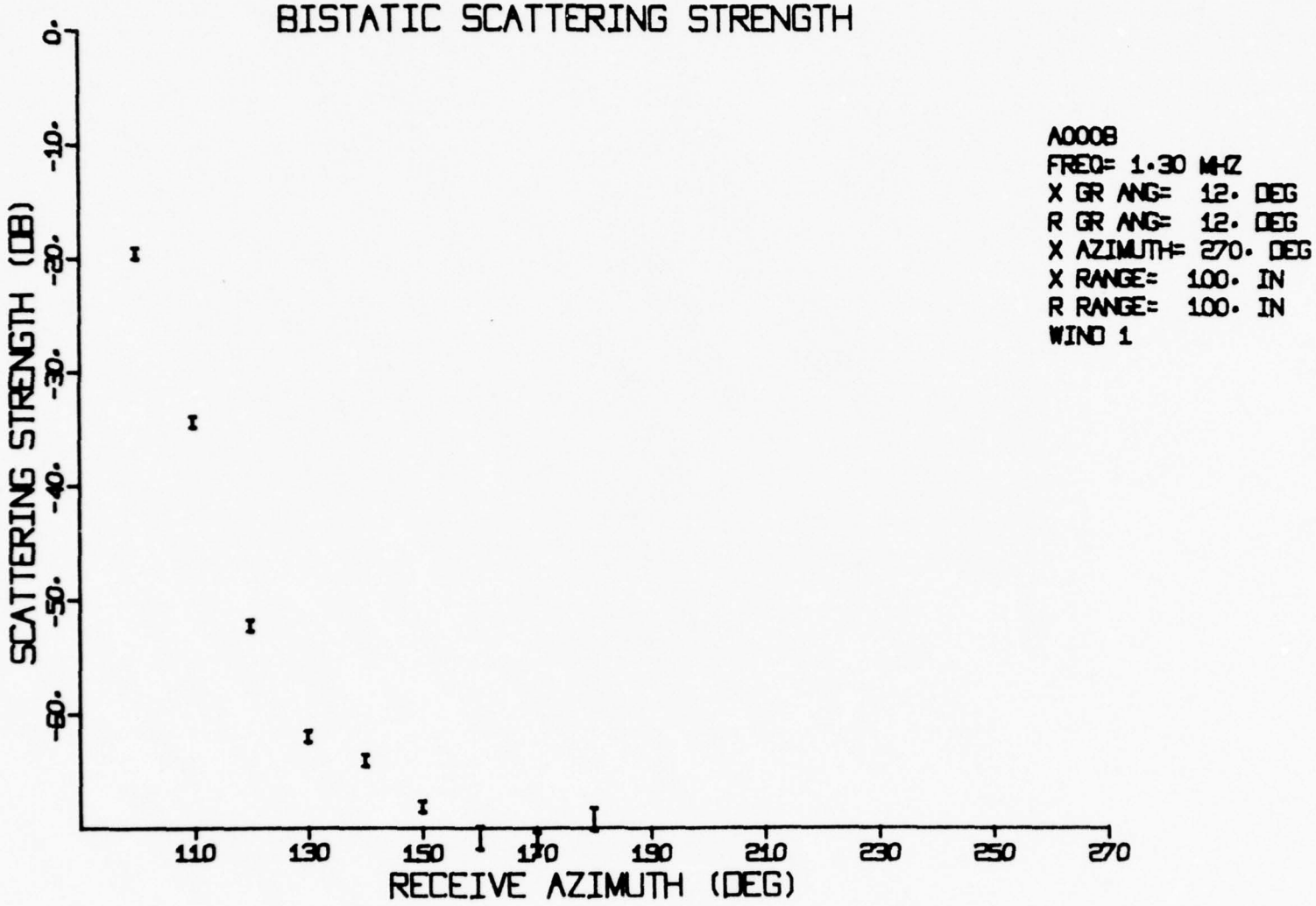
BISTATIC SCATTERING STRENGTH
A0008
FREQ= 1.30 MHZ
X GR ANG= 12. DEG
R GR ANG= 12. DEG
X AZIMUTH= 270. DEG
X RANGE= 100. IN
R RANGE= 100. IN
WIND 1
SCATTERING STRENGTH (DB)
0.
-10.
-20.
-30.
-40.
-50.
-60.
110
130
150
170
190
210
230
250
270
RECEIVE AZIMUTH (DEG)

Figure A-27

Appendix B: Scattering Strength Tabulation

This appendix contains a tabulation of the scattering strength measurements plotted in Appendix A. There are 27 tables corresponding to the figures in App. A.

A0001 9FEB77 2-Z803B
PWR PRODUCTION
1.300 TO 1.305 MHZ.
350.NS. BETWEEN SAMPLES
100.MS. BETWEEN PULSES
PROJECTOR GRAZING ANGLE = 12. DEG.
RECEIVER GRAZING ANGLE = 12. DEG.
PROJECTOR AZIMUTH = 180. DEG.
PROJECTOR RANGE = 100. IN.
RECEIVER RANGE = 100. IN.
WIND NUMBER 4

RECEIVE AZIMUTH	RECEIVE GRAZING ANGLE	SCATTERING STRENGTH
0.	12.	-7.
10.	12.	-20.
20.	12.	-34.
30.	12.	-44.
40.	12.	-51.
50.	12.	-55.
60.	12.	-57.
70.	12.	-57.
80.	12.	-58.
90.	12.	-60.
100.	12.	-59.
110.	12.	-61.
120.	12.	-61.
130.	12.	-60.
140.	12.	-60.
150.	12.	-58.
160.	12.	-61.
170.	12.	-60.
180.	12.	-60.

A0003 26JAN 77 2-Z803B
PWR PRODUCTION
1.300 TO 1.305 MHZ.
350.NS. BETWEEN SAMPLES
100.MS. BETWEEN PULSES
PROJECTOR GRAZING ANGLE = 12. DEG.
RECEIVER GRAZING ANGLE = 12. DEG.
PROJECTOR AZIMUTH = 225. DEG.
PROJECTOR RANGE = 100. IN.
RECEIVER RANGE = 100. IN.
WIND NUMBER 4

RECEIVE AZIMUTH	RECEIVE GRAZING ANGLE	SCATTERING STRENGTH
45.	12.	-6.
55.	12.	-16.
65.	12.	-33.
75.	12.	-43.
85.	12.	-48.
95.	12.	-53.
105.	12.	-56.
115.	12.	-58.
125.	12.	-59.
135.	12.	-59.
145.	12.	-60.
155.	12.	-61.
165.	12.	-62.
175.	12.	-61.
185.	12.	-60.
195.	12.	-61.
205.	12.	-62.
215.	12.	-62.
225.	12.	-62.

A0004 26JAN77 2-Z803B
PWR PRODUCTION
1.300 TO 1.305 MHZ.
350.NS. BETWEEN SAMPLES
100.MS. BETWEEN PULSES
PROJECTOR GRAZING ANGLE = 12. DEG.
RECEIVER GRAZING ANGLE = 12. DEG.
PROJECTOR AZIMUTH = 270. DEG.
PROJECTOR RANGE = 100. IN.
RECEIVER RANGE = 100. IN.
WIND NUMBER 4

RECEIVE AZIMUTH	RECEIVE GRAZING ANGLE	SCATTERING STRENGTH
90.	12.	-4.
100.	12.	-15.
110.	12.	-32.
120.	12.	-43.
130.	12.	-49.
140.	12.	-54.
150.	12.	-56.
160.	12.	-59.
170.	12.	-59.
180.	12.	-60.
190.	12.	-63.
200.	12.	-63.
210.	12.	-65.
220.	12.	-61.
230.	12.	-60.
240.	12.	-64.
250.	12.	-61.
260.	12.	-63.
270.	12.	-60.

A0010 10FEB77 2-Z803B
PWR PRODUCTION
1.300 TO 1.305 MHZ.
350.NS. BETWEEN SAMPLES
100.MS. BETWEEN PULSES
PROJECTOR GRAZING ANGLE = 12. DEG.
RECEIVER GRAZING ANGLE = 12. DEG.
PROJECTOR AZIMUTH = 315. DEG.
PROJECTOR RANGE = 100. IN.
RECEIVER RANGE = 100. IN.
WIND NUMBER 4

RECEIVE AZIMUTH	RECEIVE GRAZING ANGLE	SCATTERING STRENGTH
135.	12.	-7.
145.	12.	-14.
155.	12.	-32.
165.	12.	-44.
175.	12.	-51.
185.	12.	-56.
195.	12.	-60.
205.	12.	-63.
215.	12.	-61.
225.	12.	-62.
235.	12.	-60.
245.	12.	-58.
255.	12.	-57.
265.	12.	-56.
275.	12.	-55.
285.	12.	-51.
295.	12.	-52.
305.	12.	-49.
315.	12.	-47.

A0011 13 MAY 7 2 Z803B
PWR PRODUCTION
1.300 TO 1.305 MHZ.
350.NS. BETWEEN SAMPLES
100.MS. BETWEEN PULSES
PROJECTOR GRAZING ANGLE = 12. DEG.
RECEIVER GRAZING ANGLE = 12. DEG.
PROJECTOR AZIMUTH = 360. DEG.
PROJECTOR RANGE = 100. IN.
RECEIVER RANGE = 100. IN.
WIND NUMBER 4

RECEIVE AZIMUTH	RECEIVE GRAZING ANGLE	SCATTERING STRENGTH
180.	12.	-9.
190.	12.	-21.
200.	12.	-37.
210.	12.	-46.
220.	12.	-50.
230.	12.	-52.
240.	12.	-52.
250.	12.	-50.
260.	12.	-49.
270.	12.	-49.
280.	12.	-47.
290.	12.	-48.
300.	12.	-47.
310.	12.	-48.
320.	12.	-45.
330.	12.	-44.
340.	12.	-45.
350.	12.	-43.
360.	12.	-44.

A0020 20FEB77 2-Z803B
PWR PRODUCTION
1.300 TO 1.305 MHZ.
350.NS. BETWEEN SAMPLES
100.MS. BETWEEN PULSES
PROJECTOR GRAZING ANGLE = 17. DEG.
RECEIVER GRAZING ANGLE = 17. DEG.
PROJECTOR AZIMUTH = 180. DEG.
PROJECTOR RANGE = 82. IN.
RECEIVER RANGE = 90. IN.
WIND NUMBER 4

RECEIVE AZIMUTH	RECEIVE GRAZING ANGLE	SCATTERING STRENGTH
0.	17.	-5.
10.	17.	-10.
20.	17.	-25.
30.	17.	-36.
40.	17.	-42.
50.	17.	-48.
60.	17.	-50.
70.	17.	-52.
80.	17.	-54.
90.	17.	-55.
100.	17.	-56.
110.	17.	-56.
120.	17.	-57.
130.	17.	-57.
140.	17.	-57.
150.	17.	-57.
160.	17.	-56.
170.	17.	-57.
180.	17.	-57.

A0021 23FEB77 2-Z803B
PWR PRODUCTION
1.300 TO 1.305 MHZ.
350.NS. BETWEEN SAMPLES
100.MS. BETWEEN PULSES
PROJECTOR GRAZING ANGLE = 17. DEG.
RECEIVER GRAZING ANGLE = 17. DEG.
PROJECTOR AZIMUTH = 225. DEG.
PROJECTOR RANGE = 82. IN.
RECEIVER RANGE = 90. IN.
WIND NUMBER 4

RECEIVE AZIMUTH	RECEIVE GRAZING ANGLE	SCATTERING STRENGTH
45.	17.	-5.
55.	17.	-9.
65.	17.	-22.
75.	17.	-33.
85.	17.	-40.
95.	17.	-44.
105.	17.	-47.
115.	17.	-50.
125.	17.	-52.
135.	17.	-54.
145.	17.	-54.
155.	17.	-54.
165.	17.	-56.
175.	17.	-57.
185.	17.	-59.
195.	17.	-58.
205.	17.	-59.
215.	17.	-60.
225.	17.	-59.

A0022 23FEB77 2-Z803B
PWR PRODUCTION
1.300 TO 1.305 MHZ.
350.NS. BETWEEN SAMPLES
100.MS. BETWEEN PULSES
PROJECTOR GRAZING ANGLE = 17. DEG.
RECEIVER GRAZING ANGLE = 17. DEG.
PROJECTOR AZIMUTH = 270. DEG.
PROJECTOR RANGE = 82. IN.
RECEIVER RANGE = 90. IN.
WIND NUMBER 4

RECEIVE AZIMUTH	RECEIVE GRAZING ANGLE	SCATTERING STRENGTH
90.	17.	-4.
100.	17.	-6.
110.	17.	-19.
130.	17.	-39.
140.	17.	-45.
150.	17.	-48.
160.	17.	-52.
170.	17.	-54.
180.	17.	-56.
190.	17.	-58.
200.	17.	-60.
210.	17.	-61.
220.	17.	-61.
230.	17.	-62.
240.	17.	-63.
250.	17.	-68.
260.	17.	-64.
270.	17.	-64.

A0023 23FEB77 2-Z803B
PWR PRODUCTION
1.300 TO 1.305 MHZ.
350.NS. BETWEEN SAMPLES
100.MS. BETWEEN PULSES
PROJECTOR GRAZING ANGLE = 17. DEG.
RECEIVER GRAZING ANGLE = 17. DEG.
PROJECTOR AZIMUTH = 315. DEG.
PROJECTOR RANGE = 82. IN.
RECEIVER RANGE = 90. IN.
WIND NUMBER 4

RECEIVE AZIMUTH	RECEIVE GRAZING ANGLE	SCATTERING STRENGTH
135.	17.	-4.
145.	17.	-10.
155.	17.	-24.
165.	17.	-36.
175.	17.	-43.
185.	17.	-52.
195.	17.	-54.
205.	17.	-58.
215.	17.	-53.
225.	17.	-60.
235.	17.	-59.
245.	17.	-58.
255.	17.	-55.
265.	17.	-56.
275.	17.	-52.
285.	17.	-50.
295.	17.	-49.
305.	17.	-49.
315.	17.	-46.

A0024 23FEB77 2-Z803B
PWR PRODUCTION
1.300 TO 1.305 MHZ.
350.NS. BETWEEN SAMPLES
100.MS. BETWEEN PULSES
PROJECTOR GRAZING ANGLE = 17. DEG.
RECEIVER GRAZING ANGLE = 17. DEG.
PROJECTOR AZIMUTH = 360. DEG.
PROJECTOR RANGE = 82. IN.
RECEIVER RANGE = 90. IN.
WIND NUMBER 4

RECEIVE AZIMUTH	RECEIVE GRAZING ANGLE	SCATTERING STRENGTH
180.	17.	-5.
190.	17.	-13.
200.	17.	-26.
210.	17.	-33.
220.	17.	-38.
230.	17.	-42.
240.	17.	-42.
250.	17.	-43.
260.	17.	-42.
270.	17.	-41.
280.	17.	-43.
290.	17.	-40.
300.	17.	-40.
310.	17.	-41.
320.	17.	-37.
330.	17.	-39.
340.	17.	-38.
350.	17.	-38.
360.	17.	-37.

A0017 20FEB77 2-Z803B
PWR PRODUCTION
1.300 TO 1.305 MHZ.
350.NS. BETWEEN SAMPLES
100.MS. BETWEEN PULSES
PROJECTOR GRAZING ANGLE = 12. DEG.
RECEIVER GRAZING ANGLE = 17. DEG.
PROJECTOR AZIMUTH = 180. DEG.
PROJECTOR RANGE = 100. IN.
RECEIVER RANGE = 90. IN.
WIND NUMBER 4

RECEIVE AZIMUTH	RECEIVE GRAZING ANGLE	SCATTERING STRENGTH
0.	17.	-7.
10.	17.	-10.
20.	17.	-31.
30.	17.	-42.
40.	17.	-49.
50.	17.	-52.
60.	17.	-53.
70.	17.	-56.
80.	17.	-57.
90.	17.	-58.
100.	17.	-57.
110.	17.	-57.
120.	17.	-57.
130.	17.	-58.
140.	17.	-58.
150.	17.	-58.
160.	17.	-58.
170.	17.	-58.
180.	17.	-57.

A0016 20FEB77 2-Z803B
PWR PRODUCTION
1.300 TO 1.305 MHZ.
350.NS. BETWEEN SAMPLES
100.MS. BETWEEN PULSES
PROJECTOR GRAZING ANGLE = 12. DEG.
RECEIVER GRAZING ANGLE = 17. DEG.
PROJECTOR AZIMUTH = 225. DEG.
PROJECTOR RANGE = 100. IN.
RECEIVER RANGE = 90. IN.
WIND NUMBER 4

RECEIVE AZIMUTH	RECEIVE GRAZING ANGLE	SCATTERING STRENGTH
45.	17.	-6.
55.	17.	-11.
65.	17.	-27.
75.	17.	-37.
85.	17.	-44.
95.	17.	-48.
105.	17.	-52.
115.	17.	-53.
125.	17.	-55.
135.	17.	-56.
145.	17.	-57.
155.	17.	-58.
165.	17.	-58.
175.	17.	-59.
185.	17.	-60.
195.	17.	-60.
205.	17.	-61.
215.	17.	-61.
225.	17.	-62.

A0015 20FEB77 2-Z803B
PWR PRODUCTION
1.300 TO 1.305 MHZ.
350.NS. BETWEEN SAMPLES
100.MS. BETWEEN PULSES
PROJECTOR GRAZING ANGLE = 12. DEG.
RECEIVER GRAZING ANGLE = 17. DEG.
PROJECTOR AZIMUTH = 270. DEG.
PROJECTOR RANGE = 100. IN.
RECEIVER RANGE = 90. IN.
WIND NUMBER 4

RECEIVE AZIMUTH	RECEIVE GRAZING ANGLE	SCATTERING STRENGTH
90.	17.	-5.
100.	17.	-8.
110.	17.	-24.
120.	17.	-36.
130.	17.	-42.
140.	17.	-49.
150.	17.	-52.
160.	17.	-55.
170.	17.	-61.
180.	17.	-58.
190.	17.	-60.
200.	17.	-60.
210.	17.	-64.
220.	17.	-65.
230.	17.	-66.
240.	17.	-63.
250.	17.	-62.
260.	17.	-65.
270.	17.	-66.

A0014 16FEB77 2-Z803B
PWR PRODUCTION
1.300 TO 1.305 MHZ.
350.NS. BETWEEN SAMPLES
100.MS. BETWEEN PULSES
PROJECTOR GRAZING ANGLE = 12. DEG.
RECEIVER GRAZING ANGLE = 17. DEG.
PROJECTOR AZIMUTH = 315. DEG.
PROJECTOR RANGE = 100. IN.
RECEIVER RANGE = 90. IN.
WIND NUMBER 4

RECEIVE AZIMUTH	RECEIVE GRAZING ANGLE	SCATTERING STRENGTH
135.	17.	-7.
145.	17.	-12.
155.	17.	-26.
165.	17.	-40.
175.	17.	-46.
185.	17.	-53.
195.	17.	-59.
205.	17.	-61.
215.	17.	-61.
225.	17.	-60.
235.	17.	-59.
245.	17.	-60.
255.	17.	-56.
265.	17.	-54.
275.	17.	-53.
285.	17.	-50.
295.	17.	-49.
305.	17.	-48.
315.	17.	-45.

A0012 16FEB77 2-Z803B
PWR PRODUCTION
1.300 TO 1.305 MHZ.
350.NS. BETWEEN SAMPLES
100.MS. BETWEEN PULSES
PROJECTOR GRAZING ANGLE = 12. DEG.
RECEIVER GRAZING ANGLE = 17. DEG.
PROJECTOR AZIMUTH = 360. DEG.
PROJECTOR RANGE = 100. IN.
RECEIVER RANGE = 90. IN.
WIND NUMBER 4

RECEIVE AZIMUTH	RECEIVE GRAZING ANGLE	SCATTERING STRENGTH
180.	17.	-7.
190.	17.	-14.
200.	17.	-27.
210.	17.	-36.
220.	17.	-39.
230.	17.	-43.
240.	17.	-42.
250.	17.	-42.
260.	17.	-43.
270.	17.	-41.
280.	17.	-43.
290.	17.	-42.
300.	17.	-40.
310.	17.	-39.
320.	17.	-38.
330.	17.	-39.
340.	17.	-38.
350.	17.	-38.
360.	17.	-37.

A0034 6MAR77 2-Z803B
PWR PRODUCTION
1.300 TO 1.305 MHZ.
350.NS. BETWEEN SAMPLES
100.MS. BETWEEN PULSES
PROJECTOR GRAZING ANGLE = 17. DEG.
RECEIVER GRAZING ANGLE = 12. DEG.
PROJECTOR AZIMUTH = 180. DEG.
PROJECTOR RANGE = 82. IN.
RECEIVER RANGE = 90. IN.
WIND NUMBER 4

RECEIVE AZIMUTH	RECEIVE GRAZING ANGLE	SCATTERING STRENGTH
0.	12.	-6.
10.	12.	-15.
20.	12.	-29.
30.	12.	-39.
40.	12.	-48.
50.	12.	-52.
60.	12.	-54.
70.	12.	-56.
80.	12.	-57.
90.	12.	-57.
100.	12.	-58.
110.	12.	-58.
120.	12.	-61.
130.	12.	-59.
140.	12.	-60.
150.	12.	-60.
160.	12.	-59.
170.	12.	-59.
180.	12.	-59.

A0033 6MAR77 2-Z303B
PWR PRODUCTION
1.300 TO 1.305 MHZ.
350.NS. BETWEEN SAMPLES
100.MS. BETWEEN PULSES
PROJECTOR GRAZING ANGLE = 17. DEG.
RECEIVER GRAZING ANGLE = 12. DEG.
PROJECTOR AZIMUTH = 225. DEG.
PROJECTOR RANGE = 82. IN.
RECEIVER RANGE = 90. IN.
WIND NUMBER 4

RECEIVE AZIMUTH	RECEIVE GRAZING ANGLE	SCATTERING STRENGTH
45.	12.	-6.
55.	12.	-11.
65.	12.	-26.
75.	12.	-37.
85.	12.	-43.
95.	12.	-48.
105.	12.	-51.
115.	12.	-53.
125.	12.	-55.
135.	12.	-55.
145.	12.	-57.
155.	12.	-57.
165.	12.	-59.
175.	12.	-59.
185.	12.	-60.
195.	12.	-60.
205.	12.	-62.
215.	12.	-64.
225.	12.	-64.

A0032 6MAR77 2-Z803B
PWR PRODUCTION
1.300 TO 1.305 MHZ.
350.NS. BETWEEN SAMPLES
100.MS. BETWEEN PULSES
PROJECTOR GRAZING ANGLE = 17. DEG.
RECEIVER GRAZING ANGLE = 12. DEG.
PROJECTOR AZIMUTH = 270. DEG.
PROJECTOR RANGE = 82. IN.
RECEIVER RANGE = 90. IN.
WIND NUMBER 4

RECEIVE AZIMUTH	RECEIVE GRAZING ANGLE	SCATTERING STRENGTH
90.	12.	-5.
100.	12.	-9.
110.	12.	-25.
120.	12.	-36.
130.	12.	-44.
140.	12.	-50.
150.	12.	-52.
160.	12.	-55.
170.	12.	-57.
180.	12.	-60.
190.	12.	-60.
200.	12.	-63.
210.	12.	-65.
220.	12.	-64.
230.	12.	-67.
240.	12.	-62.
250.	12.	-66.
260.	12.	-67.
270.	12.	-65.

A0031 4 MAR 77 2-Z803B
PWR PRODUCTION
1.300 TO 1.305 MHZ.
350.NS. BETWEEN SAMPLES
100.MS. BETWEEN PULSES
PROJECTOR GRAZING ANGLE = 17. DEG.
RECEIVER GRAZING ANGLE = 12. DEG.
PROJECTOR AZIMUTH = 315. DEG.
PROJECTOR RANGE = 82. IN.
RECEIVER RANGE = 90. IN.
WIND NUMBER 4

RECEIVE AZIMUTH	RECEIVE GRAZING ANGLE	SCATTERING STRENGTH
135.	12.	-5.
145.	12.	-9.
155.	12.	-26.
165.	12.	-39.
175.	12.	-47.
185.	12.	-52.
195.	12.	-58.
205.	12.	-61.
215.	12.	-62.
225.	12.	-62.
235.	12.	-55.
245.	12.	-57.
255.	12.	-56.
265.	12.	-55.
275.	12.	-54.
285.	12.	-47.
295.	12.	-50.
305.	12.	-47.
315.	12.	-46.

A0030 27FEB77 2-Z803B
PWR PRODUCTION
1.300 TO 1.305 MHZ.
350.NS. BETWEEN SAMPLES
100.MS. BETWEEN PULSES
PROJECTOR GRAZING ANGLE = 17. DEG.
RECEIVER GRAZING ANGLE = 12. DEG.
PROJECTOR AZIMUTH = 360. DEG.
PROJECTOR RANGE = 82. IN.
RECEIVER RANGE = 90. IN.
WIND NUMBER 4

RECEIVE AZIMUTH	RECEIVE GRAZING ANGLE	SCATTERING STRENGTH
180.	12.	-6.
190.	12.	-14.
200.	12.	-29.
210.	12.	-37.
220.	12.	-41.
230.	12.	-43.
240.	12.	-44.
250.	12.	-44.
260.	12.	-43.
270.	12.	-42.
280.	12.	-42.
290.	12.	-42.
300.	12.	-41.
310.	12.	-41.
320.	12.	-39.
330.	12.	-38.
340.	12.	-39.
350.	12.	-37.
360.	12.	-38.

A0002 23JAN77 2-Z803B
LPWR PRODUCTION
1.300 TO 1.305 MHZ.
350.NS. BETWEEN SAMPLES
100.MS. BETWEEN PULSES
PROJECTOR GRAZING ANGLE = 12. DEG.
RECEIVER GRAZING ANGLE = 12. DEG.
PROJECTOR AZIMUTH = 180. DEG.
PROJECTOR RANGE = 100. IN.
RECEIVER RANGE = 100. IN.
WIND NUMBER 5

RECEIVE AZIMUTH	RECEIVE GRAZING ANGLE	SCATTERING STRENGTH
0.	12.	-10.
10.	12.	-19.
20.	12.	-29.
30.	12.	-35.
40.	12.	-40.
50.	12.	-42.
60.	12.	-42.
70.	12.	-44.
80.	12.	-45.
90.	12.	-46.
100.	12.	-47.
110.	12.	-47.
120.	12.	-47.
130.	12.	-48.
140.	12.	-48.
150.	12.	-48.
160.	12.	-48.
170.	12.	-48.
180.	12.	-49.

A0006 26JAN77 2-Z803B
PWR PRODUCRTION
1.300 TO 1.305 MHZ.
350.NS. BETWEEN SAMPLES
100.MS. BETWEEN PULSES
PROJECTOR GRAZING ANGLE = 12. DEG.
RECEIVER GRAZING ANGLE = 12. DEG.
PROJECTOR AZIMUTH = 225. DEG.
PROJECTOR RANGE = 100. IN.
RECEIVER RANGE = 100. IN.
WIND NUMBER 5

RECEIVE AZIMUTH	RECEIVE GRAZING ANGLE	SCATTERING STRENGTH
45.	12.	-10.
55.	12.	-15.
65.	12.	-25.
75.	12.	-32.
85.	12.	-36.
95.	12.	-39.
105.	12.	-41.
115.	12.	-44.
125.	12.	-44.
135.	12.	-45.
145.	12.	-46.
155.	12.	-47.
165.	12.	-45.
185.	12.	-47.
195.	12.	-46.
205.	12.	-45.
215.	12.	-45.
225.	12.	-43.

A0005 26JAN77 2-Z803B
PWR PRODUCTION
1.300 TO 1.305 MHZ.
350.NS. BETWEEN SAMPLES
100.MS. BETWEEN PULSES
PROJECTOR GRAZING ANGLE = 12. DEG.
RECEIVER GRAZING ANGLE = 12. DEG.
PROJECTOR AZIMUTH = 270. DEG.
PROJECTOR RANGE = 100. IN.
RECEIVER RANGE = 100. IN.
WIND NUMBER 5

RECEIVE AZIMUTH	RECEIVE GRAZING ANGLE	SCATTERING STRENGTH
90.	12.	-9.
100.	12.	-15.
110.	12.	-23.
120.	12.	-32.
130.	12.	-36.
140.	12.	-41.
150.	12.	-42.
160.	12.	-43.
170.	12.	-44.
180.	12.	-45.
190.	12.	-45.
200.	12.	-44.
210.	12.	-44.
220.	12.	-43.
230.	12.	-42.
240.	12.	-40.
250.	12.	-40.
260.	12.	-38.
270.	12.	-36.

A0053 14MAY77 2-Z803B
PWR PRODUCTION
1.300 TO 1.305 MHZ.
350.NS. BETWEEN SAMPLES
100.MS. BETWEEN PULSES
PROJECTOR GRAZING ANGLE = 12. DEG.
RECEIVER GRAZING ANGLE = 12. DEG.
PROJECTOR AZIMUTH = 315. DEG.
PROJECTOR RANGE = 100. IN.
RECEIVER RANGE = 100. IN.
WIND NUMBER 5

RECEIVE AZIMUTH	RECEIVE GRAZING ANGLE	SCATTERING STRENGTH
135.	12.	-9.
145.	12.	-15.
155.	12.	-26.
165.	12.	-34.
175.	12.	-40.
185.	12.	-43.
195.	12.	-45.
205.	12.	-45.
215.	12.	-44.
225.	12.	-44.
235.	12.	-44.
245.	12.	-41.
265.	12.	-39.
255.	12.	-39.
285.	12.	-37.
295.	12.	-34.
305.	12.	-34.
315.	12.	-33.

A0052 14MAY77 2-Z803B
PWR PRODUCTION
1.300 TO 1.305 MHZ.
350.NS. BETWEEN SAMPLES
100.MS. BETWEEN PULSES
PROJECTOR GRAZING ANGLE = 12. DEG.
RECEIVER GRAZING ANGLE = 12. DEG.
PROJECTOR AZIMUTH = 360. DEG.
PROJECTOR RANGE = 100. IN.
RECEIVER RANGE = 100. IN.
WIND NUMBER 5

RECEIVE AZIMUTH	RECEIVE GRAZING ANGLE	SCATTERING STRENGTH
180.	12.	-11.
190.	12.	-19.
200.	12.	-30.
210.	12.	-35.
220.	12.	-39.
230.	12.	-38.
240.	12.	-37.
250.	12.	-36.
260.	12.	-36.
270.	12.	-35.
280.	12.	-35.
290.	12.	-34.
300.	12.	-34.
310.	12.	-34.
320.	12.	-33.
330.	12.	-34.
340.	12.	-33.
350.	12.	-33.
360.	12.	-32.

A0007 31JAN77 2-Z803B
PWR PRODUCTION
1.100 TO 1.105 MHZ.
350.NS. BETWEEN SAMPLES
100.MS. BETWEEN PULSES
PROJECTOR GRAZING ANGLE = 12. DEG.
RECEIVER GRAZING ANGLE = 12. DEG.
PROJECTOR AZIMUTH = 225. DEG.
PROJECTOR RANGE = 100. IN.
RECEIVER RANGE = 100. IN.
WIND NUMBER 5

RECEIVE AZIMUTH	RECEIVE GRAZING ANGLE	SCATTERING STRENGTH
45.	12.	-10.
55.	12.	-15.
65.	12.	-24.
75.	12.	-31.
85.	12.	-35.
95.	12.	-38.
105.	12.	-41.
125.	12.	-44.
145.	12.	-45.
165.	12.	-46.
185.	12.	-46.
205.	12.	-45.
225.	12.	-43.

A0008 16MAY77 2-Z803B
PWR PRODUCTION
1.300 TO 1.305 MHZ.
350.NS. BETWEEN SAMPLES
100.MS. BETWEEN PULSES
PROJECTOR GRAZING ANGLE = 12. DEG.
RECEIVER GRAZING ANGLE = 12. DEG.
PROJECTOR AZIMUTH = 270. DEG.
PROJECTOR RANGE = 100. IN.
RECEIVER RANGE = 100. IN.
WIND NUMBER 1

RECEIVE AZIMUTH	RECEIVE GRAZING ANGLE	SCATTERING STRENGTH
90.	12.	0.
100.	12.	-20.
110.	12.	-34.
120.	12.	-52.
130.	12.	-62.
140.	12.	-64.
150.	12.	-68.
160.	12.	-71.
170.	12.	-71.
180.	12.	-69.